Programa de Doctorado en Tecnologías Industriales y de
Telecomunicación

Mejoras de eficiencia computacional y precisión para sistemas predictivos de demanda eléctrica

Alfredo Candela Esclapez

Director/a de la tesis

Dr. Sergio Valero Verdú

Codirector/a de la tesis

Dr. Miguel López García

Universidad Miguel Hernández de Elche

- 2022 -

Relación de trabajos publicados

La presente Tesis Doctoral, titulada "**Mejoras de eficiencia computacional y precisión para sistemas predictivos de demanda eléctrica**" se presenta bajo la modalidad de **tesis por compendio** de las siguientes **publicaciones**:

1. Candela Esclapez, A.; García, M.L.; Valero Verdú, S.; Senabre Blanes, C. Reduction of Computational Burden and Accuracy Maximization in Short-Term Load Forecasting. *Energies* **2022**, *15*, 3670, doi:10.3390/en15103670.

2. Candela Esclapez, A.; López García, M.; Valero Verdú, S.; Senabre Blanes, C. Automatic Selection of Temperature Variables for Short-Term Load Forecasting. *Sustainability* **2022**, *14*, 13339, doi:10.3390/su142013339.

Índice general

Listado de figuras

Listado de tablas

Resumen

Debido a la inviabilidad del almacenamiento de energía eléctrica a gran escala, la energía eléctrica se genera y consume simultáneamente. En consecuencia, las entidades eléctricas necesitan sistemas de previsión de demanda para planificar operaciones y gestionar suministros. Predicciones de demanda precisas permiten el ahorro económico de suministros de generación de energía, así como reforzar la fiabilidad del abastecimiento a los consumidores. Por otra parte, las predicciones de demanda también permiten gestionar las energías renovables en las redes eléctricas, reduciendo indirectamente las emisiones de gases de efecto invernadero.

Esta tesis se centra en mejorar, a escala peninsular, el sistema predictivo de Red Eléctrica de España (REE) y desarrollado por la Universidad Miguel Hernández (UMH). Se presenta un enfoque independiente de sus modelos matemáticos, ofreciendo metodologías aplicables a otros sistemas predictivos de otras redes eléctricas. Se exploran dos mejoras: una obtención determinista y automática del horario de cálculos y un preprocesado de datos de temperatura que da pie a análisis demográficos. Ambas mejoras también incrementan la precisión de las predicciones, siendo un criterio base de diseño.

En Europa, debido a las directivas y las nuevas tecnologías, los sistemas de predicción pasan de trabajar en intervalos horarios a cuarto-horarios, lo que reduce el tiempo de cálculo y aumenta la carga computacional. Por lo tanto, un sistema predictivo puede no disponer de tiempo suficiente para calcular todos los pronósticos futuros. Los sistemas de predicción realizan cálculos a lo largo del día, repitiendo los mismos pronósticos a medida que se acerca la hora prevista. Sin embargo, hay predicciones que no son más precisas que otras ya calculadas, lo que da pie a no ejecutarlas y emplear las predicciones previas para ahorrar esfuerzo computacional y mantener la precisión.

Con la idea de evitar cálculos contraproducentes, se desarrolla un algoritmo que estima qué pronósticos brindan mayor precisión que los anteriores, con lo que construye un horario de ejecuciones. El algoritmo se adapta a las necesidades computacionales y el sistema predictivo, con lo que se ha aplicado al sistema de predicción de REE, obteniendo un horario de ejecuciones que consigue una mayor precisión y se adapta a la carga computacional.

Por otra parte, la demanda eléctrica depende de la temperatura ambiente por el uso de equipos de aire acondicionado y calefacción. Esta tesis propone un método automático de procesamiento y selección de variables térmicas con un doble objetivo: mejorar tanto la precisión como la interpretabilidad del sistema de pronóstico global. La metodología experimental se ha realizado con el sistema predictivo de REE. La nueva forma de trabajar con las temperaturas es interpretable, ya que separan el efecto de la temperatura según la ubicación y el tiempo mediante variables con un significado específico.

Ambos estudios demuestran experimentalmente que las técnicas propuestas cumplen su cometido, mejorando la precisión y el coste computacional del sistema predictivo. También se observa que en España el calor tiene mayor influencia sobre la demanda que el frío. En los días calurosos, la temperatura del segundo día anterior tiene mayor influencia que la del anterior, mientras que en los días fríos ocurre lo contrario.

A partir de la construcción del horario de ejecuciones se ha concluido que las temperaturas afectan poco a la demanda durante la madrugada; las previsiones de temperatura de menos de cuatro días de antelación implican una mayor precisión que las de más de cuatro; y que cuanto menor es la diferencia de tiempo entre el momento de predicción y el de ejecución, mayor precisión se tiene.

Abstract

Due to the infeasibility of large-scale electrical energy storage, electrical energy is generated and consumed simultaneously. Therefore, electricity entities need demand forecasting systems to plan operations and to manage supplies. Improving the forecasts accuracy allows economic savings of energy generation supplies, as well as reinforcing the reliability of energy supply to electricity consumers. In addition, demand forecasts allow renewable energies to be managed in electricity networks, indirectly reducing greenhouse gas emissions.

This thesis focuses on improving, at peninsular scale, the forecasting system of Red Eléctrica de España (REE) developed by the Miguel Hernández University (UMH). An independent approach of mathematical models is presented, offering methodologies applicable to other forecasting systems from different electrical grids. Two improvements are tackled: a deterministic and automatic schedule obtention and a preprocessing of temperature data, which can be used as a tool for demographic studies. Both enhancements also increase the forecasting accuracy.

In Europe, due to directives and new technologies, forecasting systems are transitioning from hourly intervals to quarter-hourly intervals, which reduces the calculation time and increases the computational burden. Therefore, a predictive system may not have enough time to compute all future forecasts. Forecasting systems perform calculations throughout the day, repeating the same forecasts while the forecast time approaches. However, there are predictions that are not more accurate than others already calculated, which leads to not executing them and using previous predictions to save computational effort and maintain accuracy.

With the intention of avoiding counterproductive calculations, an algorithm is developed, that estimates which forecasts provide better accuracy than previous ones, then it builds a computing schedule. The algorithm adapts to the computational needs and the predictive system. It has been applied to the REE prediction system, obtaining a computing schedule that achieves greater precision and adapts to the computational load.

Temperature affects electricity consumption through air conditioning and heating equipment. This thesis proposes an automatic method of processing and selecting variables with a double objective: to improve both the accuracy and the interpretability of the global forecasting system. The experimental methodology has been carried out with the REE predictive system. The new way of working with temperatures is interpretable as it separates the effect of temperature based on location and time, using variables with a specific meaning.

Both studies experimentally demonstrate that the proposed techniques fulfill their purpose, improving the accuracy and computational cost of the predictive system. It is also observed that in Spain heat has a greater influence on demand than cold. On hot

days, the temperature of the second previous day has a greater influence than that of the previous one, while on cold days the opposite occurs.

Based on the construction of the execution schedule, it has been concluded that temperatures have reduced effect on demand during the early morning hours; temperature forecasts for less than four days ahead provide more accuracy than those more than four; and according as the time difference between the moment of prediction and the moment of execution decreases, the accuracy increases.

1. Introducción

Hoy en día, en las redes eléctricas no es viable almacenar energía eléctrica a escala nacional, por lo que se tiene la necesidad de generar la energía eléctrica al mismo tiempo que se consume. Para mantener este equilibrio en tiempo real, no basta con emplear sistemas de control, también es necesario planificar las operaciones y suministros que se emplearán en diferentes plazos:

- Muy corto: con una antelación de segundos a minutos. Tiene como propósito controlar los generadores de las plantas de generación eléctrica. En la literatura este ámbito predictivo se conoce como VSTLF (*Very Short-Term Load Forecasting*).
- Corto: tiene una antelación entre horas y varias semanas. Se utiliza como apoyo en las gestiones económicas, de operaciones y de suministros para entidades eléctricas como comercializadoras, agregadores de demanda, generadoras, etc. Se conoce como STLF (*Short-Term Load Forecasting*). Es el ámbito predictivo en el cual se centra la presente tesis, por su demanda por parte de REE (Réd Eléctrica de España) y el ámbito científico.
- Medio: gestiona en un plazo de meses hasta un año. Su utilidad reside en la planificación de operaciones en instalaciones; como son mantenimiento, maniobras de conmutación y sus respectivos cortes de energía. En la literatura este ámbito se conoce como MTLF (*Medium-Term Load Forecasting*).
- Largo: soporta planificaciones de varios años. Ayuda en la planificación de mantenimiento y construcción de instalaciones. Se suele demoninar LTLF (*Long-Term Load Forecasting*), siendo el tipo de plazo con menor atención en la literatura.

Dado que los métodos predictivos son la base de planificación de operaciones en las redes eléctricas, su precisión tiene un impacto directo en la fiabilidad y eficiencia de generación y transporte de energía. Predecir una mayor energía de la que se consume, deriva en mayores costes de suministro; mientras que predecir menos, supone un riesgo de no poder abastecer la demanda requerida.

Los sistemas predictivos de consumo combinados con los de generación de fuentes renovables (como eólica o solar), permiten gestionar y aprovechar mejor las energías verdes, con lo que se reduce la emisión de gases de efecto invernadero.

Las redes eléctricas distribuyen energía a escala nacional, por lo que pequeñas mejoras de precisión en las predicciones, tienen un impacto significativo en cuanto a economía y emisión de gases de efecto invernadero.

1.1 Métodos predictivos

1.1.1 Dificultades y términos

Predecir la demanda eléctrica requiere tener en cuenta múltiples variables, como son los registros de demanda previa, variables meteorológicas (como temperatura y humedad), tipo de día (laboral o festivo), etc. Además, esas variables están relacionadas entre sí, de modo que afectan a la demanda dependiendo del resto. Por ejemplo, Moral-Carcedo et al. [1] analizaron la influencia de la temperatura ambiente sobre la demanda eléctrica, concluyendo que dicha influencia sigue los ritmos circadianos a lo largo del día, de modo que en las horas de madrugada la temperatura influye mucho menos que durante las horas diurnas. Por otra parte, la demanda eléctrica siempre tiene un componente aleatorio debido a la naturaleza del comportamiento humano, lo que hace imposible determinar con plena exactitud la demanda futura.

Cada red eléctrica está localizada en una región geográfica diferente, lo que conlleva diferente clima, población y cultura. Por lo que diferentes redes eléctricas se ven influenciadas por las variables predictoras de forma diferente. Las diferencias nacionales, junto los diferentes enfoques de los investigadores, derivan en la obtención de modelos predictivos diferentes, pero cada siendo uno válido para su red y propósito. Para abordar esta incongruencia, López et al. [2] desarrollaron un método para evaluar la predictibilidad de diferentes registros de demanda, con lo que plantea una base de evaluación de diferentes modelos en diferentes redes eléctricas.

Una vez entendida la función de la predicción de demanda eléctrica y las dificultades que conlleva, conviene definir y diferenciar varios términos para prevenir confusiones más adelante.

Modelo predictivo: procedimiento matemático que obtiene la demanda predicha a partir de un conjunto de variables predictoras, que sirven de entrada. Un modelo predictivo se puede resumir en un sistema de ecuaciones o un algoritmo que parte de unos datos de entrada, para obtener un valor o conjuntos de valores de demanda predicha.

Preprocesado: el procedimiento que transforma unas variables predictoras de entrada en otras, que alimentarán el modelo predictivo para mejorar su precisión. Cabe destacar que modelo y preprocesado son dos elementos independientes, de modo que un mismo modelo puede emplear diferentes métodos de preprocesado.

Sistema predictivo: el conjunto de elementos, que al trabajar permiten obtener predicciones a partir de datos crudos. Un sistema se compone de modelos predictivos, preprocesados, técnicas y horarios en los que se ejecutarán los cálculos.

Momento de ejecución: instante en el que el sistema predictivo realiza los cálculos para obtener una o más previsiones. Se suele determinar como una hora del día; pero si un sistema predictivo trabaja en intervalos de cuartos de hora, se definirá con uno de los 96 de los cuartos de hora del día.

Momento previsto: momento futuro cuya demanda es prevista por el sistema predictivo. Para definirlo completamente es necesario especificar qué hora del día se prevé de qué día futuro.

1.1.2 Métricas de evaluación

A la hora de evaluar un sistema predictivo se pueden considerar diferentes factores para evaluar su rendimiento: el tiempo de ejecución y el error. Dado un ordenador y un sistema, el tiempo de ejecución es el intervalo requerido para obtener los resultados predictivos. Para comparar dicho tiempo entre diferentes sistemas, se debe emplear el mismo ordenador para asegurar la igualdad de condiciones. Aunque la velocidad de cálculo no tenga tanta atención como la precisión, existen algunos estudios cuyo objetivo es mejorarla para un sistema predictivo dado, como McIlvenna et al. [3], que aplicaron un método de relajación de variables para acelerar computacionalmente un sistema.

El error es el principal factor para tener en cuenta, por lo que se suele medir con diferentes métricas el cometido con registros históricos previos. Algunos ejemplos donde se evalúan sistemas predictivos son [4]–[10]. Aunque esta evaluación es indispensable a la hora de evaluar cualquier sistema o modelo, debido al impacto directo del error en las planificaciones del operador. Cada métrica interpreta el error de forma diferente, por lo que conviene elegir la métrica según la aplicación del sistema predictivo. La ecuación (1) representa el MAPE (*Mean Absolute Percentage Error*), la ecuación (2) el MAE (*Mean Absolute Error*), la (3) el RMSE (*Root Mean Square Error*), la (4) el RRMSE (RMSE relativo) y las (5) y (6) el HR (*Hit Ratio*).

$$MAPE = \frac{100}{n} \sum_{d=1}^{n} \left| \frac{F_d - L_d}{L_d} \right| \qquad (2)$$

Donde F_d es la predicción de demanda consumida durante un intervalo de tiempo d, L_d es la demanda real para el mismo intervalo y n es el número de intervalos evaluados. Como se puede ver, el MAPE es la media del error relativo, por lo que su interpretación es accesible incluso a personas no familiarizadas con el ámbito. Se trata de una de las métricas más empleadas y es útil para comparar proporcionalmente el error cometido por dos sistemas diferentes; aunque como siempre, deben compararse en igualdad de condiciones.

$$MAE = \frac{\sum_{d=1}^{n} |F_d - L_d|}{n} \qquad (2)$$

El MAE refleja el error absoluto medio, es decir, cuánto se desvían las predicciones de media en magnitud de energía. Resulta útil para entender el orden de magnitud de los fallos cometidos.

$$RMSE = \sqrt{\frac{\sum_{d=1}^{n} (F_d - L_d)^2}{n}} \qquad (3)$$

El RMSE está enfocado más al ámbito práctico que al analítico, pues las pérdidas que el operador sufre por el error de las predicciones no son lineales. Las pérdidas económicas

del operador por el error se asemejan a una relación cuadrática, que penaliza más a un patrón de errores variable que a uno continuo.

$$RRMSE = \sqrt{\frac{\sum_{d=1}^{n} \left(\frac{F_d - L_d}{L_d}\right)^2}{n}} \tag{4}$$

El RRMSE es muy similar al RMSE, con la diferencia de estar expresado de forma relativa, por lo que representa el coste que al operador le puede suponer, aunque de forma relativa al orden de magnitud con el que trabaja.

$$HR = \frac{100}{n} \sum_{d=1}^{n} S_d \tag{5}$$

$$S_d = \begin{cases} 0, & \left|\frac{F_d - L_d}{L_d}\right| \geq E \\ 1, & \left|\frac{F_d - L_d}{L_d}\right| < E \end{cases} \tag{6}$$

Donde S se puede interpretar como la serie temporal de aciertos de predicciones, mientras que E es el umbral de acierto, el cual se debe elegir según cuánto error se considera perjudicial para el sistema. El HR estima la probabilidad de que un sistema acierte una predicción por debajo de un umbral de error, por lo que también tiene una connotación práctica, pues puede que al operador sólo le preocupen aquellos fallos que superen cierto umbral.

1.2 Motivación de la tesis

Una vez explicado el contexto, se explica la motivación y utilidad de la tesis que surgen del mismo.

La principal motivación reside en resolver un problema de sistema tecnológico de gran escala, como es la península española. El sistema predictivo de REE, desarrollado por la UMH (Universidad Miguel Hernández), tiene potencial de mejora, que si se aplica a la gestión de la energía peninsular puede suponer un gran ahorro económico y medioambiental.

Al mismo tiempo, se pretende aportar algo nuevo al estado del arte. La cantidad de modelos predictivos desarrollados en la literatura es inmensurable, tal y como Hong et al. denunciaron en su revisión [11]. Por lo que se considera que desarrollar nuevos modelos no aportaría nada similar que se pueda conseguir buscando en la inmensa literatura. En conclusión, desarrollar un modelo diferente queda descartado, queda como opción estudiar otras mejoras para sistemas predictivos. Además, unas mejoras que no dependan del modelo predictivo también pueden ser útiles para otros sistemas predictivos con un modelo ya establecido.

1.3 Problemas planteados

Se plantean dos problemas a resolver, cada uno desarrollado en su respectivo artículo. Por un lado se tiene la transición de sistemas horarios a cuarto-horarios [12] y por otro la gestión de datos de temperatura [13].

1.3.1 Transición de intervalos

Los sistemas predictivos STLF calculan frecuentemente nuevas predicciones para las horas y días futuros, normalmente a cada hora y prediciendo la demanda consumida en intervalos horarios. Los sistemas deben calcular las predicciones dentro de un plazo para que el operador tenga tiempo de leer los datos y comenzar a gestionar sus operaciones. Sin embargo, los sistemas de medida tienden a intervalos cuarto-horarios, de hecho, el artículo 19 de la Comisión de Regulación (EU) 2017/2195 del 23 de noviembre de 2017 ya lo requiere.

Frente a esta necesidad de cambio de intervalos surge un problema doble. Al predecir cuartos de hora en lugar de horas, se deben calcular el cuádruple de valores. Además, se tienen menos de 15 minutos para calcular el intervalo siguiente, por lo que se tiene aproximadamente un cuarto del tiempo. La velocidad de cálculo se debe acelerar aproximadamente 16 veces más para una tarea computacionalmente ya pesada, pues el operador español necesita predecir 19 regiones eléctricas a nivel nacional para obtener su total. Incluso con el sistema horario no se calculaban todas las horas futuras que podía abarcar el sistema, pues predecir una hora nacional cuesta 2,5 segundos en un procesador i7-8700 con 16 GB de RAM.

Previamente ya se tenía un horario que determinaba qué horas futuras se calculaban en cada hora del día. Sin embargo, no resulta viable una transición directa del sistema horario al cuarto-horario con el mismo horario de cálculos, por lo que surge la necesidad de elaborar un horario nuevo que no implique pérdidas de precisión. Al mismo tiempo se exige que este horario se adapte a la potencia computacional disponible, variando así en función de las necesidades de quien utiliza el sistema predictivo.

1.3.2 Gestión de temperaturas

Existe una fuerte relación entre demanda eléctrica y temperatura ambiente [14]–[16], por lo que es habitual utilizarla como variable predictora. Investigadores previos analizaron la relación temperatura-demanda para extraer conclusiones acerca del uso de equipos de climatización [16]–[18], siendo la relación temperatura-demanda un objeto de estudio en diferentes regiones geográficas.

Frente la importancia que las variables térmicas tienen en los sistemas predictivos, se plantea la necesidad de encontrar un método de preprocesado térmico que cumpla tres características: interpretabilidad, para que los resultados del preprocesado puedan ser objeto de estudio; mejor precisión en el sistema de REE que el preprocesado antiguo; y automatización, para que sea fácilmente aplicable a otros sistemas eléctricos.

La automatización de preprocesado térmico también resulta deseable para aplicaciones que pretenden construir sistemas de forma automática sin la intervención de expertos,

como el de Wang et al. que usan auto-sklearn y TPOT [19] o el de Duan et al., que elaboran un algoritmo para elegir un modelo a partir de una librería [20].

1.4 Revisión de la literatura

Esta tesis se centra en el STLF, un campo con décadas de desarrollo con una basta cantidad de publicaciones, tal y como reflejan las revisiones de la literatura [11], [21], [22].

1.4.1 Métodos predictivos

La predicción eléctrica es un ámbito científico con décadas de desarrollo, con miles de publicaciones por parte de investigadores de todo el mundo. Por lo que se han desarrollado modelos predictivos desde múltiples enfoques para adaptarse a diferentes redes eléctricas.

Los métodos predictivos se suelen agrupar en tres categorías de acuerdo con su innovación: estadísticos, inteligencia artificial e híbridos.

Los métodos estadísticos se basan en definir la relación entre demanda y variables predictoras. Algunos ejemplos son: autorregresivo [23], [24], suavizamiento exponencial [25] o ARIMA (*AutoRegressive Integrated Moving Average*) [26]. Los modelos de inteligencia artificial no definen la relación entre demanda y predictores, por el contrario, se entrenan con registros históricos para obtener las relaciones de forma automática, pero no interpretable al ser heurística; posteriormente pueden calcular predicciones en base a los respectivos predictores de entrada. Algunos ejemplos de inteligencia artificial son: redes LSTM (*Long-Short Term Memory*) [27], regresión mediante lógica difusa [28], redes neuronales convolucionales con redes LSTM [29] y redes neuronales con máquina de soporte vectorial [30]. Los métodos híbridos combinan ambos tipos de técnicas en un mismo sistema, como un suavizado exponencial con una red neuronal [31], un modelo SARIMAX (*Seasonal ARIMA eXogenous*) con una red LSTM [32] o un modelo autorregresivo con una red NARX (*Neural AutoRegressive eXogenous*) [33], que es el objeto de estudio principal de esta tesis.

También existen estudios enfocados en el VSTLF, como el de Zhang et al. [34], quienes elaboran un sistema predictivo para la gestión de energía en microgrids. Así como estudios acerca del MTLF, con Han et al. [35] con una red neuronal convolucional y una red LSTM. En LTLF se tiene de ejemplo a Hong et al. [36] al emplear datos de *smart grid* en predicciones de largo plazo.

Weimar et al. [37] demostraron, en Calirfornia, cómo mejoras en la precisión de un sistema predictivo de demanda pueden derivar en ahorros económicos significativos.

1.4.2 Horarios de ejecución

No se tiene constancia de artículos que hayan afrontado el problema de los horarios de ejecución, evaluando las diferentes antelaciones para decidir qué momentos ejecutar los cálculos. En esta sección se muestran algunos trabajos que se relacionan con el

problema planteado, ya sea porque han abordado un problema similar, o bien porque no lo han planteado y se podrían beneficiar en trabajos futuros.

Jiang et al. [38] evaluaron diferentes modelos predictivos de STLF, teniendo en cuenta error y tiempos de cómputo. Incluso consideraron diferentes antelaciones para evaluar los modelos. Sin embargo, compararon el rendimiento entre modelos completos, no entre antelaciones de un mismo modelo, requisito indispensable para elaborar un horario de ejecuciones.

Mohammed et al. [39] evaluaron un modelo de suavizado exponencial, una red neuronal y uno híbrido (combinando ambos). Sin embargo, evaluaron los modelos por separado, sin considerar tampoco los diferentes momentos de ejecución. Veljanovski et al. [40] emplearon una red neuronal, junto los datos semanales de temperatura y tipo de día, para predecir con un día de antelación la demanda; tampoco evaluaron diferentes antelaciones para analizar la evolución de la precisión.

Weyermüller et al. [41] construyeron un modelo de inferencia difuso neuronal adaptativo, que utiliza la demanda previa, el día de la semana y el mes del año como entradas. Pronostica con 24 horas de antelación, por lo que la investigación de la que parte esta tesis [12] podría aplicarse para organizar el horario de cálculo, para ello bastaría con agregar más horas de pronóstico al modelo. Sin embargo el trabajo mencionado [41] es sólo un ejemplo de sistema predictivo al cual se le puede aplicar el estudio de horarios de ejecución [12], pues también se puede estudiar su implementación en cualquier sistema que compute predicciones a lo largo del día.

El enfoque de mejora computacional se suele centrar en disminuir la carga computacional a la hora de generar predicciones, como es el caso de McIlvenna et al. [3] en su cambio de variables.

También se propone implementar la obtención de horarios en trabajos que no saltan del ámbito académico al industrial; como Panapongpakorn et al. [42] que elaboran un sistema híbrido de redes neuronales y series temporales, pero no predicen más allá de los 30 minutos. Otro ejemplo es el de Shuai et al. [43], que construye un modelo de máquina de soporte vectorial de mínimos cuadrados, aunque no dan el paso de trasladarlo a un sistema predictivo en ese artículo.

Tampoco se tiene constancia de trabajos que aborden el problema en otros campos que empleen predicciones de series temporales. Un ejemplo es el trabajo de Clements et al. [44], quienes predicen el ratio de desempleo con un conjunto de modelos; los evalúan mediante ocho dicotomías o factores planteados, junto un método de Monte Carlo, sin embargo evalúan modelos completos sin entrar en la evolución de las ejecuciones previas.

Zhou et al. [45] evaluaron diferentes métodos predictivos de precio del petróleo, con una comparativa multidimensional. Cheng et al. [46] evaluaron modelos predictivos de riadas, con un coeficiente de eficiencia y otro de persistencia. Benavides et al. [47] compararon modelos para el ratio de cambio entre el dólar estadounidense y el peso mejicano, con el error medio cuadrático y la varianza como indicadores con datos

intradiarios. Pereira [48] puso a prueba varios métodos predictivos de demanda de transfusiones de sangre en un hospital; como indicadores usó la bondad de ajuste, la tasa de cobertura y la tasa de desactualización. Los trabajos mencionados se enfrentan al problema de evaluar diferentes modelos predictivos con diferentes métricas, pero no evalúan diferentes antelaciones de un mismo modelo, sino conjuntos de predicciones de modelos completos para seleccionar el mejor candidato.

1.4.3 Gestión de temperaturas

A la hora de predecir demanda eléctrica, elegir y procesar las variables de entrada que recibirá el modelo es una tarea tan importante como elegir el propio modelo. Por lo que otros investigadores han trabajado en procesar la temperatura con el fin de generar predicciones precisas. Ruzic et al. [49] predijeron la demanda con un modelo regresivo cuyos coeficientes de temperatura se actualizan según datos previos similares, usando la distancia euclídea como métrica de similitud.

La lógica difusa también ha sido empleada como método de preprocesado térmico por parte de Zhichao et al. [50], permitiendo que un modelo LSTM se adapte al clima sin alterar significativamente su precisión. El efecto isla de calor fue tenido en cuenta por Wang et al. [14], junto las temperaturas de días previos para alimentar a una red neuronal Elman; sin embargo los datos satelitales son raramente accesibles en el ámbito de la predicción de demanda. El trabajo de Rajbhandari et al. [15] desarrolla un modelo predictivo neuronal que usa temperatura actual y de días previos, así como el tipo de día, hora y mes del año. Además, analizan la sensibilidad demanda/temperatura diferenciando entre días cálidos y fríos, con lo que diferencian el uso entre equipos de calefacción y de refrigeración.

Otros trabajos [14], [49], [50] han empleado las variables climáticas para incrementar la precisión de sistemas predictivos, pero dejando de lado la interpretabilidad de dichas variables durante el preprocesamiento. Por el contrario, otros artículos se centran en la relación temperatura/demanda como el de Tung et al. [16], quienes extrajeron la correlación mediante un modelo de regresión lineal, analizando su evolución a lo largo del año. Shi et al [17] analizaron la relación temperatura/demanda empleando dos ecuaciones lineales, una para las temperaturas que superen un umbral y otra para las que no, por lo que no se contempla un rango de temperaturas templado. La relación temperatura/demanda puede llevar a conclusiones socio-económicas, como es el caso de Anderson et al. [18], quienes infieren en la demanda de bombas de calor del Reino Unido según las bajas temperaturas.

En España, previamente al trabajo base de la tesis [13], Moral-Carcedo et al. [1] desarrollaron un modelo que usa la temperatura diferenciada y la luz solar como entradas para cada hora del día. Se trata de un modelo de regresión con suave transición de doble umbral, que permite distinguir la sensibilidad demanda/temperatura según los periodos de actividad o descanso económico. De modo que el enfoque del trabajo es analítico más que predictivo, preprocesando la temperatura con una función polinomial de tercer grado frente a la demanda logarítmica.

A la hora de buscar alternativas en el preprocesado de temperaturas, se plantea un problema de reducción dimensional, pues se parte de 28 estaciones meteorológicas con datos muy similares entre sí debido a su cercanía geográfica. Existen múltiples técnicas de reducción dimensional, como el análisis de componentes principales aplicado por Bao et al. [51], así como la descomposición en valores singulares por Wang et al. [52], sin embargo proyectan los datos sobre un espacio vectorial carente de interpretabilidad al tratar de maximizar la varianza en dimensiones.

Por el contrario, en el trabajo base [13], la temperatura se procesa de una forma con interpretabilidad directa, linealizándola mediante tres funciones rectas según el rango de temperaturas. Además, el sistema trabaja con un modelo para cada hora de ejecución, por lo que implícitamente también tiene en cuenta los ciclos diarios, incluso también tiene en cuenta indirectamente la luz solar al combinarse con el mes como dato de entrada. Incluso las 54 variables que definen el tipo de día refuerzan la información de la actividad económica.

1.4.4 Automatización

Ya en 1997 existía el concepto de automatización en sistemas predictivos de demanda eléctrica, como el caso de Hyde et al. [53] y su sistema regresivo con la predicciones y entrenamientos periódicos automatizados. Incluso tenía un sistema de eliminación de datos atípicamente extremos.

Hoy en día la automatización sigue siendo un término perseguido en el ámbito. Antoja et al. [54] elaboraron otro sistema automático incluyendo una interfaz gráfica de usuario, aunque la automatización ya ha ido un paso más allá y existen proyectos de construcción automática de modelos predictivos para usuarios poco experimentados. Auto-Sklearn y TPOT son librerías de Python que generan modelos de inteligencia artificial, un ejemplo de su aplicación en el ámbito es la predicción de consumo por parte de electrodomésticos en un hogar y unas oficinas, tal y como hicieron [19] et al. También existe la posibilidad de trabajar en un punto medio, partiendo de una librería de modelos y eligiendo el más apto con un proceso de automático. Duan et al. [20] lo hicieron mediante un proceso semi-Markov y una cadena de Markov oculta.

1.5 Contribuciones

Ambos estudios base de esta tesis [12], [13] han probado sus técnicas en el sistema predictivo de REE [33] mejorando su rendimiento, con lo que se contribuye directamente a la mejora de dicho sistema. Las mejoras desarrolladas no dependen del modelo predictivo, por lo que también son aplicables a otros sistemas diferentes. Por lo que indirectamente se contribuye a la amplia variedad de sistemas predictivos ya disponibles. Ambos estudios también contribuyen a la automatización de construcción de sistemas predictivos, una ambición perseguida por otros investigadores, incluso de otras ramas como la econometría con Liu et al. [55].

Para predecir la demanda de la península española, el anterior sistema de REE disponía de datos de temperatura de 28 estaciones meteorológicas, de las que se utilizaban 5. Las estaciones fueron elegidas mediante un estudio previo, siguiendo criterios

demográficos y climatológicos de las regiones españolas. En consecuencia, el sistema anterior no estaba construido de forma repetible, tampoco tenía una forma interpretable de procesar las temperaturas, pues algunos coeficientes de los modelos autorregresivos tenían signos opuestos, lo que compensa unos efectos respecto otros y dificulta su lectura. Además, tenía 30 variables para representar las temperaturas del día pronosticado y los dos anteriores, lo que, como se muestra en esta tesis, es una cantidad innecesaria.

La nueva construcción de variables térmicas [13] determina cuantas estaciones meteorológicas usar, cuales y cuantos días previos se deben tener en cuenta. Para ello emplea cuatro nuevos tipos de variable: temperatura media de las estaciones seleccionadas, promedios de temperatura de días anteriores, temperaturas individuales de las estaciones elegidas y temperaturas individuales de días anteriores. Estas nuevas variables, aportan mejor precisión e interpretabilidad que el sistema antiguo de REE de acuerdo con los ensayos experimentales.

Por otra parte, el estudio mencionado [12] ofrece una métrica para evaluar las predicciones más útiles que se pueden calcular, para así poder decidir cuáles computar en cada momento y optimizar el reducido tiempo disponible. Dicha métrica sirve como base para un algoritmo que calcula el horario óptimo a partir de un sistema predictivo y un límite computacional. Además, se ha analizado el horario obtenido en REE, obteniendo conclusiones sobre la relación entre la información que llega al sistema y la incertidumbre de horas futuras. Dado que el algoritmo no depende del modelo predictivo, la obtención de horarios y su respectivo análisis es aplicable a otros sistemas predictivos.

Cabe recordar que la presente tesis no pretende aportar un nuevo modelo predictivo, sino unas mejoras para sistemas predictivos. Pues los trabajos realizados no modifican el modelo empleado, sólo lo usan como objeto de estudio alterando el resto del sistema.

2. Sistema predictivo de REE

En este apartado se explica el sistema predictivo original de REE, que ha servido como objeto de estudio. No incluye las modificaciones que plantean los estudios en base a esta tesis [12], [13].

El sistema STLF implementado en REE [33] fue desarrollado por la UMH. Tras su implementación, se ha seguido trabajando en mejoras y análisis [56]–[58] gracias a proyectos de colaboración con la propia REE. Este sistema se considera como una referencia de estudio adecuada por permanecer como principal predictor durante más de cinco años, a pesar de que REE estuviese abierto a nuevas alternativas.

Se trata de un sistema híbrido compuesto por un modelo autorregresivo y una red NARX, cuyos resultados se ponderan y suman para obtener una predicción más precisa que cualquiera de ambas. Es capaz de predecir desde la hora siguiente hasta las 24:00 del noveno día posterior.

De forma resumida, los datos de entrada que alimentan los modelos son los siguientes:

- Demanda media de las 52 semanas anteriores.
- Predicciones de temperatura para el día actual y los próximos nueve días.
- Demanda peninsular de la última hora disponible.
- Información del tipo de día.

La salida es la demanda eléctrica pronosticada para una hora de uno de los siguientes nueve días o el actual. Para obtener varias horas pronosticadas, se entrenan tantos modelos diferentes como horas se deseen prever. De modo que todos los modelos tienen la misma definición matemática, pero sus coeficientes obtenidos son diferentes, pues se entrenan con sus respectivos datos de entrada y salida.

Cada hora de ejecución dispone de diferentes datos de entrada, pues los datos disponibles se actualizan a cada momento. La temperatura disponible también varía, pues las predicciones se actualizan cada día a las 9:00 de la mañana. En consecuencia, cada hora de ejecución debe disponer de su propio conjunto de modelos para predecir las horas futuras. Por ejemplo, para predecir las 17:00 del día siguiente ejecutando a las 11:00, se usará un modelo diferente que al ejecutar a las 14:00.

2.1 Datos de entrada

Los datos de temperatura son provistos por AEMET (Agencia Estatal de Meteorología), siendo información pública disponible en su página web https://opendata.aemet.es. Las temperaturas se componen de mediciones y pronósticos que abarcan de uno a nueve días de antelación, teniendo dos valores para cada día: temperatura máxima y mínima.

El tipo de día distingue diferentes festivos nacionales y regionales incluyendo Navidad, días laborables, días anteriores y posteriores al cambio de hora, mes del año y semana de agosto. El día se define con 54 variables, López et al. desarrollaron esta construcción

de variables mediante un estudio previo [56]. Para obtener las variables que definen el día, se parte de la información de festivos que publica el BOE (Boletín Oficial del Estado).

REE proporciona los registros de demanda histórica, siendo también datos públicos disponibles en su respectiva página web https://www.esios.ree.es/es/analisis/1293?compare_indicators=545,544&start_date=10-07-2021T00:00&geoids=.

La hora que se prevé también es intrínsecamente una variable de entrada al sistema, pues hace que los modelos empleados varíen.

Los conjuntos datos se clasifican en tres tipos según su propósito: entrenamiento, validación y test. Los datos de entrenamiento se utilizan para calcular los coeficientes internos de los modelos predictivos. Por otra parte, algunos datos de entrada no se aplican directamente a los modelos, sino que se procesan previamente mediante coeficientes llamados hiperparámetros. Los datos de validación se utilizan para probar y corregir estos hiperparámetros después de entrenar modelos. Los datos de test se utilizan para poner a prueba y valorar modelos entrenados. El conjunto de datos de test debe ser independiente y no tener ninguna coincidencia con los otros conjuntos de datos para garantizar la generalización; de lo contrario, las pruebas realizadas estarán fuertemente sesgadas para unos datos concretos.

REE actualiza sus modelos al comienzo de cada año, entrenándolos de nuevo con los últimos 7 años de prueba. Por lo que el operador no requiere de datos de validación y prueba, pues estas denominaciones se usan normalmente en ámbitos experimentales.

2.2 Modelos

2.2.1 Combinación

La predicción combinada es el valor final que obtendrá el operador o usuario del sistema predictivo. Se obtiene de una media ponderada de las predicciones de ambos modelos, tal y como expresa la ecuación (7).

$$F = F_{NARX} \cdot k + F_{AR} \cdot (1 - k) \tag{7}$$

Donde F es la predicción combinada, F_{NARX} es el resultado del método predictivo NARX, F_{AR} es el resultado predictivo AR y k es el coeficiente de ponderación, cuyo valor se restringe entre 0 y 1. El coeficiente k se calcula minimizando el MAPE de los últimos 30 días a partir de la misma ecuación (7).

2.2.2 Autorregresivo

El modelo autorregresivo se puede representar con la ecuación (8).

$$\ln(F_h) = \sum_{k=1}^{n} X_{k\,h}\,\delta_k + \sum_{i=1}^{d} E_i\,\omega_i + \varepsilon_h \tag{8}$$

Donde F_h es la demanda prevista para la hora h, $X_{k\,h}$ es la variable exógena de entrada k para predecir la hora h, n es el número de variables exógenas, δ_k es su respectivo coeficiente, E_i es el error cometido en la misma hora hace i días, ω_i es su respectivo coeficiente, d es el número de días previos que se tienen en cuenta y ε es un valor aleatorio de distribución gaussiana con media cero.

Nótese que un modelo autorregresivo debe incluir, por definición, los valores previos como entrada. La ecuación (8) lo hace, pero implícitamente como error E, pues este es la diferencia entre el valor real y el predicho previamente.

Los coeficientes ω y δ se consiguen mediante un entrenamiento de máxima verosimilitud, mientras que el parámetro d se obtuvo empíricamente resultando un valor de 7 días.

2.2.3 NARX

En el sistema de REE, cada modelo NARX se compone de 10 redes NARX que generan su predicción por separado, después el mayor y el menor valor se descartan para hacer la media con los 8 restantes. La media resultante es el valor predictivo del modelo.

Cada red NARX se compone de una red neuronal retroalimentada, es decir, incluyendo en su entrada un número de salidas previas, tal y como muestra la Figura 1.
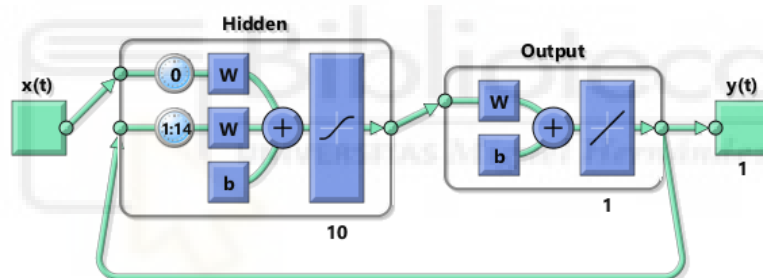

Figura 1. Esquema NARX

En la figura se pueden observar dos capas de redes neuronales: *Hidden* y *Output*. La primera se compone de 10 neuronas, de modo que para cada predicción t, cada neurona multiplica cada valor del vector de entradas $X(t)$ por un peso, luego cada neurona suma los valores más un *bias*, finalmente aplica una función de activación para otorgar el resultado como salida. El proceso que sigue una neurona en una red neuronal típica se refleja en la ecuación (9).

$$S(t) = f\left(b + \sum_{k=1}^{n} W_k\, X(t)_k \right) \tag{9}$$

Donde $S(t)$ es el valor resultante de la neurona para un instante t, f es la función de activación, b es el bias, W_k es el peso para la variable k, n es el número de variables y $X(t)_k$ es la variable de entrada k para el instante t.

En el caso de la capa *Hidden* de la red NARX, también se tiene como entrada los 14 valores previos de salida, que se tratan como si fueran otras 14 entradas $X(t)_k$. La función

de activación puede variar según la red, en este caso es la tangente hiperbólica con entrada *x* y salida *f(x)* de la ecuación (10).

$$f(x) = \frac{e^x - e^{-x}}{e^x + e^{-x}}$$

(10)

Las 10 salidas de la capa *Hidden* pasan luego a la capa *Output*, que tiene sólo una neurona y por consiguiente una salida. Esta capa tiene como función de activación una conexión directa como refleja la ecuación (11).

$$f(x) = x$$

(11)

El entrenamiento es el proceso mediante el cual se obtienen los pesos y *bias* a partir de registros históricos. Durante el entrenamiento, el algoritmo empleado es el Levenberg-Marquardt implementado en Matlab, de forma que el bucle permanece abierto con entradas reales sustituyendo la retroalimentación. El número de neuronas, el desfase de retroalimentación y el número de redes por modelo se obtuvo de forma empírica sopesando precisión y coste computacional.

El motivo por el cual se usan múltiples redes por modelos reside en la naturaleza estocástica de las redes. Cuando se inicia el entrenamiento, los valores internos son aleatorios, por lo que el resultado final varía imprevisiblemente con cada entrenamiento. Para minimizar el efecto aleatorio se hace la media con varias redes, que en conjunto tienen un comportamiento más estable, sobre todo si se descartan valores extremos que tienen mayor riesgo de ser anómalos.

2.3 Horario

Al comenzar la investigación de horarios de ejecución [12] REE empleaba el representado en la Tabla 1, la cual muestra las horas previstas para cada tiempo de ejecución. Cada celda de la tabla contiene las horas futuras del día a pronosticar, de modo que el 0 corresponde al intervalo de tiempo entre las 0:00 a.m. y la 1:00 a.m. Las filas indican la hora del día en que se ejecuta el sistema y las columnas indican el día de previsión futuro, además los guiones indican la predicción de los intervalos intermedios. Existe la posibilidad de predecir la hora actual, ya que sigue siendo útil para el operador durante los primeros 10 minutos de la misma hora. Por ejemplo, en el tiempo de ejecución 0:00, en la primera fila de la subtabla (a), sólo se pronostica el noveno día siguiente. Otro ejemplo es el de las 9:00 en la subtabla (a), se pronostican todos los días siguientes excepto el segundo, también se pronostica el día actual desde las 9:00 hasta las 23:00 (todo el resto del día).

Tabla 1. *Horario de ejecución antiguo de REE.*

(a)						(b)					
Run Time	Future Day Whose Load Is Forecast					Run Time	Future Day Whose Load Is Forecast				
	Current Day	1	2	3–8	9		Current Day	1	2	3–8	9
0					0–23	12	12–23				
1						13	13–23	0–23			
2						14	14–23				
3	3–23					15	15–23				
4						16	16–23				
5	5–23	0–23	0–23			17	17–23	0–23	0–23		
6						18	18–23				
7	7–23	0–23				19	19–23				
8	8–23	0–23	0–23			20	20–23				
9	9–23	0–23		0–23	0–23	21	21–23	0–23			
10	10–23					22	22–23				
11	11–23	0–23				23	23	0–23			

(a) Horario de 0:00 a 12:00. (b) Horario de 12:00 a 24:00.

Este horario no se decidió a partir de un análisis formal. Sin embargo, se tuvo en cuenta que todos los días a las 9:00 se recibían los datos de temperatura de AEMET. Al disponer de información actualizada se ejecutaban la mayoría de predicciones, pues se presupuso que serían más precisas.

2.4 Preprocesado de temperaturas

La relación entre la temperatura y la demanda no es lineal, lo cual queda reflejado en estudios previos [16], [59], [60]. Además, entender cómo influye en la temperatura es crucial para minimizar el error debido a su incertidumbre [61].

Esa relación no lineal se resume de forma intuitiva con la siguiente relación causa-efecto: cuando las temperaturas son bajas, la gente usa los equipos de calefacción y cuando son frías usa los equipos de aire acondicionado, mientras que en rangos intermedios la temperatura no afecta. Este enfoque es el que tiene el sistema predictivo de REE en su preprocesado térmico, el cual divide el espectro térmico en tres rangos: frío, templado y caliente, de modo que los tres rangos se separan con dos umbrales.

Cuando la temperatura de una zona *z* desciende por debajo del umbral de temperaturas frías, se calcula la diferencia entre la temperatura y dicho umbral, con lo que ya se obtiene una variable de entrada llamada CD_z reflejada en la ecuación (12).

$$CD_z = \begin{cases} 0, & T_z \geq Thc_z \\ Thc_z - T_z, & T_z < Thc_z \end{cases} \tag{12}$$

Donde Thc_z es el umbral de temperaturas frías para la zona *z* y T_z es la temperatura media de la zona *z*. De forma análoga se obtiene la variable HD_z para temperaturas cálidas de acuerdo con la ecuación (13), siendo Thh_z el umbral de temperaturas cálidas.

$$HD_z = \begin{cases} 0, & T_z \leq Thh_z \\ T_z - Thh_z, & T_z > Thh_z \end{cases} \tag{13}$$

Ambas ecuaciones se aplican a 5 regiones de la península española definidas por la localización de estaciones meteorológicas. Se realizó una evaluación demográfica para decidir qué estaciones emplear. También se aplica ambas ecuaciones a las temperaturas de los dos días previos al que se predice, por lo que se tiene 6 variables por cada zona con un total de 30 variables térmicas.

3. Obtención de horario de ejecuciones

3.1 Primer enfoque

El artículo de horarios [12] se enfrentó, con un primer enfoque en el estado del arte, a la toma de decisiones para determinar qué horas futuras se calculan en cada momento. Por lo que fue necesario establecer una métrica que defina la utilidad de las predicciones, de modo que en cada momento del día se calculen las más útiles.

Con lo que surge una cuestión ¿Qué hace que una predicción sea útil? Dado que el operador de red busca maximizar precisión en todo momento, una predicción le resulta útil de acuerdo con la reducción de error que le proporciona. Pues ejecuta predicciones repetidamente a medida que el momento predicho se aproxima en el tiempo.

La intuición dice que a medida que se aproxima el momento que se prevé, el error desciende debido a que la información disponible está más próxima. Sin embargo, tal y como muestra la Figura 2, esa tendencia no siempre se cumple en cortos intervalos de tiempo.
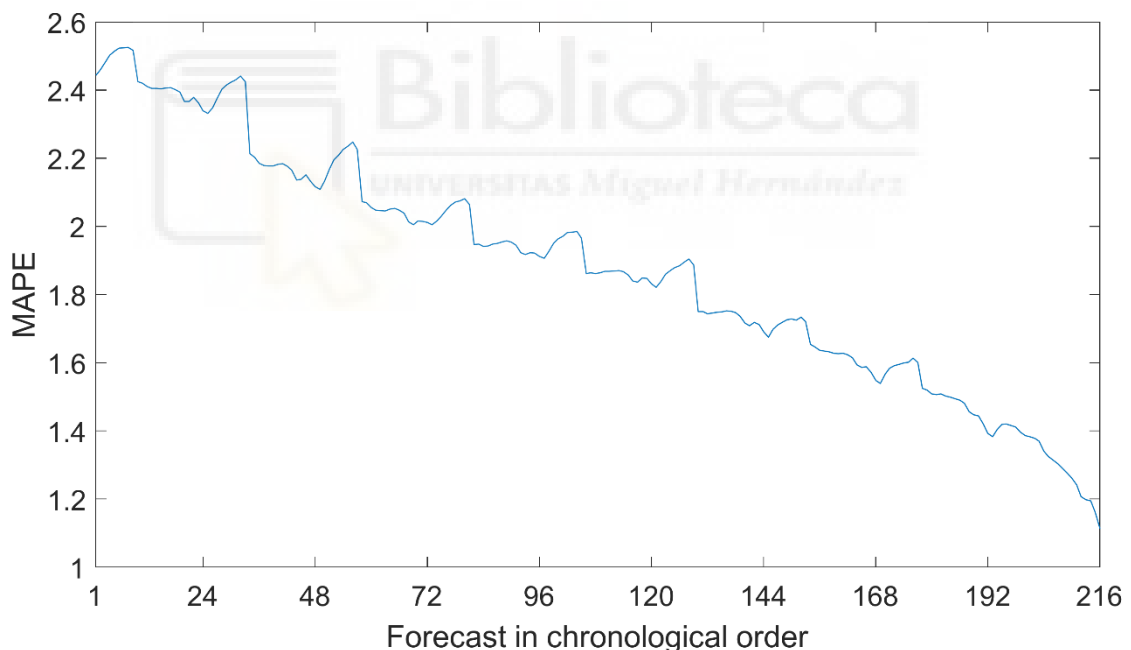

Figura 2. *Error de modelo autorregresivo en 2019*

Se pueden apreciar picos de subida contraproducentes. Si en esos picos no se realizasen cálculos predictivos y se emplease las predicciones anteriores, no se tendría esos incrementos locales de error, mejorando la precisión y ahorrando cálculos al sistema.

Al predecir una demanda *L* de un intervalo de tiempo específico, ejecutando los cálculos en diferentes momentos, se tiene una serie temporal P_t de predicciones, siendo *t* el momento en el que se calcula la ejecución. Con lo que se puede definir la utilidad de las predicciones como una serie temporal llamada *AIE* (*Accuracy Improvement Expectation*) en la ecuación (14).

$$\text{AIE}_t = 100 \left| \frac{P_{t-1} - L}{L} \right| - 100 \left| \frac{P_t - L}{L} \right| \qquad (14)$$

La variable *AIE* es la métrica de utilidad del estudio [12]. Se puede interpretar como la diferencia de dos MAPEs: el de la predicción anterior y el de la predicción actual. Ambos errores se multiplican por 100 para mostrar esa interpretabilidad. Si *AIE* resulta positivo, indica que la predicción actual es útil al ejecutarla para disminuir el error; si resulta negativo, indica que no vale la pena ejecutar la predicción actual.

Sin embargo, aplicar el *AIE* para decidir si vale la pena ejecutar una predicción no es una tarea directamente aplicable a un sistema predictivo en marcha, pues no se conoce la demanda real futura *L*. Sin embargo, sí que es posible estimar ambos errores en base a registros históricos del año pasado. Dicha estimación se realiza mediante el mismo algoritmo que elabora el horario de ejecuciones, explicado en el propio artículo [12].

3.2 Metodología experimental

Para entender el algoritmo, primero hay que localizarlo en el contexto reflejado en la Figura 3. El algoritmo tiene en cuenta el máximo número de predicciones que se puede obtener según las restricciones computacionales, de modo que devuelve un horario que no sobrepasa ese límite en ninguna hora del día. Para estimar los errores de las predicciones, emplea los registros históricos de error del año pasado, lo que hace que sea adaptable a cualquier base de datos.
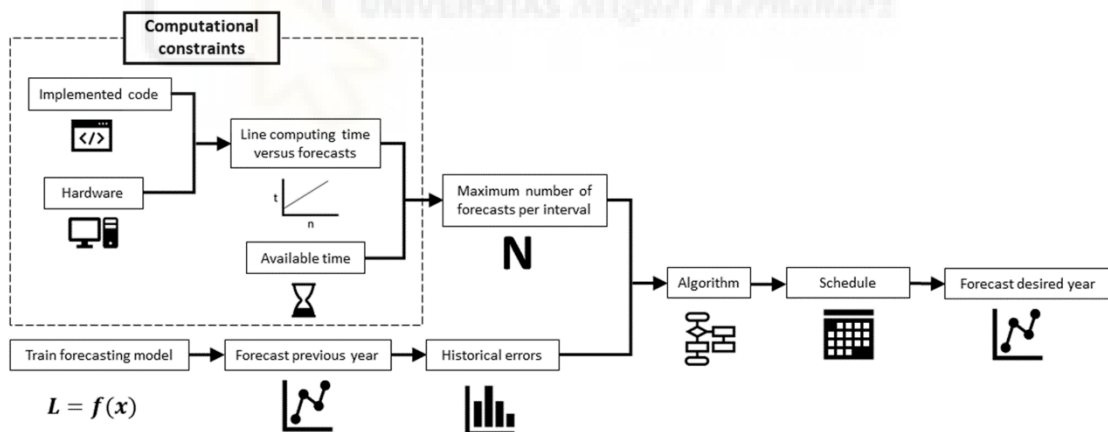

Figura 3. *Resumen de la metodología de obtención de horarios*

El número máximo de predicciones *N* de la figura depende de dos factores. Uno es el tiempo de cálculo disponible, que depende del ritmo al que trabaja el sistema predictivo. El otro factor es la velocidad de cálculo del sistema predictivo, que depende de la eficiencia del código de programación y el *hardware* que lo ejecuta.

El algoritmo primero registra los errores históricos, para ello calcula la media del MAPE de todas las anticipaciones para cada momento de ejecución. Luego ejecuta una simulación de ejecución del sistema predictivo. Dado que se desea elaborar un horario para un año futuro, no se disponen de los errores reales, por lo que en la simulación sólo se tiene en cuenta los registros de error. La simulación consiste en iterar cada momento

de ejecución para cada día del año a predecir, de manera que en cada momento de ejecución se compara el MAPE de las predicciones calculadas con el MAPE de las que se podrían calcular. Posteriormente elige las *N* predicciones que más reduzcan el MAPE estimado, registrando en memoria dicho MAPE para volver a comparar en los siguientes momentos de ejecución. El resultado de cada iteración es una lista de las *N* horas futuras cuya demanda se predice, así como los registros de sus respectivos MAPEs estimados.

En muchas ocasiones de la simulación, se tienen predicciones que no se han calculado. Esas ocasiones son las primeras horas del año y la primera de cada día; pues al comenzar un nuevo día, el noveno día posterior entra dentro del horizonte predictivo. Aquellas predicciones que se pueden ejecutar por primera vez, se consideran de utilidad infinita, pues permiten salir de un estado de nula información. Por lo tanto, las predicciones primerizas se elegirán primero, priorizando las más cercanas al momento de ejecución. En las simulaciones se observó que el horario de ejecuciones se estabiliza en torno al segundo o tercer día del año, por lo que no es necesario simular un año completo.

En el caso del sistema predictivo de REE, en un procesador i7-8700 con 16GB de memoria RAM, se tarda 0,633 segundos en iniciar los cálculos y 0,134 en obtener cada hora futura. También hay que tener en cuenta que se tiene un total de 240 horas futuras como horizonte. Además, se calculan 19 regiones eléctricas para obtener la demanda peninsular, con lo que se tiene un total de 4560 posibles valores a predecir y ascendiendo el tiempo total de ejecución a más de 10 minutos; lo que resulta para trabajar con intervalos cuarto-horarios que requieren menos de 7 minutos por exigencias de REE. Para tardar menos de 7 minutos se deben calcular menos de 3140 valores totales, que al dividir por 19 se tienen 165 para cada región eléctrica, siendo éste el límite *N* del sistema.

Sin embargo, que el ordenador permita ejecutar 165 cálculos por intervalo no es razón suficiente para elegir dicho número. Existe la posibilidad de que el límite computacional no se corresponda con el número óptimo de cálculos, algo que ocurre al analizar la curva de precisión frente al número de predicciones límite en la Figura 4.
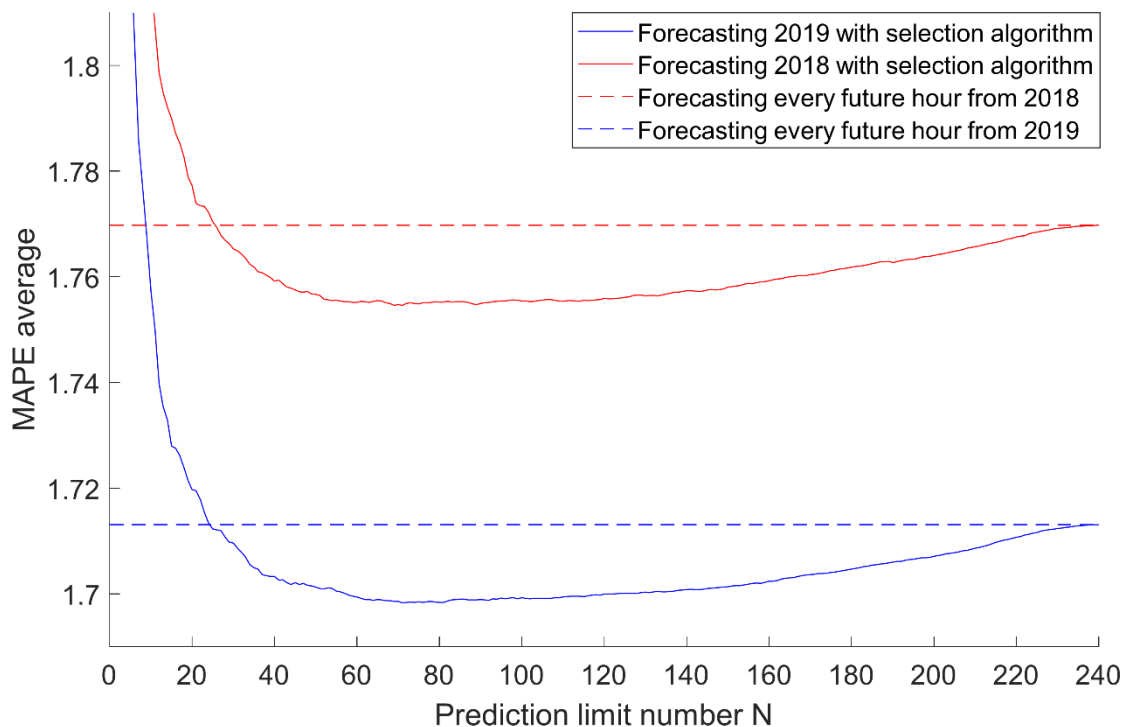
Figura 4. *Precisión del sistema predictivo en 2018 y 2019 al aplicar el algoritmo*

La curva se calculó aplicando el algoritmo con todos los posibles valores de *N*. Las rectas discontinuas muestran el valor con *N* máximo. Se puede observar que hay un intervalo de precisión muy parecido para ambos años entre 60 y 140 predicciones, teniendo el mínimo para 2018 en 71. Por lo que 71 es el número de predicciones límite elegido para ejecutar el algoritmo, en lugar de 165 que muestra mayor error en sus registros históricos (con la curva de 2018).

3.4 Resultados

Una vez obtenido el valor de *N* con el límite computacional y simulaciones del año previo, se ejecutó el algoritmo con un valor de 71 para *N* obteniendo la Tabla 2, que se lee del mismo modo que la Tabla 1. Sin embargo, la tabla 2 resulta visualmente más caótica debido a que muchas predicciones futuras no están encadenadas y quedan sueltas reflejando muchos números por celda. Un ejemplo de lectura es la hora de ejecución 19 (7:00 p.m.), para el segundo día futuro, las horas previstas son 12, 14, 16, 17, 18, 19 y 21; es decir, los períodos comprendidos entre las 12:00 y las 13:00 horas, entre las 14:00 y las 15:00 y entre las 16:00 y las 22:00.

Tabla 2. *Horario de ejecuciones para 2019 con N=71*

Run Time	Current Day	1	2	3	4	5	6	7	8	9
0	0–1, 5, 9, 23	0, 18, 22	2–5, 10, 14, 16–18, 22–23	1, 10, 19, 21–23	4, 18, 22	2, 4, 13, 16, 22	11, 14, 22–23	2, 19–20, 23	2, 7, 12, 16, 22–23	0–23
1	1–5, 7, 22	1–2, 5–6, 9, 11, 23	0, 2–3, 7–8, 18–19	0–1, 4, 10, 17	0–4, 15, 18, 21	0, 3, 6–7, 11	0, 9, 19–20, 23	3, 5, 11–12, 15, 21	0, 3, 12, 14, 19	0–5, 7–8, 10–11, 13–14, 16–17, 19, 22
2	2–6, 8, 10, 13–14, 22	0–1, 6–7, 10–11, 17–18	2, 7, 10, 19, 21	1–2, 10, 12, 15, 18–19, 22	2–3, 12–13, 15, 18, 21	5, 10, 12–14, 18, 23	10, 12, 14	0, 4, 7, 11–12, 18, 21	0, 3, 12–13	0, 5–6, 9–14, 17, 19, 22
3	3–7, 9, 12–13, 18, 20	1–4, 6–7, 10, 12, 21	0, 6–7, 11, 18–19, 23	4, 8, 10, 13–14, 18–20	2–3, 13–14, 17–18, 22	3, 12, 15, 18	0, 2, 13, 19, 22–23	0, 11, 13, 23	0, 3, 11–14, 23	2–4, 9, 13–15, 18, 22
4	4–7, 10, 14, 16, 19, 22	1–6, 8, 10, 13, 18–19	1, 4, 7, 10, 15, 18–19, 21, 23	2–4, 7, 10, 12–13, 19	0, 2–3, 5, 17–18, 22	3, 10, 13, 15	11–12, 14–15, 17, 19, 23	0, 10, 12, 16, 18, 22	3, 12, 18	4, 10–12, 14, 18, 23
5	5–8, 12, 14, 16–17, 20–21	2, 4–5, 7, 17, 19	2, 5, 7, 10–11, 17, 21	7, 12–15, 17–20	2–3, 10, 13, 16, 18, 21–22	2, 4–5, 10, 12, 16–17, 22–23	8, 12, 15, 20, 23	0, 10, 12, 15, 18, 23	11, 19, 23	0, 5, 7, 11–13, 15, 18
6	6–9, 12, 14, 17, 19, 21, 23	0, 3–7, 9, 17, 20, 23	0, 3, 14–15, 22	1–2, 4–5, 9, 12–14, 16–18	2–3, 8, 12, 17–18, 21	2, 6, 13–14, 16, 22	0, 9, 15, 17, 22	0, 10–11, 15, 21, 23	3, 6, 10–11, 13, 18, 23	6, 8, 20, 22
7	7–9, 11–20, 22–23	0–3, 5–6, 8–9, 15, 18–20, 23	0,2–5,9,11–12	1, 5, 7, 13, 18	2,16,22	2, 4, 12–14, 16–17, 19, 22	0,8,15, 19,21–22	0,11,21	13,18,23	0,5,9–10, 13,23
8	8–10, 16–18, 23	0–1, 4, 6–8, 10–12, 15,17, 19–20, 23	1,11,13, 22–23	2, 9, 11, 14, 17, 20, 23	0,2,19,21	4–5,8, 17–19,22	0,10,15, 18,20–23	0,7,9,15, 17,19,22–23	13,18–19	2,4,6,13, 15,17,21,23
9	9		3, 19	15	0, 2, 8–14, 18, 20–21	8,10,12–14, 16,22	8–10,14–23	0,2–7,10, 13,15–23	3,6,9, 13–19,21–23	2,13,20–21
10	10–12, 18	6	2, 5, 13, 22–23	1,13,17, 21–23	3,6,15–17, 19,22–23	0–1,3–4, 11,16–21,23	0,2,4–5, 11,13,22	1,8–9,11–12, 14,16	0–2,5–6, 10–12,20	0,4–6,10,12, 15,17–19, 22–23
11	11–20, 23	4, 7–10, 18, 23	1–2, 17–18, 21	2,6,8,11–12, 14,18–20, 22–23	1,5,9,16–17	0,2,5–7, 9,15,23	3,6–7, 12–13,23	1,8–9,18,20	0,2,4,7–8, 15,22	11,13, 15–17,20
12	12–17, 19–21, 23	0, 4, 6, 9, 11, 14, 18, 22	4,7–9,12,15, 17–18,20–21	0,4,7,9–11, 13–16,19–21	4,7,14,16,23	1,5,15	0–1,6, 11–12,14–16	2–4,7–8,14	1,3,7–8	1,14,17,23
13	13–23	10, 15, 17, 20	0,5,10,12,14,16,20–21	0–2,4–5, 13–14, 16,18,20,23	7,13	2–3,5, 12,17–18	1,6,11–12, 17,22	0,2,5,8,11, 14,16,18–20	0,3–4, 10,18,22	3,7,9,11,13,16, 19
14	14–19, 21,23	1, 3, 10–12, 14, 16–17, 22	4, 11, 13, 15–16, 18–20, 23	3, 5, 7, 9, 12, 18–19, 23	5,8,13–14, 16–17,21,23	4,9,18	0–1,21–23	0,7,9–10,12 13,15–16, 19,21	1,5,20	1,3,11,15,17,1 9,22–23
15	15–23	0–1,4–6,8, 13,15–17,23	2,9,11–13, 16,20	7,10–12, 14,16,20	4,6,8–9, 12–13, 15,19–21	13–14,17–18	1,5,21–22	0–1,4,8–9, 12–13,20,23	1,4,9, 16–18,20	5,16,18
16	16–22	0–3,10–11,13, 16,18–19,22	0,2,4,12–13, 17–18,23	1,9,11–12, 17–18,23	1,17–18,20	2,12,22	2–3,12–13, 21–22	1,5,7,11–13, 15,18–21,23	2–3,18,20	1,3,6–7, 11–13,19,23
17	17–22	0,2–5, 11–13, 15–19,21	1,4,10–11, 14,17–18, 20,22	0,5,9–11,18	4,9,11,14–15, 20–21,23	14,17	5,21,23	0–2,7,9,12, 19,21,23	1,11–12, 18–19,22–23	1,3,6,8,17, 19,23
18	18–20,22–23	1–2,5,9,11, 13–15, 17,19–22	2,4,12, 15–17,20,22	3,10–11,13, 16–17,19, 21,23	4,10,12–15	1,7,9,14, 17,21–22	0,5–6,8,12,18	1,5,8–9,11, 15–16,22–23	1,5,11, 19–20	7,12–13
19	19–23	0,2,9,12–13, 18–20,22–23	12,14,16–21	11,14, 16–19,21,23	0,2,12, 14,20,22	4–5,13,17–18, 20–22	1–3,12, 14,16,21–23	12,20,23	0–3,11, 13,19,21	3,10,15, 17,19–20
20	20–23	0,2,5,10, 14–20,22–23	1,3,9–11, 16–18,23	10,15,18–20	2,14,16–17, 19–21	1,3,9,20–22	11,14–15, 21,23	1,4,6,14, 19,23	0,2,4,8–9, 18,20–21	1,3–4,7,12, 19,22–23
21	21–23	0–2,4,8–9, 11,14,17, 20,22–23	3,14, 16–17,20	1,4,11, 16,18–20	1–2,10, 14,17,19–21	3,11,15, 18–23	0,2–3, 13–14,17,23	4,8,12,14, 16,18–19,23	3,11–12, 18,22–23	3,7,9, 19–20,22
22	22–23	0–1,13, 18–21	0,2–4,9–10, 17–23	0,4,10–11, 13,18,20,23	1,5,10,13, 15,17–23	3,9,21–22	2–3,11, 14,17–18	0,4,12, 19–20,23	1,3,8,18–19	0,3,6–7, 18–20,23
23	23	2,4,7,9–10, 19–20,22–23	1–2,9,18, 20–23	1–2,7,19, 21–23	1,4,10,17, 21–22	1–2,4–5, 18–19,21–22	0,3,5,12–13, 15–16,20–21	1–2,7–8, 18–20,22–23	1,4,11,15, 18,20–22	1,9,12, 18,20–21

Se realizó una comparativa analítica entre los patrones de los errores predictivos al aplicar el algoritmo y sin aplicar el algoritmo, ejecutando todas las horas futuras con esta última opción. Con lo que se observó que el algoritmo detectó y corrigió los patrones pertinentes para mejorar la precisión. Para ello, sin aplicar el algoritmo se predijo 2019 ejecutando todas las horas futuras, posteriormente se obtuvieron los errores y se observaron tres patrones:

Influencia de la temperatura en la madrugada: los datos de temperatura presentaron menor correlación con la demanda durante las horas de madrugada que durante el resto del día.

Influencia de la temperatura en días distantes: al actualizar los datos de temperatura se obtuvo una mayor mejora de precisión para días distantes (del cuarto en adelante) que para días cercanos (antes del tercero). Esto se puede justificar con la gran precisión que tienen los días cercanos, por lo que resulta difícil mejorar más su precisión. También se puede explicar con la mayor relevancia que tienen los registros históricos de demanda para predecir días cercanos.

Influencia de la demanda de horas previas: cuanto menor es la diferencia de tiempo entre el momento de predicción y el de ejecución, mayor precisión se tiene, de manera que las tres siguientes horas al momento de ejecución tienen una precisión significativamente mayor que el resto.

Posteriormente se aplicó el algoritmo para obtener el horario de ejecuciones representado con la Tabla 2, a partir de la cual se pueden extraer análogamente las deducciones previas:

Influencia de la temperatura en la madrugada: a las 9:00 se predice pocas horas de madrugada, lo que concuerda con el análisis de errores, que infiere en un menor impacto de la temperatura sobre la demanda de la madrugada.

Influencia de la temperatura en días distantes: a las 9:00 se predicen muy pocas horas futuras correspondientes a los primeros 4 días, lo que vuelve a coincidir con el análisis de errores en su relación entre temperatura y días distantes.

Influencia de la demanda de horas previas: durante la mayoría de horas de ejecución se calculan las tres siguientes, lo que se justifica con la mayor correlación entre la demanda de cada hora y las tres siguientes.

Se predijo el año 2019 con diferentes horarios y se midió el error para cada antelación. Los resultados se muestran en la Figura 5, donde la curva naranja corresponde a predecir todas las horas futuras, la rosa discontinua al antiguo de REE (véase Tabla 1), la azul al algoritmo (véase Tabla 2) y la gris al horario que predice el día actual y el día futuro que más tiempo lleve sin actualizar.
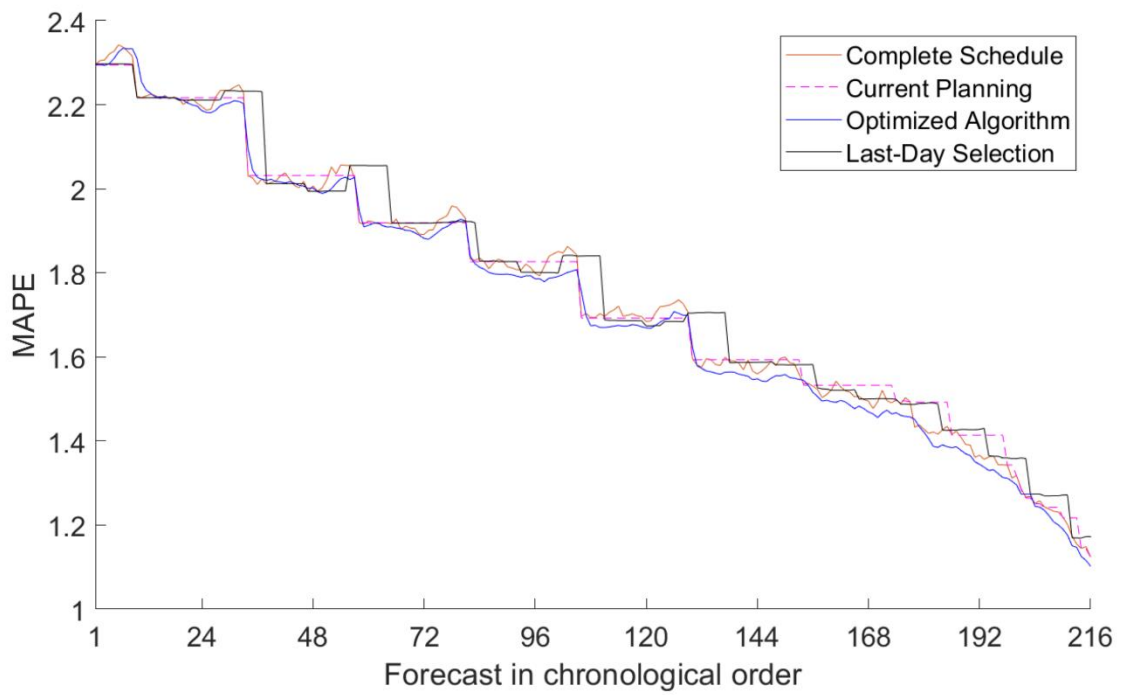
Figura 5. *Precisión del sistema predictivo respecto la antelación*

Como se puede apreciar, el algoritmo supera a todas las alternativas incluyendo el horario original de REE.

4. Preprocesado de temperaturas

4.1 Preprocesado interpretable, automático y preciso

En el apartado "1.4.3 Gestión de temperaturas" se han presentado técnicas de preprocesamiento de variables. Ninguna de ellas satisface los tres requisitos que se buscan en la investigación de la presente tesis [13]: interpretabilidad, precisión y automatización. Pues el estado del arte tiende a centrarse en algún aspecto específico. Dado que el procesamiento que se pretende diseñar tiene unos requisitos tan específicos, resulta difícil buscar en la literatura algún trabajo que haga lo mismo.

La interpretabilidad planteada [13] se basa en calcular unas nuevas variables de entrada para el modelo, de manera que se pueda explicar intuitivamente su significado. Las variables obtenidas se resumen en la Tabla 3.

Tabla 3. Variables resultantes del preprocesado térmico

Input variables		
Symbol	**Name**	**Explanation**
CN	Cold degree for national mean.	Cold effect for the entire peninsula
HN	Heat degree for national mean.	Heat effect for the entire peninsula
PC_l	Previous cold degree.	Effect of previous day l being colder than today.
PH_l	Previous heat degree.	Effect of previous day l being hotter than today.
IC_z	Individual cold degree difference.	Effect of region z being colder than the nation.
IH_z	Individual heat degree difference.	Effect of region z being hotter than the nation.
$PIC_{z\,l}$	Previous individual cold degree.	Effect of region z being colder than the nation, for one previous day.
$PIH_{z\,l}$	Previous individual heat degree.	Effect of region z being hotter than the nation, for one previous day.

Las variables *CN* y *HN* representan el frío y calores de la media nacional, *PC* y *PH* simbolizan el mismo efecto para días previos. De forma análoga *IC* e *IH* indican el frío y el calor de ciertas regiones, mientras que *PIC* y *PIH* conceptualizan lo mismo para días previos. Con lo que se tiene una lista de variables que indican aspectos concretos de la temperatura del territorio nacional. Una vez entrenados los modelos autorregresivos se tendrán unos coeficientes para estas variables, que si se analizan se pueden extraer conclusiones acerca de la relación temperatura/demanda.

Las variables se obtienen con la lista de ecuaciones de (15) a (23).

$$TM_t = \frac{1}{nz}\sum_{z=1}^{nz} T_{z\,t} \tag{15}$$

$$HN_t = \begin{cases} 0, & TM_t \leq Thh_n \\ TM_t - Thh_n, & TM_t > Thh_n \end{cases} \tag{16}$$

$$CN_t = \begin{cases} 0, & TM_t \geq Thh_n \\ Thh_n - TM_t, & TM_t < Thh_n \end{cases} \tag{17}$$

Donde *TM* es la serie temporal de media nacional de temperatura, *t* es el día previsto, T_z es la serie temporal de la temperatura de la zona *z*, *nz* es el número de zonas que se tienen en cuenta, Thc_n es el umbral de frío nacional y Thh_n el umbral de calor nacional. Dichos umbrales varían su valor según la hora del día que se prevé

$$PC_{nl\,t} = CN_{t-nl} - CN_t \qquad (18)$$

$$PH_{nl\,t} = HN_{t-nl} - HN_t \qquad (19)$$

Donde *nl* indica el día previo que se tiene en cuenta.

$$IC_{z\,t} = CD_{z\,t} - CN_t \qquad (20)$$

$$IH_{z\,t} = HD_{z\,t} - HN_t \qquad (21)$$

$$PIC_{z\,zl\,t} = CD_{z\,t-zl} - CN_{t-zl} \qquad (22)$$

$$PIH_{z\,zl\,t} = HD_{z\,t-zl} - HN_{t-zl} \qquad (23)$$

No obstante, para calcular las variables expuestas, tal y como indican las ecuaciones se requiere la obtención de otras variables previas llamadas hiperparámetros, las cuales son: Thh_z, Thc_z, Thh_n, Thc_n, *nz, z, nl* y *zl*.

Para obtener los hiperparámetros se puso a prueba cuatro alternativas con diferentes enfoques, siendo su finalidad maximizar la precisión del sistema predictivo en su conjunto. En las cuatro alternativas, primero se obtiene los umbrales locales Thh_z y Thc_z con el mismo procedimiento que el sistema predictivo original [33], es decir, minimizando el RMSE de las tres rectas temperatura/demanda que linealizan su relación. El procedimiento que siguen después se resume a continuación:

Fuerza Bruta Combinacional: consiste en probar todas las combinaciones de zonas y desfases, calculando el R cuadrado entre *CD* y *HD* con la demanda para quedarse la combinación con mayor correlación. Luego se calcula Thh_n y Thc_n con las zonas elegidas. Finalmente se pone a prueba todas las combinaciones posibles de *zl* y *nl* calculando el MAPE del sistema predictivo resultante.

Fuerza Bruta Secuencial: es similar a Fuerza Bruta Combinacional, con la diferencia de que las zonas se agregan una a una a la lista según su correlación en lugar de probar combinaciones; al agregarse una a una se tienen 5 listas posibles que se ponen a prueba en fusión del número de zonas elegidas.

Combinación Completa: es similar a Fuerza Bruta Combinacional, empleando la máxima información disponible, por lo que sólo se prueban combinaciones de 5 zonas y el número de días previos a utilizar se establece como 2 para nación (*nl*) y para cada región (*zl*).

Secuencia Completa: también es similar a Fuerza Bruta Secuencial maximizando la información empleada, de manera que se emplean todas las 5 zonas y 2 días previos para nación y para cada región.

El sistema antiguo de REE empleaba los mismos umbrales para las 24 horas del día, sin embargo, todas las alternativas propuestas funcionan con una pareja de umbrales para cada hora del día. Por lo que surge una pregunta ¿La mejora de precisión conseguida se debe únicamente a los nuevos umbrales? Para responderla se puso a prueba una quinta alternativa: el sistema predictivo original de REE con umbrales horarios, llamándose esta variante como Sistema Predictivo Actualizado.

4.2 Ensayos y resultados

Una vez definidas los preprocesamientos, se tiene cinco sistemas predictivos cuya precisión se puso a prueba prediciendo 2019 y calculando los errores resultantes. Por un lado, se puso a prueba la parte autorregresiva del sistema, pues es crucial que sea precisa por sí sola para obtener una base sólida en la interpretación de sus coeficientes. Por otro lado, se testeó el sistema completo, es decir la predicción combinada, para justificar el uso del nuevo preprocesado en el ámbito práctico del operador eléctrico.

4.2.1 Precisión de los sistemas autorregresivos

La precisión del modelo autorregresivo con cada uno de los preprocesados se muestra en la Figura 6 en función de la antelación, de modo que el eje de abscisas muestra el orden de ejecución a medida que se aproxima el momento que se prevé.
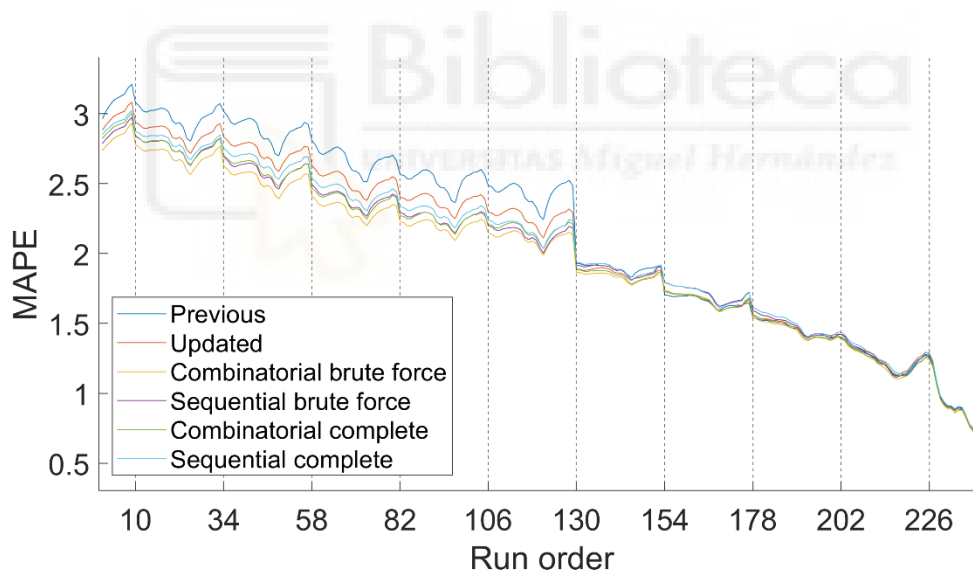

Figura 6. Error de sistemas autorregresivos en función de la antelación

El sistema Fuerza Bruta Combinacional resulta ser consistentemente el más preciso hasta el sexto día de ejecución y luego todos los sistemas son muy similares. Sin embargo, se tiene una anomalía en la ejecución 130 como un salto exagerado de precisión, que se corresponde a las 9:00 el sexto día de ejecución. Las anomalías pueden deberse a dos causas: una mala ejecución experimental o un fenómeno desconocido.

En el momento del salto sólo dos variables cambian: última demanda registrada y temperaturas. Para distinguir cuál es la causa de la anomalía, se testeó el sistema original de REE con dos modificaciones.

Empleo de temperaturas adelantadas: antes de la ejecución 130 se tienen las previsiones de temperatura con 4 días de antelación (que son las mismas condiciones que en el salto).

Empleo de demanda adelantada: antes de la ejecución 130 se tiene la demanda registrada con 4 días de antelación.
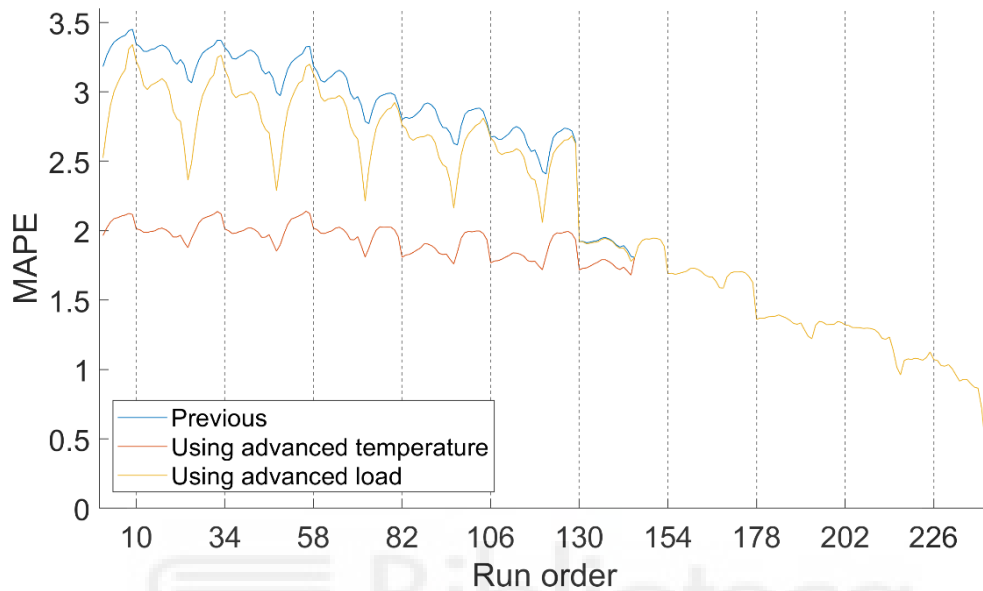

Figura 7. Error del sistema previo y sus variantes con variables adelantadas

Los resultados apuntan a la temperatura como culpable del salto de precisión. Sin embargo, para confirmarlo se realizó un segundo experimento en el que se calcula el R cuadrado de *CD*, *HD* y sus versiones desfasadas respecto la demanda real. Esas variables se calcularon con la información disponible para todas las antelaciones, obteniendo la curva naranja de la Figura 8. La curva azul se corresponde a la correlación de las variables térmicas del sistema antiguo.
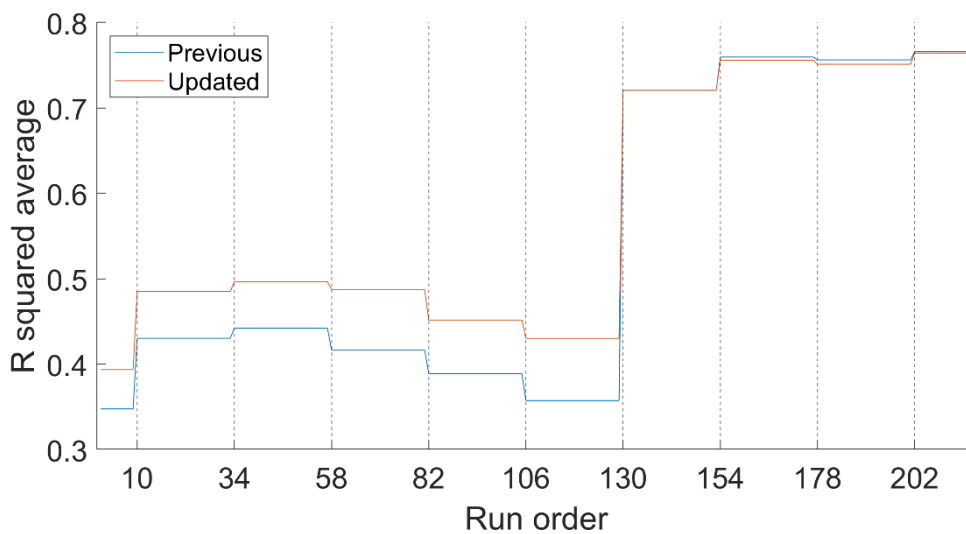

Figura 8. R cuadrado de variables de temperatura

Como se puede apreciar, el salto de correlación se corresponde con el salto de precisión. Además, para ambos sistemas, hay una diferencia de correlación antes de la ejecución y una fuerte similitud después, lo que justifica la mejora de precisión antes de la ejecución 130.

4.2.2 Precisión de los sistemas híbridos

La Figura 9 muestra la precisión del preprocesado aplicado al sistema completo combinado, demostrando la mejora consistente del preprocesado Fuerza Bruta Combinacional respecto los demás.
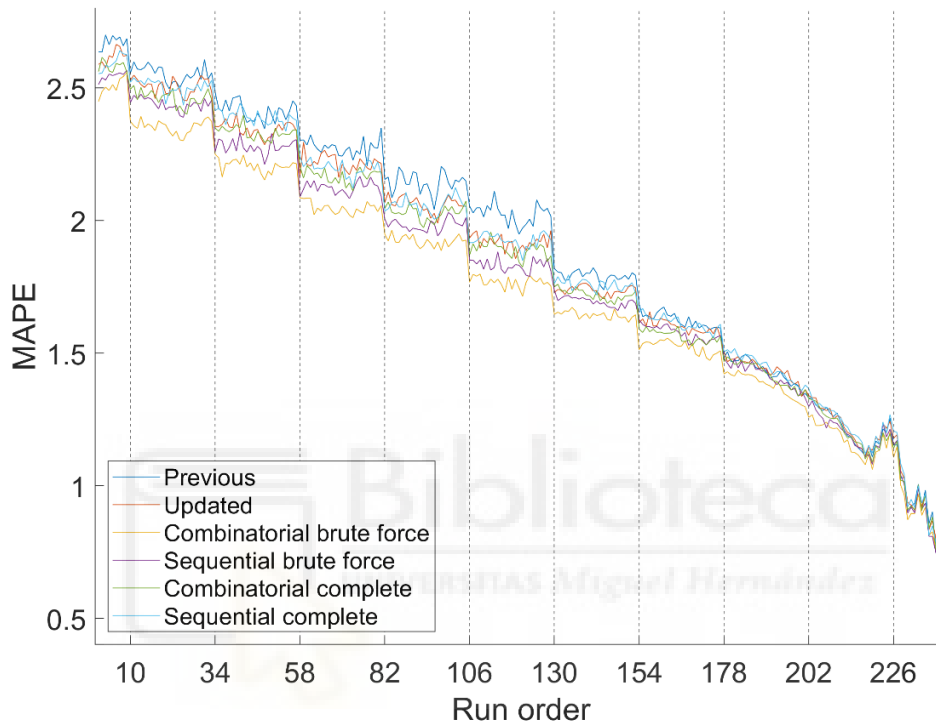

Figura 9. Error de los sistemas híbridos en función de la antelación

4.3.3 Interpretabilidad del modelo autorregresivo

Una vez validado el preprocesamiento térmico, se puede extraer las variables del sistema autorregresivo para dibujar alguna conclusión analítica. La forma más habitual de interpretar la influencia de una variable sobre otra es la sensibilidad, es decir, la derivada del modelo matemático respecto la variable que se desea analizar. Por lo que la sensibilidad de una variable K a interpretar se obtiene mediante la ecuación (24) que surge de despejar F_h en la ecuación (8) y derivar.

$$S_k = \frac{\partial F_h}{\partial k} = F_h\, \delta_k \qquad (24)$$

Aplicando la ecuación (24) a las predicciones de 2019 se obtuvieron las figuras 10, 11 y 12.
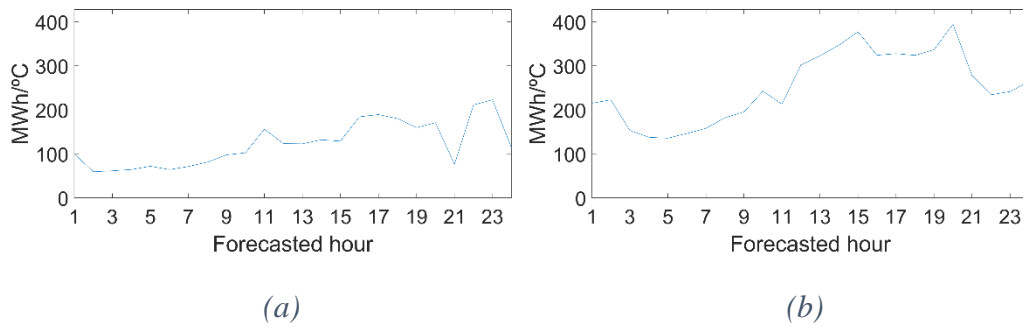
(a) *(b)*

Figura 10. *Sensibilidad de las variables peninsulares para cada hora predicha. (**a**) Peninsular cold degree sensitivity (CN). (**b**) Peninsular heat degree sensitivity (HN).*
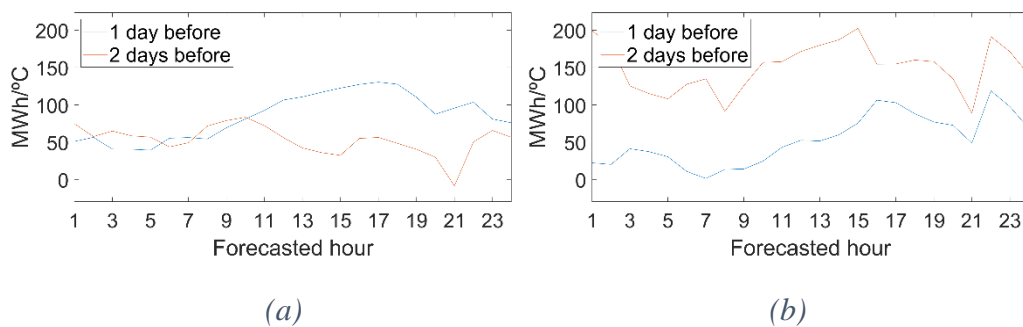

(a) *(b)*

Figura 11. *Sensibilidad de las variables peninsulares previas para cada hora predicha (**a**) Previous cold degree sensitivity (PC). (**b**) Previous heat degree sensitivity (PH).*
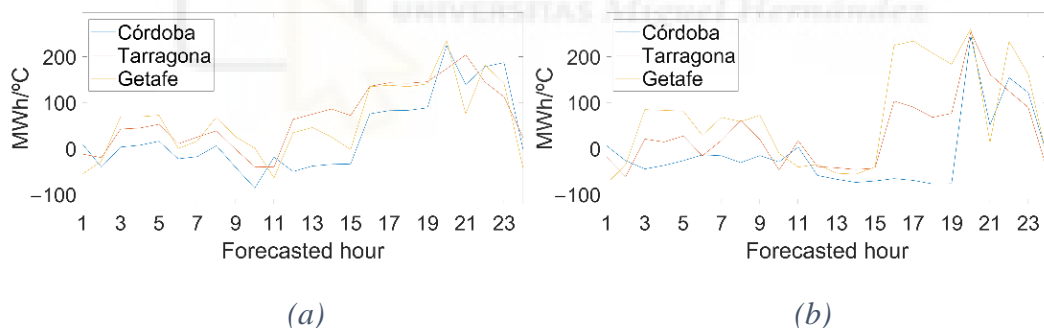

(a) *(b)*

Figura 12. *Sensibilidad de variables locales para cada hora predicha. (**a**) Individual cold degree difference (IC). (**b**) Individual heat degree difference (IH).*

En el cálculo de hiperparámetros mediante Fuerza Bruta Combinacional se obtuvieron cero días previos, por lo que no se tienen las variables *PIC* y *PIH*. La conclusión que se obtiene de ahí es que no aportan información lo suficientemente relevante como para mejorar la precisión.

De las curvas se extraen las siguientes conclusiones:

- El efecto del calor es mayor que el del frío.
- La temperatura tiene menor influencia en horas de madrugada.
- Si durante los días anteriores ha hecho más frío o más calor que el actual, la demanda aumentará.

- En épocas de calor la temperatura del segundo día anterior tiene mayor influencia que la del anterior, mientras que en épocas de frío ocurre lo contrario.

Además, se puede ver que se ha obtenido un total de 12 variables, 18 menos que las que empleaba el sistema de REE. Esta reducción dimensional beneficia al modelo NARX, pues las inteligencias artificiales tienden a rendir mejor si se elimina variables con información redundante [62], lo que justificaría la ligera mejora de rendimiento del sistema híbrido a partir del sexto día de ejecución.

5. Conclusiones

Se han planteado y resumido diferentes técnicas para mejorar el sistema predictivo de REE, con procedimientos automáticos que no requieren estudios previos a la hora de ser ejecutados, lo que permite una implementación directa en otros sistemas predictivos. Para que las técnicas fueran automáticas se ha mantenido un enfoque que únicamente emplea variables predictoras, sin recurrir a ninguna otra base de datos particular de España o sus regiones que implique toma de decisiones fuera del automatismo.

La obtención de horarios y nuevas variables de temperatura mejoran la precisión a escala peninsular; lo que deriva en un ahorro económico en la generación de energía eléctrica, un suministro más fiable y una mejor gestión de energías renovables. Estas contribuciones derivan en una mayor sostenibilidad energética desde el punto de vista económico y medioambiental.

La precisión no es proporcional a la frecuencia de actualización de las predicciones. Por lo que se ha establecido un criterio para decidir qué predicciones se ejecutan y elaborar así horarios de ejecución. El algoritmo que elabora el horario se adapta a las exigencias computacionales y el sistema predictivo empleado, resolviendo la transición a intervalos cuarto-horarios en consonancia con el resto de los operadores europeos.

La presente tesis ofrece un primer enfoque a la mejora de los sistemas de previsión a través de la planificación del cálculo, no sólo para sistemas predictivos de demanda eléctrica, también para otros sistemas predictivos de series temporales. La aplicación de un estudio similar a otros sistemas de predicción de series temporales podría mejorarlos de manera similar en cuanto a precisión y velocidad de cálculo.

El análisis del horario obtenido y sus respectivos errores proporciona una comprensión más profunda de cómo cada actualización del pronóstico de temperatura reduce el error en los días distantes, pero no tanto en los próximos. También demuestra que las demandas recientes afectan a la precisión drásticamente en las siguientes tres horas previstas.

Por otra parte, se ha desarrollado un nuevo preprocesado de datos de temperatura que cumple con tres requisitos: precisión, automatización e interpretabilidad. Por lo que se propone como sustituto al preprocesado antiguo y como herramienta de análisis demográfico en futuros trabajos. También ser propone emplearlo en otros operadores eléctricos fuera de España gracias a su automatización.

Al aplicar el preprocesado a un modelo autorregresivo se ha observado una anomalía en el patrón de errores. Al indagar en dicha anomalía, se ha observado la relación entre la disponibilidad de previsiones de demanda y la precisión del sistema. Con lo que la disponibilidad de previsiones de temperatura afecta notoriamente a la precisión, de manera que previsiones de temperatura de más de cuatro días de antelación son mucho menos útiles que las de tres o menos. También se ha concluido que la temperatura de

los dos días previos afecta a la demanda, por lo que conviene usarlos como variables de entrada

Las técnicas de preprocesamiento térmico también se pueden aplicar a otros campos donde se utilicen múltiples temperaturas ambientales como entrada. Un ejemplo es la previsión de velocidad del viento y en consecuencia, la previsión de generación en aerogeneradores; lo que construye una sinergia con los sistemas predictivos de demanda a la hora de gestionar las energías renovables.

En resumen, el compendio de mejoras presentadas contribuye a la construcción de una red eléctrica más limpia, económica y fiable; al mismo tiempo que aporta una pequeña herramienta de análisis demográfico en la relación temperatura/demanda.

Bibliografía

[1]   J. Moral-Carcedo y J. Pérez-García, «Time of day effects of temperature and daylight on short term electricity load», *Energy*, vol. 174, pp. 169-183, may 2019, doi: 10.1016/j.energy.2019.02.158.

[2]   M. Lopez Garcia, S. Valero, C. Senabre, y A. Gabaldon Marin, «Short-Term Predictability of Load Series: Characterization of Load Data Bases», *IEEE Trans. Power Syst.*, vol. 28, n.º 3, pp. 2466-2474, ago. 2013, doi: 10.1109/TPWRS.2013.2250317.

[3]   A. McIlvenna, A. Herron, J. Hambrick, B. Ollis, y J. Ostrowski, «Reducing the computational burden of a microgrid energy management system», *Computers & Industrial Engineering*, vol. 143, p. 106384, may 2020, doi: 10.1016/j.cie.2020.106384.

[4]   A. Kapoor y A. Sharma, «A Comparison of Short-Term Load Forecasting Techniques», en *2018 IEEE Innovative Smart Grid Technologies - Asia (ISGT Asia)*, may 2018, pp. 1189-1194. doi: 10.1109/ISGT-Asia.2018.8467788.

[5]   W. Jie-sheng y Z. Qing-wen, «Short-term electricity load forecast performance comparison based on four neural network models», en *The 27th Chinese Control and Decision Conference (2015 CCDC)*, may 2015, pp. 2928-2932. doi: 10.1109/CCDC.2015.7162426.

[6]   S. T. Mehmood y M. El-Hawary, «Performance Evaluation of New and Advanced Neural Networks for Short Term Load Forecasting», en *2014 IEEE Electrical Power and Energy Conference*, nov. 2014, pp. 202-207. doi: 10.1109/EPEC.2014.45.

[7]   X. Sun *et al.*, «An Efficient Approach to Short-Term Load Forecasting at the Distribution Level», *IEEE Transactions on Power Systems*, vol. 31, n.º 4, pp. 2526-2537, jul. 2016, doi: 10.1109/TPWRS.2015.2489679.

[8]   S. H. Rafi y N.-A.-M. Nahid-Al-Masood, «Highly Efficient Short Term Load Forecasting Scheme Using Long Short Term Memory Network», en *2020 8th International Electrical Engineering Congress (iEECON)*, mar. 2020, pp. 1-4. doi: 10.1109/iEECON48109.2020.229546.

[9]   W. Kong, Z. Y. Dong, Y. Jia, D. J. Hill, Y. Xu, y Y. Zhang, «Short-Term Residential Load Forecasting Based on LSTM Recurrent Neural Network», *IEEE Transactions on Smart Grid*, vol. 10, n.º 1, pp. 841-851, ene. 2019, doi: 10.1109/TSG.2017.2753802.

[10]   S. H. Rafi, Nahid-Al-Masood, S. R. Deeba, y E. Hossain, «A Short-Term Load Forecasting Method Using Integrated CNN and LSTM Network», *IEEE Access*, vol. 9, pp. 32436-32448, 2021, doi: 10.1109/ACCESS.2021.3060654.

[11]   T. Hong y S. Fan, «Probabilistic electric load forecasting: A tutorial review», *International Journal of Forecasting*, vol. 32, n.º 3, pp. 914-938, jul. 2016, doi: 10.1016/j.ijforecast.2015.11.011.

[12]   A. Candela Esclapez, M. L. García, S. Valero Verdú, y C. Senabre Blanes, «Reduction of Computational Burden and Accuracy Maximization in Short-Term Load Forecasting», *Energies*, vol. 15, n.º 10, Art. n.º 10, ene. 2022, doi: 10.3390/en15103670.

[13]   A. Candela Esclapez, M. López García, S. Valero Verdú, y C. Senabre Blanes, «Automatic Selection of Temperature Variables for Short-Term Load Forecasting», *Sustainability*, vol. 14, n.º 20, Art. n.º 20, ene. 2022, doi: 10.3390/su142013339.

[14]   M. Wang, Z. Yu, Y. Chen, X. Yang, y J. Zhou, «Short-term load forecasting considering improved cumulative effect of hourly temperature», *Electric Power Systems Research*, vol. 205, p. 107746, Abril 2022, doi: 10.1016/j.epsr.2021.107746.

[15]   Y. Rajbhandari *et al.*, «Impact Study of Temperature on the Time Series Electricity Demand of Urban Nepal for Short-Term Load Forecasting», *Applied System Innovation*, vol. 4, n.º 3, 2021, doi: http://dx.doi.org/10.3390/asi4030043.

[16]   N. X. Tung, N. Q. Dat, T. N. Thang, V. K. Solanki, y N. T. N. Anh, «Analysis of temperature-sensitive on short-term electricity load forecasting», en *2020 IEEE-HYDCON*, sep. 2020, pp. 1-7. doi: 10.1109/HYDCON48903.2020.9242910.

[17]   H. Shi, W. Weng, Z. Zhai, y X. Zhang, «The relationship analysis of temperature and electric load», *Applied Mechanics and Materials*, vol. 256-259, n.º PART 1, pp. 2644-2647, 2013, doi: 10.4028/www.scientific.net/AMM.256-259.2644.

[18]   A. Anderson, B. Stephen, R. Telford, y S. McArthur, «A Probabilistic Model for Characterising Heat Pump Electrical Demand versus Temperature», en *2020 IEEE PES Innovative Smart Grid Technologies Europe (ISGT-Europe)*, oct. 2020, pp. 1030-1034. doi: 10.1109/ISGT-Europe47291.2020.9248942.

[19]   C. Wang, T. Bäck, H. H. Hoos, M. Baratchi, S. Limmer, y M. Olhofer, «Automated Machine Learning for Short-term Electric Load Forecasting», en *2019 IEEE Symposium Series on Computational Intelligence (SSCI)*, dic. 2019, pp. 314-321. doi: 10.1109/SSCI44817.2019.9002839.

[20]   Q. Duan, J. Liu, y D. Zhao, «Short term electric load forecasting using an automated system of model choice», *International Journal of Electrical Power & Energy Systems*, vol. 91, pp. 92-100, oct. 2017, doi: 10.1016/j.ijepes.2017.03.006.

[21]   A. A. Mamun, Md. Sohel, N. Mohammad, Md. S. Haque Sunny, D. R. Dipta, y E. Hossain, «A Comprehensive Review of the Load Forecasting Techniques Using Single and Hybrid Predictive Models», *IEEE Access*, vol. 8, pp. 134911-134939, 2020, doi: 10.1109/ACCESS.2020.3010702.

[22]   H. S. Hippert, C. E. Pedreira, y R. C. Souza, «Neural networks for short-term load forecasting: a review and evaluation», *IEEE Trans. Power Syst.*, vol. 16, n.º 1, pp. 44-55, feb. 2001, doi: 10.1109/59.910780.

[23]   F. Lisi y I. Shah, «Forecasting next-day electricity demand and prices based on functional models», *Energy Syst*, vol. 11, n.º 4, pp. 947-979, nov. 2020, doi: 10.1007/s12667-019-00356-w.

[24] Z. Baharudin y N. Kamel, «Autoregressive method in short term load forecast», en *2008 IEEE 2nd International Power and Energy Conference*, dic. 2008, pp. 1603-1608. doi: 10.1109/PECON.2008.4762735.

[25] P. Ji, D. Xiong, P. Wang, y J. Chen, «A Study on Exponential Smoothing Model for Load Forecasting», en *2012 Asia-Pacific Power and Energy Engineering Conference*, mar. 2012, pp. 1-4. doi: 10.1109/APPEEC.2012.6307555.

[26] L. Wei y Z. Zhen-gang, «Based on Time Sequence of ARIMA Model in the Application of Short-Term Electricity Load Forecasting», en *2009 International Conference on Research Challenges in Computer Science*, dic. 2009, pp. 11-14. doi: 10.1109/ICRCCS.2009.12.

[27] S. Bouktif, A. Fiaz, A. Ouni, y M. A. Serhani, «Multi-Sequence LSTM-RNN Deep Learning and Metaheuristics for Electric Load Forecasting», *Energies*, vol. 13, n.º 2, Art. n.º 2, ene. 2020, doi: 10.3390/en13020391.

[28] T. Hong y P. Wang, «Fuzzy interaction regression for short term load forecasting», Hugo Steinhaus Center, Wroclaw University of Technology, HSC Research Reports HSC/13/14, dic. 2013. Accedido: 5 de febrero de 2022. [En línea]. Disponible en: https://econpapers.repec.org/paper/wuuwpaper/hsc1314.htm

[29] M. Alhussein, K. Aurangzeb, y S. I. Haider, «Hybrid CNN-LSTM Model for Short-Term Individual Household Load Forecasting», *IEEE Access*, vol. 8, pp. 180544-180557, 2020, doi: 10.1109/ACCESS.2020.3028281.

[30] M. Imani, «Electrical Load-Temperature CNN for Residential Load Forecasting», *Energy*, vol. 227, p. 120480, mar. 2021, doi: 10.1016/j.energy.2021.120480.

[31] W. Sulandari, S. Subanar, S. Suhartono, y H. Utami, «Forecasting electricity load demand using hybrid exponential smoothing-artificial neural network model», *International Journal of Advances in Intelligent Informatics*, vol. 2, n.º 3, Art. n.º 3, nov. 2016, doi: 10.26555/ijain.v2i3.69.

[32] N. Pooniwala y R. Sutar, «Forecasting Short-Term Electric Load with a Hybrid of ARIMA Model and LSTM Network», en *2021 International Conference on Computer Communication and Informatics (ICCCI)*, ene. 2021, pp. 1-6. doi: 10.1109/ICCCI50826.2021.9402461.

[33] M. López, S. Valero, A. Rodriguez, I. Veiras, y C. Senabre, «New online load forecasting system for the Spanish Transport System Operator», *Electric Power Systems Research*, vol. 154, pp. 401-412, ene. 2018, doi: 10.1016/j.epsr.2017.09.003.

[34] Z. Zhang, C. Dou, D. Yue, y B. Zhang, «Predictive Voltage Hierarchical Controller Design for Islanded Microgrids Under Limited Communication», *IEEE Transactions on Circuits and Systems I: Regular Papers*, vol. 69, n.º 2, pp. 933-945, feb. 2022, doi: 10.1109/TCSI.2021.3117048.

[35]   L. Han, Y. Peng, Y. Li, B. Yong, Q. Zhou, y L. Shu, «Enhanced Deep Networks for Short-Term and Medium-Term Load Forecasting», *IEEE Access*, vol. 7, pp. 4045-4055, 2019, doi: 10.1109/ACCESS.2018.2888978.

[36]   T. Hong, J. Wilson, y J. Xie, «Long Term Probabilistic Load Forecasting and Normalization With Hourly Information», *IEEE Transactions on Smart Grid*, vol. 5, n.º 1, pp. 456-462, ene. 2014, doi: 10.1109/TSG.2013.2274373.

[37]   M. Weimar *et al.*, «Benefit Cost Analysis of Improved Forecasting for Day-Ahead Hourly Regulation Requirements», en *2018 IEEE Power Energy Society General Meeting (PESGM)*, ago. 2018, pp. 1-5. doi: 10.1109/PESGM.2018.8586106.

[38]   H. Jiang, Y. Zhang, E. Muljadi, J. J. Zhang, y D. W. Gao, «A Short-Term and High-Resolution Distribution System Load Forecasting Approach Using Support Vector Regression With Hybrid Parameters Optimization», *IEEE Transactions on Smart Grid*, vol. 9, n.º 4, pp. 3341-3350, jul. 2018, doi: 10.1109/TSG.2016.2628061.

[39]   J. Mohammed, S. Bahadoorsingh, N. Ramsamooj, y C. Sharma, «Performance of exponential smoothing, a neural network and a hybrid algorithm to the short term load forecasting of batch and continuous loads», en *2017 IEEE Manchester PowerTech*, jun. 2017, pp. 1-6. doi: 10.1109/PTC.2017.7980816.

[40]   G. Veljanovski, M. Atanasovski, M. Kostov, y P. Popovski, «Application of Neural Networks for Short Term Load Forecasting in Power System of North Macedonia», en *2020 55th International Scientific Conference on Information, Communication and Energy Systems and Technologies (ICEST)*, sep. 2020, pp. 99-101. doi: 10.1109/ICEST49890.2020.9232674.

[41]   E. Weyermüller, H. J. Vermeulen, y M. Groch, «Short-Term Load Forecasting using Minimalistic Adaptive Neuro Fuzzy Inference Systems», en *2020 International SAUPEC/RobMech/PRASA Conference*, ene. 2020, pp. 1-6. doi: 10.1109/SAUPEC/RobMech/PRASA48453.2020.9041124.

[42]   T. Panapongpakorn y D. Banjerdpongchai, «Short-Term Load Forecast for Energy Management Systems Using Time Series Analysis and Neural Network Method with Average True Range», en *2019 First International Symposium on Instrumentation, Control, Artificial Intelligence, and Robotics (ICA-SYMP)*, ene. 2019, pp. 86-89. doi: 10.1109/ICA-SYMP.2019.8646068.

[43]   S. Di, «Power System Short Term Load Forecasting Based on Weather Factors», en *2020 3rd World Conference on Mechanical Engineering and Intelligent Manufacturing (WCMEIM)*, dic. 2020, pp. 694-698. doi: 10.1109/WCMEIM52463.2020.00149.

[44]   M. P. Clements y D. F. Hendry, «Evaluating a Model by Forecast Performance*», *Oxford Bulletin of Economics and Statistics*, vol. 67, n.º s1, pp. 931-956, 2005, doi: 10.1111/j.1468-0084.2005.00146.x.

[45]   Z. Zhou, Q. Jin, J. Peng, H. Xiao, y S. Wu, «Further Study of the DEA-Based Framework for Performance Evaluation of Competing Crude Oil Prices' Volatility

Forecasting Models», *Mathematics*, vol. 7, n.º 9, p. 827, sep. 2019, doi: 10.3390/math7090827.

[46]   K. Cheng, Y. Lien, Y. Wu, y Y. Su, «On the criteria of model performance evaluation for real-time flood forecasting», *Stochastic Environmental Research and Risk Assessment; Heidelberg*, vol. 31, n.º 5, pp. 1123-1146, 2017, doi: http://dx.doi.org.publicaciones.umh.es:8080/10.1007/s00477-016-1322-7.

[47]   G. Benavides y C. Capistrán, «Forecasting exchange rate volatility: The superior performance of conditional combinations of time series and option implied forecasts», *Journal of Empirical Finance*, vol. 19, n.º 5, pp. 627-639, dic. 2012, doi: 10.1016/j.jempfin.2012.07.001.

[48]   A. Pereira, «Performance of time-series methods in forecasting the demand for red blood cell transfusion», *Transfusion*, vol. 44, n.º 5, pp. 739-746, 2004, doi: 10.1111/j.1537-2995.2004.03363.x.

[49]   S. Ruzic, A. Vuckovic, y N. Nikolic, «Weather sensitive method for short term load forecasting in Electric Power Utility of Serbia», *IEEE Transactions on Power Systems*, vol. 18, n.º 4, pp. 1581-1586, nov. 2003, doi: 10.1109/TPWRS.2003.811172.

[50]   R. Zhichao, C. Chao, D. Yingying, Z. Wentao, W. Jun, y Z. Ruixiao, «Short-term load forecasting of multi-layer LSTM neural network considering temperature fuzzification», en *2020 IEEE Sustainable Power and Energy Conference (iSPEC)*, nov. 2020, pp. 2398-2404. doi: 10.1109/iSPEC50848.2020.9351188.

[51]   G. Bao, Q. Lin, D. Gong, y H. Shao, «Hybrid Short-term Load Forecasting Using Principal Component Analysis and MEA-Elman Network», en *Intelligent Computing Methodologies*, Cham, 2016, pp. 671-683. doi: 10.1007/978-3-319-42297-8_62.

[52]   Z. Wang *et al.*, «Singular value decomposition-based load indexes for load profiles clustering», *IET Generation, Transmission and Distribution*, vol. 14, n.º 19, pp. 4164-4172, 2020, doi: 10.1049/iet-gtd.2019.1960.

[53]   O. Hyde y P. F. Hodnett, «An adaptable automated procedure for short-term electricity load forecasting», *IEEE Transactions on Power Systems*, vol. 12, n.º 1, pp. 84-94, feb. 1997, doi: 10.1109/59.574927.

[54]   A. J. D. Antoja, P. A. O. Lafamia, C. A. B. Yang, G. V. Magwili, y R. V. M. Santiago, «Automated Short-Term Load Forecasting Using Modified Stochastic Hour Ahead Proportion (SHAP) Analysis», en *2019 IEEE 11th International Conference on Humanoid, Nanotechnology, Information Technology, Communication and Control, Environment, and Management (HNICEM)*, nov. 2019, pp. 1-6. doi: 10.1109/HNICEM48295.2019.9073407.

[55]   S. Liu, S. Gu, y T. Bao, «An Automatic Forecasting Method for Time Series», *Chinese Journal of Electronics*, vol. 26, n.º 3, pp. 445-452, 2017, doi: https://doi.org/10.1049/cje.2017.01.011.

[56]   M. López, C. Sans, S. Valero, y C. Senabre, «Classification of Special Days in Short-Term Load Forecasting: The Spanish Case Study», *Energies*, vol. 12, n.º 7, p. 1253, abr. 2019, doi: 10.3390/en12071253.

[57]   M. López, C. Sans, S. Valero, y C. Senabre, «Empirical Comparison of Neural Network and Auto-Regressive Models in Short-Term Load Forecasting», *Energies*, vol. 11, n.º 8, p. 2080, ago. 2018, doi: 10.3390/en11082080.

[58]   M. López, «Daylight effect on the electricity demand in Spain and assessment of Daylight Saving Time policies», *Energy Policy*, vol. 140, p. 111419, may 2020, doi: 10.1016/j.enpol.2020.111419.

[59]   S. M. Moghaddas-Tafreshi y M. Farhadi, «A linear regression-based study for temperature sensitivity analysis of Iran electrical load», en *2008 IEEE International Conference on Industrial Technology*, abr. 2008, pp. 1-7. doi: 10.1109/ICIT.2008.4608590.

[60]   Nahid-Al-Masood, M. Z. Sadi, S. R. Deeba, y R. H. Siddique, «Analyzing the impact of temperature on electrical load», en *2010 4th International Power Engineering and Optimization Conference (PEOCO)*, jun. 2010, pp. 238-343. doi: 10.1109/PEOCO.2010.5559225.

[61]   Tao Hong, Pu Wang, A. Pahwa, Min Gui, y S. M. Hsiang, «Cost of temperature history data uncertainties in short term electric load forecasting», en *2010 IEEE 11th International Conference on Probabilistic Methods Applied to Power Systems*, Singapore, Singapore, jun. 2010, pp. 212-217. doi: 10.1109/PMAPS.2010.5529001.

[62]   I. P. Panapakidis, T. Perifanis, y A. S. Dagoumas, «The effect of dimensionality reduction methods in short-term load forecasting performance», en *2018 15th International Conference on the European Energy Market (EEM)*, jun. 2018, pp. 1-5. doi: 10.1109/EEM.2018.8628002.

Anexos

Anexo A. Reduction of Computational Burden and Accuracy Maximization in Short-Term Load Forecasting.

Reduction of Computational Burden and Accuracy Maximization in Short-Term Load Forecasting

Alfredo Candela Esclapez*, Miguel López García, Sergio Valero Verdú and Carolina Senabre Blanes.

Electrical Engineering Area, Miguel Hernández University, Av. de la Universidad, s/n, 03202 Elche, Spain

*Author to whom correspondence should be addressed.

Abstract

Electrical energy is consumed at the same time as it is generated, since its storage is unfeasible. Therefore, short-term load forecasting is needed to manage energy operations. Due to better energy management, precise load forecasting indirectly saves money and CO_2 emissions. In Europe, owing to directives and new technologies, prediction systems will be on a quarter-hour basis, which will reduce computation time and increase the computational burden. Therefore, a predictive system may not dispose of sufficient time to compute all future forecasts. Prediction systems perform calculations throughout the day, calculating the same forecasts repeatedly as the predicted time approaches. However, there are forecasts that are no more accurate than others that have already been made. If previous forecasts are used preferentially over these, then computational burden will be saved while accuracy increases. In this way, it will be possible to optimize the schedule of future quarter-hour systems and fulfill the execution time limits. This paper offers an algorithm to estimate which forecasts provide greater accuracy than previous ones, and then make a forecasting schedule. The algorithm has been applied to the forecasting system of the Spanish electricity operator, obtaining a calculation schedule that achieves better accuracy and involves less computational burden. This new algorithm could be applied to other forecasting systems in order to speed up computation times and to reduce forecasting errors.

Keywords: short-term load forecasting; computational burden; forecasting schedule; performance evaluation

1. Introduction

Short-term load forecasting (STLF) is used to manage the production and distribution of electricity, and operate electricity markets from the current hour to the following days. If the electricity operator overestimates future electricity load, there will be extra

production costs that will lead to economic losses. On the other hand, if the electricity demand is underestimated, power plants may not have sufficient reserves for their generators to meet the energy demanded by the grid, compromising its stability and risking the possibility of a blackout. In addition, an accurate demand forecast indirectly facilitates the management of electrical energy from renewable energies.

In addition to the STLF, there are very short-term load forecasting systems, which forecast load for the forthcoming seconds or minutes for control purposes, such as that developed by Zhang et al. [1]; medium-term load forecasting for more than 3 weeks to manage operations, such as that made by Han et al. [2]; and long-term load forecasting for the months or years ahead, forecasting for facilities planning, for example the system presented by Hong et al. [3].

Electricity networks are systems that distribute power at both a regional and national scale, therefore even a slight improvement in the accuracy of STLF supposes a significant economic saving, which increases the competitiveness and development of multiple large-scale companies. In addition to electricity operators, other entities benefit from accurate electricity load forecasts, such as power marketers, independent system operators, or load aggregators.

Forecasting systems must process multiple variables whose relationships among them vary with location and weather: previous loads, meteorological data, calendar day, etc. Furthermore, electric load always contains a random unpredictable variation. Forecasting electricity load is a complex problem, which has been approached through various methods and from different points of view over the last few decades, which has led to a great variety of forecasting algorithms implemented in different electricity networks.

Many techniques are based on neural networks [4,5,6,7,8]. Other algorithms use statistical methods [9,10]. Hybrid systems that combine neural networks with other techniques are also common [11,12,13,14].

1.1. Main Problem

STLF systems calculate forecasts frequently—most likely hourly. The system must obtain fast forecasts, so the operator can read the results and manage the actions that adjust to future load. The latest measurement systems tend to use quarter-hour intervals. In addition, forecasts within the EU must be calculated at quarter-hour intervals, as required by article 19 of Commission Regulation (EU) 2017/2195, of 23 November 2017, establishing a guideline on electricity balancing. The STLF systems that currently work with hourly intervals will considerably increase their computational burden, whenever they change to quarter-hour intervals. They will have to forecast four times more values due to increased granularity and they will do this four times more often, due to an increase in frequency. This paper addresses the problem of computational burden while attempting to increase the accuracy of the STLF systems already implemented.

The Spanish transmission system operator (TSO) is Red Eléctrica de España (REE) and it is working on hourly intervals. It needs forecasts for 19 electrical regions, which is 19 times more calculations than a single STLF, with a total of 2.5 s for every hour that is predicted nationwide. Due to time limits for submitting predictions, it is not always feasible to calculate all future hours. Therefore, there is a schedule that determines which future intervals are predicted during each hour of the day.

The REE forecasting system cannot keep the previous forecasting schedule with quarter-hour intervals, since it is too computationally heavy to work within the time restriction. Therefore, there is need for a new schedule to forecast only the most useful intervals. Furthermore, the new schedule must be based on a criterion that numerically

determines which predictions are most useful. Satisfying the need for a systematic method to optimize schedules is the main motivation of this work.

1.2. Solution Approach

It was assumed that as we approach the forecast moment, the forecast becomes more accurate. However, this hypothesis does not always hold true. As an example, Figure 1 represents the mean absolute percentage error (MAPE) when predicting each hour of the Spanish national load, in 2019. Predicted values are distributed along the abscissa axis as they are executed hourly from 9 days before until the previous day. These forecasts are calculated with the auto-regressive model from REE [11]. There is an obvious trend in which accuracy increases as more recent information (weather and load) becomes available. Nevertheless, there seem to be some periods in which new forecasts are actually less accurate. The temperature data availability produces sudden drops in error, but during some periods the error increases. If accuracy loss periods can be known in advance, then the unproductive forecasts made at these times can be spared, saving computational effort while achieving a more accurate forecast. This paper aims to determine the optimal schedule of forecasts so that the system only computes new forecasts when an accuracy improvement is expected.
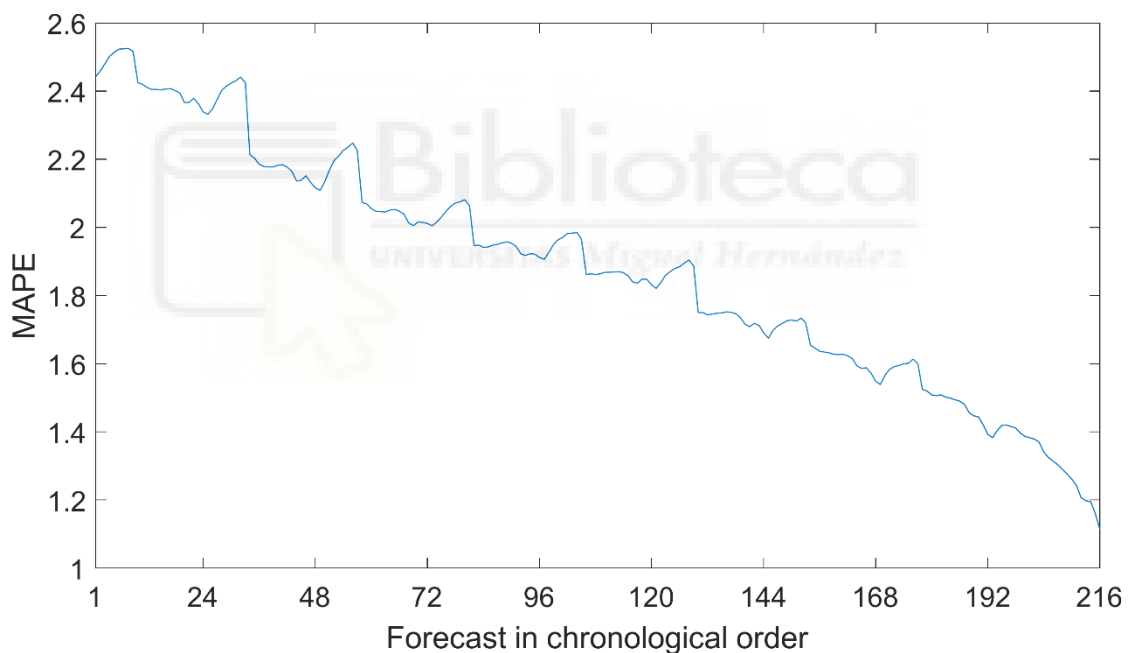

Figure 1. Error of auto-regressive forecasts in 2019.

The variations in precision are due to the availability of temperature and demand data. However, the objective of this paper is not to improve the input selection, but to determine at which moments it should be executed. The input selection problem had already been studied and solved [11].

The forecast needs to be computed within a time limit; therefore, each computer has a limit of N hourly values, beyond which the forecast would arrive late. This limit depends on the time allowed and the calculation speed, which again depends on the computer itself and on the forecasting algorithm used. To sum up, it may not be feasible to predict the whole range needed, therefore, in order to select the best N forecasts that can be calculated at each moment—a method to prioritize them needs to be developed. In addition, even if

all predictions can be calculated, they may be counterproductive, since some of them have a greater predictive error than some of the previous ones.

1.3. Literature Review

The STLF field is extensive, since innumerable works have been published for decades; consequently, reviews of the state of the art have been published, such as those made by Mamum et al. [15], Hippert et al. [16], or Hong et al. [17].

The previous work on the STLF system used in this paper [18] compared the autoregressive and neural models used. The research defined which one performs better in different contexts, being determined by the model configuration, availability of data and the use of exogenous variables. The performance of both models was studied, in such a way that predictions that were calculated in the same time intervals with different models were compared; the time lapse between the execution moment and the predicted one is not a variable. On the other hand, the proposed research took into account the performance of the same model for different time lapses.

Other researchers [19,20,21,22,23,24,25] built and compared different STLF mathematical models employing error measures as performance indicators. After that, they did not consider how to apply those models in an optimized schedule, to avoid producing larger errors than past predictions that had already been calculated. J. Mohammed et al. [26] did something similar, which also included reliability indicators to assess the model's performance.

Another example is the work carried out by G. Veljanovski et al. [27], in which they proposed a forecasting system based on a neural network, that uses the day type and air temperature of the last seven days as inputs to obtain day-ahead load forecasts as output. The system was executed one day before the forecast day but they did not consider the best time at which to obtain data and execute the computation.

E. Weyermüller et al. [28] built a minimalistic adaptive neuro-fuzzy inference model, which uses the hourly load at the same time for the preceding day, day of week, and month of yearas input. It forecasts the load of one hour 24 h before, so this research could be applied to organize the calculation schedule if more forecast hours are added to the model.

The present work could complement automatic forecasting systems. This paper offers an automated extra step at the end of the modeling process, in order to obtain an optimized execution schedule. An example of automatically modeled systems is the work conducted by L. Shufen et al. [29], in which they proposed an algorithm to automate time series forecasting for nonexperts.

The analysis proposed in this work could be applied to future works of theoretical research. For example, T. Panapongpakorn et al. [30] developed a STLF system for Mae Hong Son, Thailand. It is made up of two different time series models and three different neural networks. It predicts 30 min ahead by employing historical load, temperature, irradiance, and ATR. If the forecast horizon is extended beyond 30 min in order to build a practical system, the main ideas of this work could be applied to make an appropriate schedule. Another example is the work by D. Shuai [31]; he created a least-squares support vector machine model to forecast load from relative humidity, rainfall, maximum, minimum, and average temperature. If a complete forecasting system is built with his ideas, this paper could be applied to help improve its performance.

H. Jiang et al. [32] examined their model for different anticipation times; they also compared different STLF models, taking into account error and computation times. However, anticipation times varied just from 5 min to 16 h ahead and they were used to assess models, in the same way that calculation times were employed to compare entire models. On the other hand, this work employs accuracy from different anticipation times

to assess them and optimize calculation schedules, whilst computation times govern how many calculations can be chosen.

There is research which focuses on reducing computational burden, such as that by A. McIlvenna et al. [33], who modified a forecasting system through the reduction of integer variables by relaxation. This paper aims to optimize the use of a previously built forecasting system regardless of which one it is.

With a different approach, M. Weimar et al. [34] evaluated the improvement of a STLF system according to the economic savings with an econometric model. This is an example of how improving accuracy offers benefits that overcome developing costs.

1.4. Paper Contributions

The contributions of this paper can be summarized as follows.

This article offers a method to evaluate, at each moment of the day, the most useful predictions that are calculated and renewed on the prediction horizon. As far as we know there is nothing similar in the state of the art, making this is a first approach to evaluating single predictions. The most similar found works evaluate complete forecasting systems, for example H. Jiang et al. [32] or M. Weimar et al. [34].

The forecast evaluation allows the creation of an an optimal forecast schedule that reduces computational burden and increases overall accuracy, instead of focusing on improving computationally a single model, such as in the work by A. McIlvenna et al. [33].

The analysis of the prioritized schedule provides an understanding of the effect of new information on the quality of forecasts for both near and distant hours. This analysis could be applied to other researches, which use different inputs to understand its influence in accuracy, such as T. Panapongpakorn et al. [30] or D. Shuai [31].

According to Hong et al. [17], there is already a high number of STLF models for point predictions. For this reason, the present work does not develop a new model, but rather develops a technique with the potential to improve existing ones with respect to precision and particularly to computational burden.

1.5. Sections Summary

The paper is organized as follows. Section 2 gives an overview of the forecasting system used in this research. Section 3 explains the predictive scheduling algorithm in detail. Section 4 analyzes the accuracy of the algorithm when applied to the forecasting system. Its performance is compared with the current system. Section 5 summarizes the conclusions obtained.

2. Forecasting System Employed

The STLF system used in this research is that developed by the UMH [11], which was implemented in REE. The system has been operating for more than 4 years, and during this time REE and UMH have continued to collaborate in continuous improvement efforts [18,35].

The system entails an auto-regressive exogenous model and an exogenous autoregressive neural network (NARX) model. Each technique provides a separate forecast, which is then combined into a final forecast. This combination is more accurate than each separate result, so it is employed as final result by the operator.

The auto-regressive exogenous model employed by REE is described by Equation (1).

$$ln(Y_t) = \sum_{i=1}^{d} E_{t-i}\, \alpha_i + \sum_{v=1}^{n} X_{v\,t}\, \Phi_v + \varepsilon_t \qquad (1)$$

Where Y is the time series of forecast load for an interval of the day t, E is the error time series from previous forecasts, α coefficients associated with the error time series, d is the number of previous days that are taken into account, X is the input vector to predict a day t composed of a number n of variables v, Φ are their respective coefficients, and ε is a Gaussian random variation with mean zero.

This model is named auto-regressive since it takes into account previous forecasts through variable E. In addition, it is exogenous due to the input vector X, which incorporates all the inputs mentioned previously.

The NARX model is a category of neural networks; it is a modification of feed-forward neural networks, which only have exogenous inputs. NARX models have an extra input: the forecast value from previous steps; then they have a feedback loop. To train the network or compute single-step forecasts, the feedback loop is replaced by the real load as input, since the real load from preceding load is available.

Both models have the same inputs to forecast the peninsular load, which are the following: temperature forecasts of the current and next 9 days for Madrid, Barcelona, Seville, Zaragoza, and Biscay; peninsular demand of the previous hour to execution; average demand for the 52 weeks prior to the last week; and calendar information [35], which distinguishes the following day variables: weekdays, the different national and provincial holidays including Christmas, the previous and following days, days after the time change, month of the year, and August weeks. As output, the STLF system provides the predicted loads for the current day and the next nine, as required by the Spanish TSO. Furthermore, this horizon will be increased in five more days in future years. In addition, each forecast may have different relevance: the accuracy of the current day and the next day is more important than that of the 8th or 9th.

Both models employ the same input preprocessing. A filtering system is included in the forecasting system to identify and correct misleading information about historical load; it identifies and corrects abnormalities by comparing them to previous data. Temperatures are linearized using three linear equations that model load versus temperature, each one for different temperature levels classified as cooling, heating, and warm; the last one is not employed, so there are two variables (cooling and heating) to define each temperature value. Calendar information is represented as one-hot code for every variable about type of day.

2.1. Forecasting Schedule

The system schedule with the current configuration of the electricity operator is represented in Table 1, which shows the ranges of forecast hours for each run time. Each cell in the table contains the future hours of the day to forecast, so that 0 corresponds to the time span between 0:00 a.m. and 1:00 a.m. The hours in between are also predicted. Rows indicate the time of the day when the system is running, and columns indicate the future forecast day. There is the possibility of predicting the current hour, since it is still useful for the operator during the first 10 min of the hour itself. For example, at run time 0:00, on the first row of table (a), only the ninth following day is forecast. As another example, at run time 9:00 a.m., on the first row of table (a), all the following days except

for the second are forecast, also the current day is forecast from 9:00 until 23:00 (the entire rest of the day).

Table 1. Current schedule employed by REE.

| (a) | | | | | | (b) | | | | | |
| Run Time | Future Day Whose Load Is Forecast | | | | | Run Time | Future Day Whose Load Is Forecast | | | | |
	Current Day	1	2	3–8	9		Current Day	1	2	3–8	9
0					0–23	12	12–23				
1						13	13–23	0–23			
2						14	14–23				
3	3–23					15	15–23				
4						16	16–23				
5	5–23	0–23	0–23			17	17–23	0–23	0–23		
6						18	18–23				
7	7–23	0–23				19	19–23				
8	8–23	0–23	0–23			20	20–23				
9	9–23	0–23		0–23	0–23	21	21–23	0–23			
10	10–23					22	22–23				
11	11–23	0–23				23	23	0–23			

(a) Schedule from 0 to 11. (b) Schedule from 12 to 23.

2.2. Data Employed

During training and forecasting, the STLF system uses calendar data. Holiday information is obtained from the Spanish Official State Gazette, known as Boletín Oficial del Estado (BOE). It also uses the historical load of the national network, which is provided by REE. Additionally, the system uses historical records and forecasts of maximum and minimum daily temperatures, which are provided by the State Meteorological Agency.

The data employed by the algorithm is divided into three groups: training, validation, and test.

- The training group is employed to train the STLF models, these are the data from the years from 2012 to 2018 inclusive. Therefore, the 7 years prior to the desired year to forecast was selected, as recommended in the analysis of the STLF system performance [18].
- The validation group is used by the algorithm to obtain error records, comprising the year prior to the test period: 2018, therefore it coincides with the last year of training. The validation period coincides with the end of training because it must be done with data from the 7 years prior to the year to be predicted. Moreover, the post-training data cannot be used, since the validation is simulated without it.
- The test group is used to verify the performance of the forecasting system with the implemented algorithm. In this case the year 2019 was selected.

3. Methodology

This study has been performed with a CPU i7-8700, 16 GB RAM and Windows Home 64 bits as the operating system. The STLF system employed runs in Matlab, so all the calculations from this paper have been carried out with the same software, version R2020a.

The time a computer needs to calculate a set of predictions depends on three factors: the time that it takes to load new input data (I), the number of forecasts (n), and the time

that it takes to make each prediction (P). So, the run time (t) can be modeled with the linear Equation (2).

$$t = I + P \cdot n \tag{2}$$

Variables I and P depend on the computer and code employed. At the beginning of each hour, the forecasting system loads new input data (temperatures and previous measured load). This task requires 0.6329 s approximately, so this is the value for I. Moreover, every forecast hour requires different auto-regressive and neuronal models, since there is a model of both to forecast every hour from every run hour and previous day. Loading models from hard drive is not needed since they do not change throughout the year, therefore they can be kept in RAM memory to save loading times. Calculating each future hour with both models and combining the results requires 0.1336 s, then this is the p value.

As mentioned before, due to the limitation of accuracy or computational burden, for each execution, there is a maximum number, N, of predictions that can be performed without exceeding the response time limit. Therefore, for each execution period, up to N predictions with greater value can be selected.

The algorithm does not depend on the mathematical model used, but on the errors that it makes regarding historical records. Therefore, the major benefit of applying the algorithm is the error reduction sparing us from calculations with worse errors than previous ones already executed. In this way, it can be applied to a system that is organized by time intervals and it is possible to choose which intervals to predict in each hour of the day.

To measure error, the methodology employs the MAPE as indicator, described in Equation (3), where F is the forecast load at time d, L is the actual load, and n is the number of evaluated forecasts.

$$MAPE = \frac{100}{n} \sum_{d=1}^{n} \left| \frac{F_d - L_d}{L_d} \right| \tag{3}$$

The Figure 2 shows how to use the algorithm in a forecasting system. First, the maximum number of predictions that can be calculated per interval is obtained, which depends on available time and computing power. At the same time, the previous year can be predicted to calculate historical error records. Finally, the algorithm is applied to obtain a schedule that will serve to forecast load during the next year.
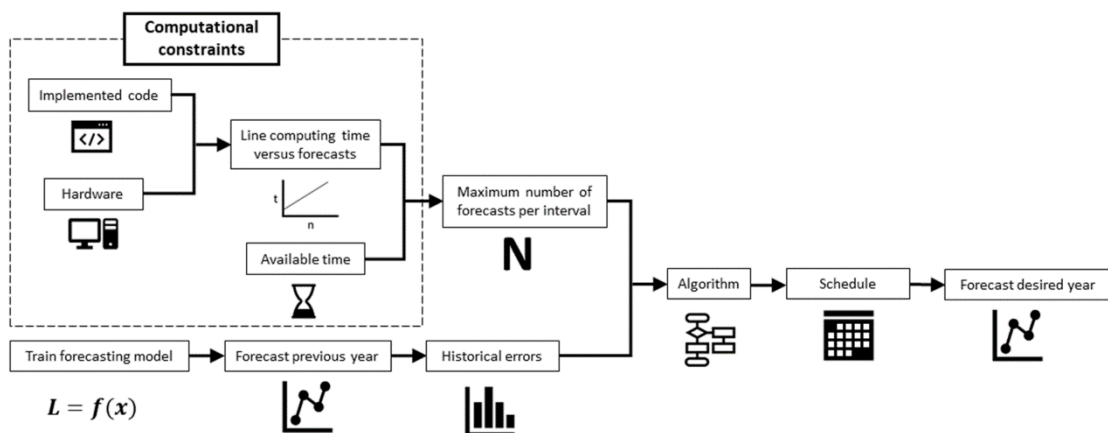

Figure 2. Process summary.

Other scheduling alternatives have been tested to compare the performance of the proposed algorithm. They are explained in Table 2.

Table 2. Scheduling options

Name	Explanation
Proposed algorithm	Employ the proposed algorithm to obtain a schedule and then use it to forecast during the entire year.
Complete schedule	Predict every future intervals up to 9 days in advance, at every hour of the day.
Current planning	Use the current schedule from REE, which is explained with Table 1.
Optimized algorithm	Employ the proposed algorithm with the optimal forecast number.
Random selection	Forecast a number, N, of random future intervals at each hour of the day.
Last-day selection	This algorithm, at each moment, predicts the current day. It also forecasts the future day that has gone the longest time without updating, prioritizing those days which have never been forecast.

4. Proposed Algorithm

To measure the value of a prediction, a numerical indicator called accuracy improvement expectation (AIE) is used. As the name suggests, it reflects the expectation of improvement in accuracy of a predicted demand if it is recalculated. To calculate this parameter, historical records of predictions calculated under the same conditions are used; that is, forecasts calculated at the same time of day with the same advance period.

In order to define AIE, let P be a series of predictions, which have been calculated at different intervals of time, t. Each value in P predicts a load, L, of one same hour of a given future day. Then, the AIE_t of a specific prediction P_t is defined by Equation (4) as the difference of percentage errors between such prediction and a prediction of the same load made one interval before. Relative errors are multiplied by 100, so they are expressed as percentages.

$$AIE_t = 100 \left| \frac{P_{t-1} - L}{L} \right| - 100 \left| \frac{P_t - L}{L} \right| \tag{4}$$

The implemented algorithm prioritizes the hourly forecasts according to larger AIE over the results of a full year, so only the first N values will be predicted in order to adhere to the time allowed.

Before executing the algorithm, the forecasting systems must be trained with the training data and ready to calculate forecasts. It is also necessary to determine the number of maximum forecasts, N, that the computer employed can execute. This is determined empirically by its computational speed and the calculation time limit. The data preprocessing from the original forecasting system is used in the same way, since it is not modified.

The algorithm core consists of two matrices named H and R. Matrix H is computed at algorithm initialization, so it remains constant during the rest of the process. It represents the historical records of the errors made in the validation period. It is used as a reference to estimate the error that the predictive model will have if it is executed at a given time to obtain the demand for a future hour. The matrix R varies with each iteration, representing the estimated error of the predicted demands in the prediction horizon. The values of matrix R are obtained by copying them from matrix H, according to the execution moment and the hour whose demand is expected.

The flowchart of the algorithm is described in Figure 3 and explained in depth in the following paragraphs:
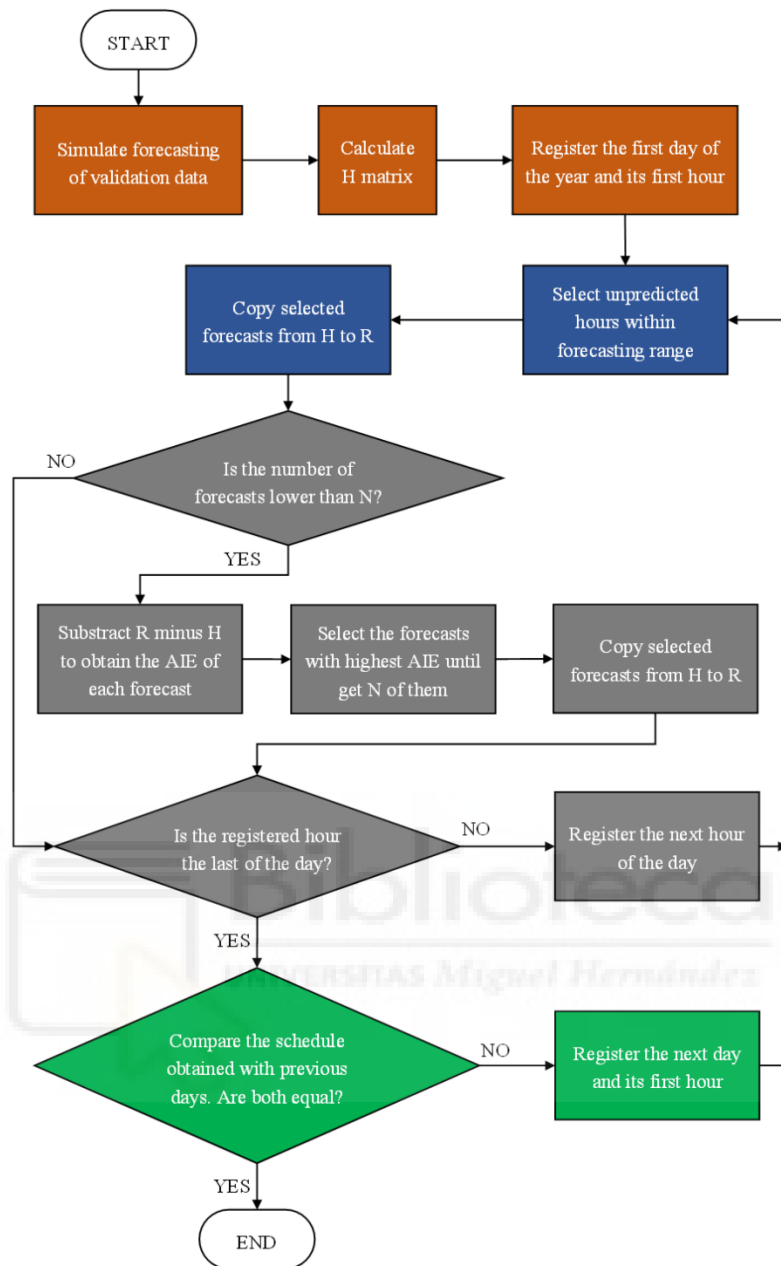
Figure 3. Algorithm flow chart.

Initialization: as a reference to estimate the AIE of each forecast, the algorithm forecasts the validation period. Each hour is predicted between 216 and 240 times, from the first time it enters the forecasting horizon until such an hour actually occurs. These reference forecasts make it possible to elaborate the H_{ijk} reference matrix, which contains the MAPE of the predicted hour, i, with j days of anticipation, where j = 1 the current day and j = 10 the ninth before, executed at time of the day k. The matrix H is obtained according to Equation (5), where F is the forecast load, L is the real load, t is the forecast day, and n is the number of days employed.

$$H_{ijk} = \frac{100}{n} \sum_{t=1}^{n} \left| \frac{F_{tijk} - L_{ti}}{L_{ti}} \right| \tag{5}$$

Hourly iterations: For each of the 24 h on the first day of the year, the algorithm selects the N possible values within the forecasting horizon that will reduce the prediction error

the most. To do this, it first checks if there are values without prior predictions, and it includes them among the selected ones. In addition, it copies the selected values from matrix H to matrix R as indicated in Equation (6). In this way, matrix R_{ij} contains the expected error of the last prediction made for hour i of future day j. At this point, all values within the horizon have either a current or a previous forecast. Next, if the number of predictions to be calculated is less than N, the rest of the forecasts are prioritized according to their AIE. To do this, according to time k, the submatrix H_{ij} is subtracted from R_{ij}. The models whose difference is greater will be included among those selected and the values of H will be transferred to R until the N predictions are completed. This process is carried out for 24 h until a list of predictions to be calculated for each hour is obtained, so matrix R changes with every hourly iteration.

$$R_{ij} = H_{ijk} \tag{6}$$

Daily iterations: The algorithm repeats the previous iterations with the following days of the year, thus obtaining a schedule of executions for each day. The algorithm ends when two consecutive days get the same schedule for all 24 h.

5. Results

The result obtained by applying the algorithm is a schedule similar to the one in Table 3. Each cell in the table contains the future hours of the day to forecast, so that 0 corresponds to the time span between 0:00 a.m. and 1:00 a.m. Hours separated by a dash indicate that the hours in between are also predicted. Rows indicate the times of the day when the system is running and columns indicate the future forecast days. For example, at run time 19 (7:00 p.m.), for the second future day, hours forecast are 12, 14, 16, 17, 18, 19, and 21; in other words, periods between 12:00 and 13:00, between 14:00 and 15:00, and between 16:00 and 20:00. The relationship between the algorithm and Table 3 is described as follows: The algorithm uses the variable k as "hour of forecast", the variable j as "future day whose load is forecast", and the variable i as the "forecast hour". The combination of three variables is stored during the execution of the algorithm as explained in hourly iterations.

Table 3. Schedule for combined model.

Run Time	Current Day	Future Day Whose Load Is Forecast								
		1	2	3	4	5	6	7	8	9
0	0–1, 5, 9, 23	0, 18, 22	2–5, 10, 14, 16–18, 22–23	1, 10, 19, 21–23	4, 18, 22	2, 4, 13, 16, 22	11, 14, 22–23	2, 19–20, 23	2, 7, 12, 16, 22–23	0–23
1	1–5, 7, 22	1–2, 5–6, 9, 11, 23	0, 2–3, 7–8, 18–19	0–1, 4, 10, 17	0–4, 15, 18, 21	0, 3, 6–7, 11	0, 9, 19–20, 23	3, 5, 11–12, 15, 21	0, 3, 12, 14, 19	0–5, 7–8, 10–11, 13–14, 16–17, 19, 22
2	2–6, 8, 10, 13–14, 22	0–1, 6–7, 10–11, 17–18	2, 7, 10, 19, 21	1–2, 10, 12, 15, 18–19, 22	2–3, 12–13, 15, 18, 21	5, 10, 12–14, 18, 23	10, 12, 14	0, 4, 7, 11–12, 18, 21	0, 3, 12–13	0, 5–6, 9–14, 17, 19, 22
3	3–7, 9, 12–13, 18, 20	1–4, 6–7, 10, 12, 21	0, 6–7, 11, 18–19, 23	4, 8, 10, 13–14, 18–20	2–3, 13–14, 17–18, 22	3, 12, 15, 18	0, 2, 13, 19, 22–23	0, 11, 13, 23	0, 3, 11–14, 23	2–4, 9, 13–15, 18, 22
4	4–7, 10, 14, 16, 19, 22	1–6, 8, 10, 13, 18–19	1, 4, 7, 10, 15, 18–19, 21, 23	2–4, 7, 10, 12–13, 19	0, 2–3, 5, 17–18, 22	3, 10, 13, 15	11–12, 14–15, 17, 19, 23	0, 10, 12, 16, 18, 22	3, 12, 18	4, 10–12, 14, 18, 23
5	5–8, 12, 14, 16–17, 20–21	2, 4–5, 7, 17, 19	2, 5, 7, 10–11, 17, 21	7, 12–15, 17–20	2–3, 10, 13, 16, 18, 21–22	2, 4–5, 10, 12, 16–17, 22–23	8, 12, 15, 20, 23	0, 10, 12, 15, 18, 23	11, 19, 23	0, 5, 7, 11–13, 15, 18
6	6–9, 12, 14, 17, 19, 21, 23	0, 3–7, 9, 17, 20, 23	0, 3, 14–15, 22	1–2, 4–5, 9, 12–14, 16–18	2–3, 8, 12, 17–18, 21	2, 6, 13–14, 16, 22	0, 9, 15, 17, 22	0, 10–11, 15, 21, 23	3, 6, 10–11, 13, 18, 23	6, 8, 20, 22
7	7–9, 11–20, 22–23	0–3, 5–6, 8–9, 15, 18–20, 23	0,2–5,9,11–12	1, 5, 7, 13, 18	2,16,22	2, 4, 12–14, 16–17, 19, 22	0,8,15, 19,21–22	0,11,21	13,18,23	0,5,9–10, 13,23
8	8–10, 16–18, 23	0–1, 4, 6–8, 10–12, 15,17, 19–20, 23	1,11,13, 22–23	2, 9, 11, 14, 17, 20, 23	0,2,19,21	4–5,8, 17–19,22	0,10,15, 18,20–23	0,7,9,15, 17,19,22–23	13,18–19	2,4,6,13, 15,17,21,23
9	9		3, 19	15	0, 2, 8–14, 18, 20–21	8,10,12–14, 16,22	8–10,14–23	0,2–7,10, 13,15–23	3,6,9, 13–19,21–23	2,13,20–21
10	10–12, 18	6	2, 5, 13, 22–23	1,13,17, 21–23	3,6,15–17, 19,22–23	0–1,3–4, 11,16–21,23	0,2,4–5, 11,13,22	1,8–9,11–12, 14,16	0–2,5–6, 10–12,20	0,4–6,10,12, 15,17–19, 22–23
11	11–20, 23	4, 7–10, 18, 23	1–2, 17–18, 21	2,6,8,11–12, 14,18–20, 22–23	1,5,9,16–17	0,2,5–7, 9,15,23	3,6–7, 12–13,23	1,8–9,18,20	0,2,4,7–8, 15,22	11,13, 15–17,20
12	12–17, 19–21, 23	0, 4, 6, 9, 11, 14, 18, 22	4,7–9,12,15, 17–18,20–21	0,4,7,9–11, 13–16,19–21	4,7,14,16,23	1,5,15	0–1,6, 11–12,14–16	2–4,7–8,14	1,3,7–8	1,14,17,23
13	13–23	10, 15, 17, 20	0,5,10,12,14, 16,20–21	0–2,4–5, 13–14, 16,18,20,23	7,13	2–3,5, 12,17–18	1,6,11–12, 17,22	0,2,5,8,11, 14,16,18–20	0,3–4, 10,18,22	3,7,9,11,13,1 6,19
14	14–19, 21,23	1, 3, 10–12, 14, 16–17, 22	4, 11, 13, 15–16, 18–20, 23	3, 5, 7, 9, 12, 18–19, 23	5,8,13–14, 16–17,21,23	4,9,18	0–1,21–23	0,7,9–10,12 13,15–16, 19,21	1,5,20	1,3,11,15,17, 19,22–23
15	15–23	0–1,4–6,8, 13,15–17,23	2,9,11–13, 16,20	7,10–12, 14,16,20	4,6,8–9, 12–13, 15,19–21	13–14,17–18	1,5,21–22	0–1,4,8–9, 12–13,20,23	1,4,9, 16–18,20	5,16,18
16	16–22	0–3,10– 11,13, 16,18–19,22	0,2,4,12–13, 17–18,23	1,9,11–12, 17–18,23	1,17–18,20	2,12,22	2–3,12–13, 21–22	1,5,7,11–13, 15,18–21,23	2–3,18,20	1,3,6–7, 11–13,19,23
17	17–22	0,2–5, 11–13, 15–19,21	1,4,10–11, 14,17–18, 20,22	0,5,9–11,18	4,9,11,14–15, 20–21,23	14,17	5,21,23	0–2,7,9,12, 19,21,23	1,11–12, 18–19,22–23	1,3,6,8,17, 19,23
18	18–20,22–23	1–2,5,9,11, 13–15, 17,19–22	2,4,12, 15–17,20,22	3,10–11,13, 16–17,19, 21,23	4,10,12–15	1,7,9,14, 17,21–22	0,5–6,8,12,18	1,5,8–9,11, 15–16,22–23	1,5,11, 19–20	7,12–13

Table 3 shows the 2019 schedule with the combined model and a forecasting limit per interval, N, of 71. The table is somewhat cumbersome as it describes all hours to be forecast at any given time. Nevertheless, the following conclusions can be extracted from it and are further substantiated in the following sections:

1. At 9:00 a.m., only 18.3% of forecasts are for the first 8 h of each future day. This allows us to infer that there is usually not a significant accuracy improvement in forecasting the first 8 h of each future day at 9:00 a.m. This conclusion is further developed in Section 5.1. "Temperature Influence on Early Morning".

2. At 9:00 a.m., only 5.6% of the predictions executed correspond to the first 4 days (including the current day). This selection makes sense since obtaining temperature data benefits more distant days than close ones, as seen in Section 5.1 "Temperature Influence on distant days".

3. For all running hours, the next hour is always forecast; while 22 of 24 running hours forecast the next two future hours and 21 of 24 forecast the next three. This fact coincides with the reasoning from Section 5.1 "Recent Loads", as it states that hours prior to the forecast moment tend to perform a great accuracy improvement.

5.1. Error Analysis

Error analysis has been performed on the results of both the auto-regressive and the NARX models. Nevertheless, the NARX model shows a more random behavior than the AR model and, even though the same conclusions apply to both, the identified patterns appear more clearly in the AR model. Therefore, for clarity reasons, the following section focuses on the conclusions obtained using the results of the AR model. Notwithstanding, all conclusions are valid for the AR, the NARX, and the combined model.

5.1.1. AIE and Error Analysis

The STLF system has been used to predict 2019, without applying the selection algorithm, so that it always calculates all future hours up to and including the ninth day after. The errors have been analyzed to detect patterns.

Temperature Influence on Early Morning

In order to quantify the effect of temperature updates, the MAPE of the entire forecasting horizon has also been calculated for each time of the day when forecasts are calculated. These errors are drawn in Figure 4; in order to distinguish the effects of temperature updates when predicting early morning and the rest of the day, the hours of the day that are predicted have been separated into two graphs.
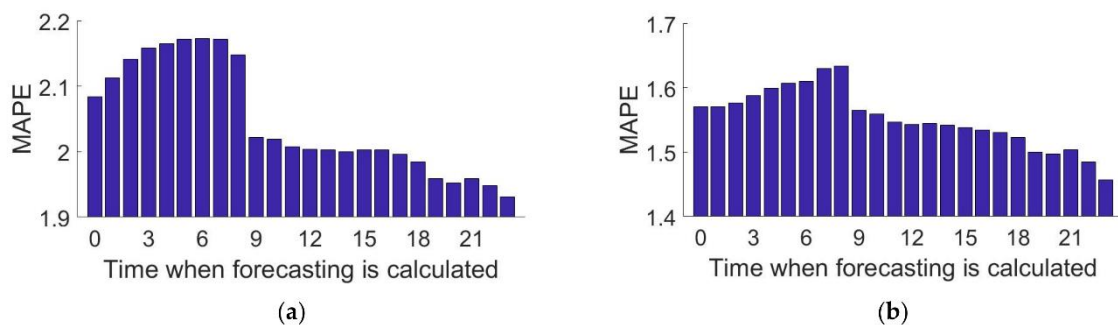

Figure 4. MAPE of every forecast moment during previous days. (**a**) Forecasting load consumed at 8:00 to 24:00. (**b**) Forecasting load consumed at 24:00 to 8:00.

Waking hours (8 a.m.–11 p.m.) experience an error decrease of 0.126% when executed at 9:00 a.m. compared to 8:00 a.m. On the other hand, resting hours have an error decrease of 0.068% at 9:00 a.m. compared to 8:00 a.m. At 9:00 a.m. the forecasting system receives new temperature data, then there is a larger correlation between temperature and load during waking hours than resting hours.

Temperature Influence on Distant Days

Figure 5 shows the AIE average of all the predictions at 9:00 a.m. from the previous 8 days to the preceding day.
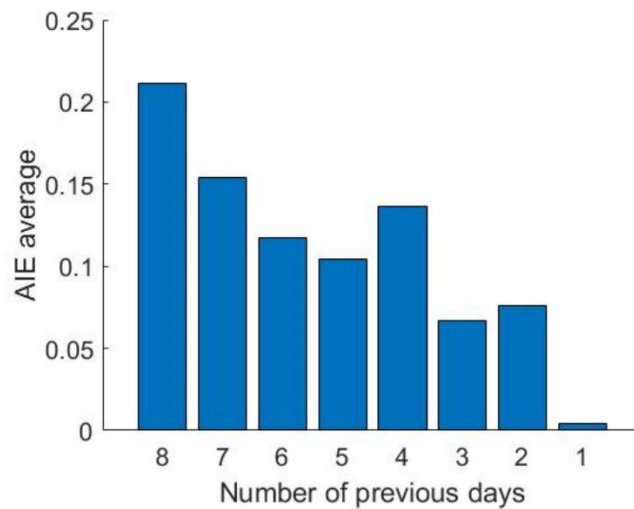

Figure 5. AIE average of previous days at 9:00 a.m.

The new temperature data results in greater improvements for distant days while not so much for proximate ones. Two reasons explain this: on one hand, temperature forecasts 2 or 3 days ahead are almost completely accurate and, therefore, each new forecast does not add any value beyond that point. On the other hand, other variables (recent load) become more relevant than temperature as the forecasting hour approaches. Day 9 is not represented in Figure 5 because the temperature received at 9:00 a.m. is not an update, but brand-new information (there was no previous temperature forecast).

Recent Loads

To visualize the impacts that the latest demands have on forecast accuracy, actual temperature registers as opposed to forecasts have been used to avoid confusion between both variables. Figure 6 shows the MAPE made by the latest forecasts, which are distributed on the abscissa axis so that the first one corresponds to the most recent one.
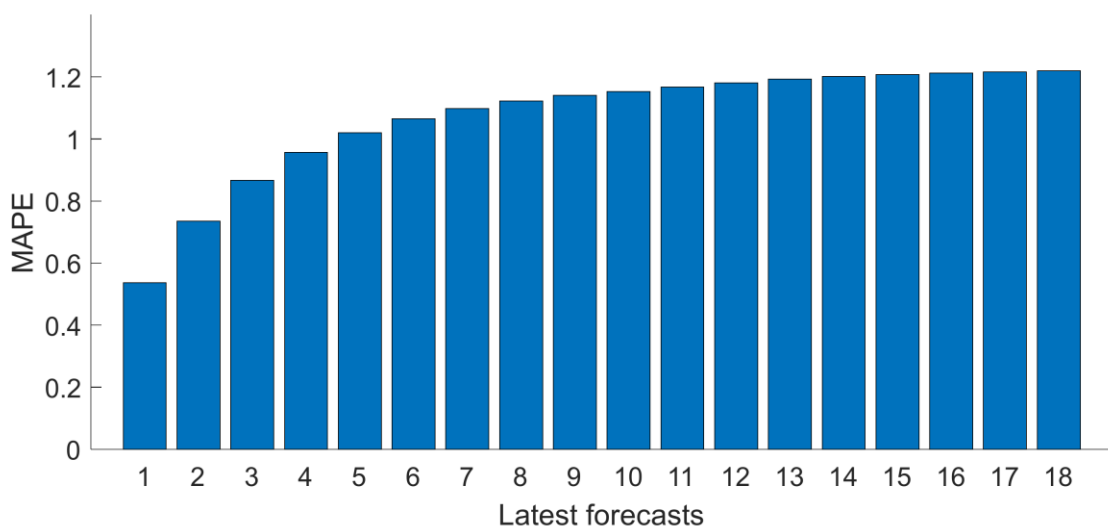

Figure 6. MAPE of latest forecasts.

According to Figure 6, the 3 h prior to the forecast moment have a higher error reduction than the rest. The greatest reduction in MAPE occurs on the latest forecast with 0.299%; the previous ones have a reduction of 0.131% and 0.090%, in that order. Therefore, it follows that there is a close correlation between the load for one hour and the previous ones.

5.2. Obtaining the Optimal Forecast Number

The algorithm has been applied to predict 2018 and 2019; so that to predict 2018, the years from 2011 to 2017 have been used as training and 2018 as validation datasets, while to predict 2019, the years from 2012 to 2018 have been used as training and 2018 as validation datasets. Figure 7 shows the MAPE average for each number of predictions that the system calculates. The solid lines refer to the STLF system with the algorithm applied and the dashed lines to the error made in predicting all the future hours that the system can cover; that is, the entire forecasting horizon, also understood as N equal to 240.
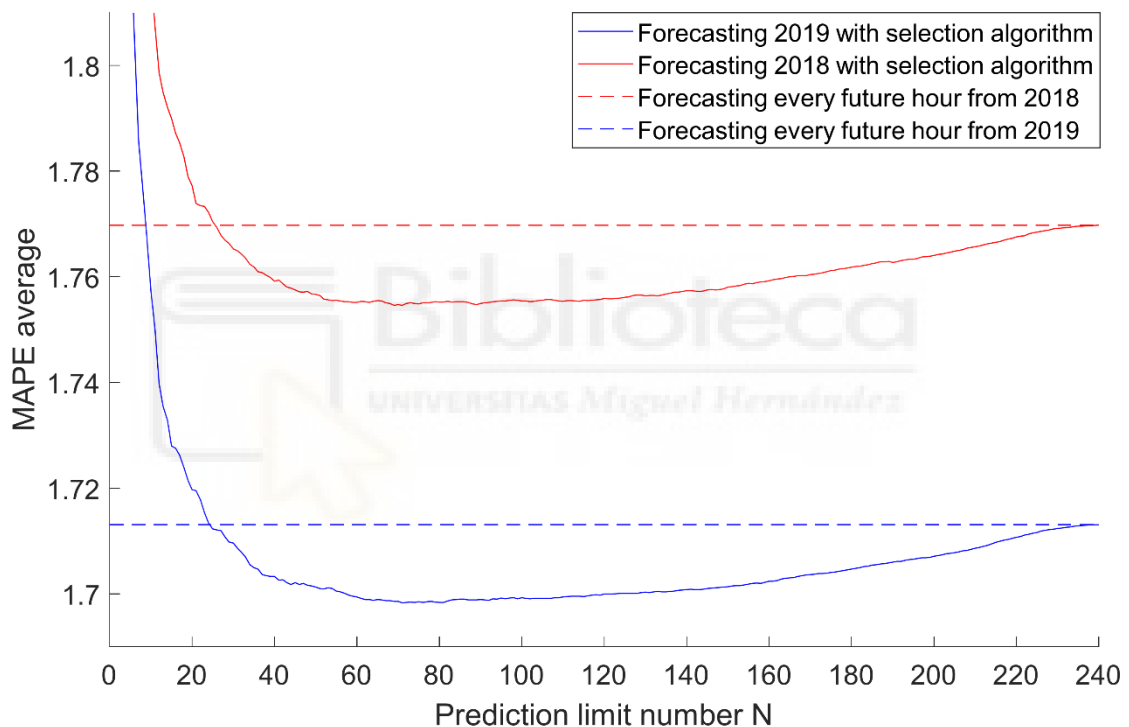

Figure 7. Accuracy of STLF system in 2018 and 2019.

A pattern can be seen in which accuracy increases with more forecasts up to a certain point, beyond which allowing more forecasts increases computational burden, but does not improve accuracy. Both curves present a minimum between 60 and 100, which proves not only that the priority determined with data from previous years is valid for the next year but also that the optimal amount of forecast can also be established from such data.

The minimum MAPE of 2018 is 1.755% and achieved with N = 71; for this reason, the N value has been applied when obtaining the prediction times. Coincidentally, the optimal N value coincides with the 2019 minimum with N = 71 and 1.698% of MAPE.

5.3. Accuracy Results of Optimized Scheduling

In order to test the proposed algorithm, the year 2019 has been predicted, with each one of the scheduling options explained in Table 2. The MAPE average has been

calculated for all the advances of all the hours of the year. Figure 8 shows the mean of the MAPE for each scheduling method. Methods with dashed lines are those that have a predetermined number, N, of future predictions.
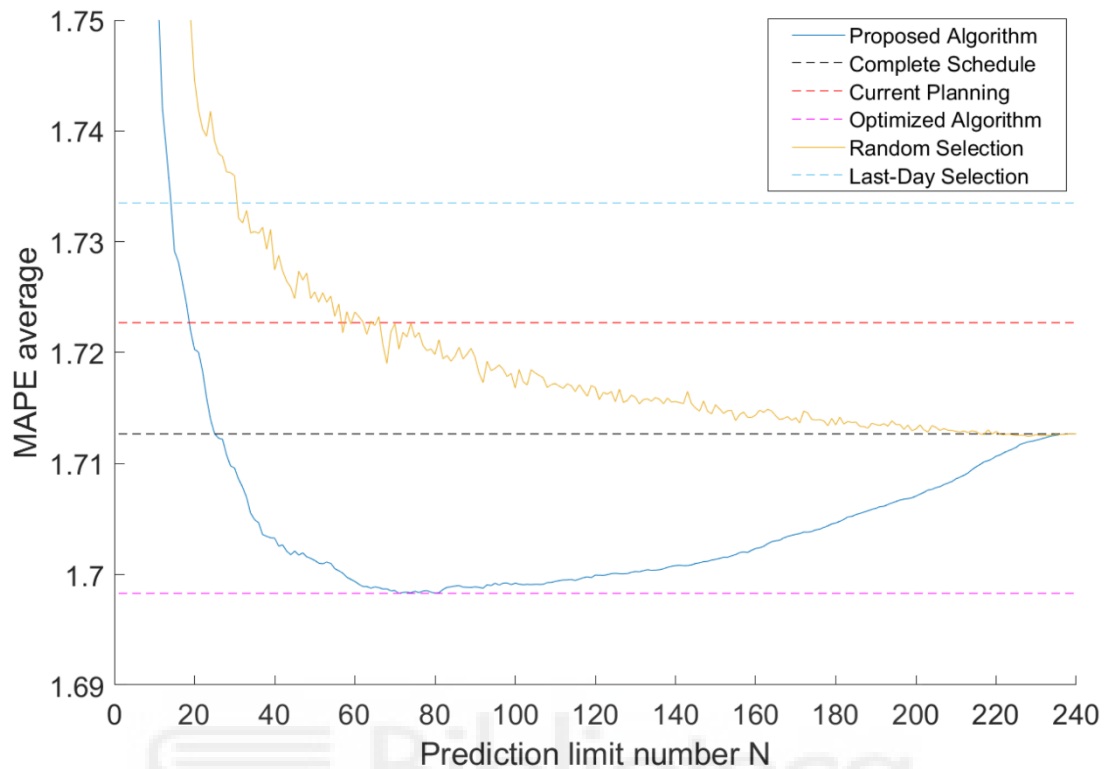

Figure 8. Accuracy of STLF system with different scheduling.

According to the test, random selection could perform worse for almost all cases; it is also inconsistent, so it is ruled out as a candidate. On the contrary, the proposed algorithm offers significantly better precision than the rest of the methods, using between 60 and 100 limit predictions.

As a final test, the year 2019 has been predicted with every method. Figure 9 represents the MAPE obtained with forecasts made every hour from the previous 9 days until the previous day.

In most advances, the optimized algorithm performs better than other methods. Certain combinations of execution time and future forecast days do not occur; in consequence, the last-day selection method has constant error periods due to a lack of updates.

As a final result, the year 2019 has been predicted with the current REE schedule, the algorithm with N = 71, and by calculating all future hours. Table 4 shows the MAPE of the entire year for each schedule and day in advance.

Table 4. MAPE of 2019 when employing each schedule and advance.

Schedule	Current	Days in Advance								
		1	2	3	4	5	6	7	8	9
Current Planning	1.089%	1.276%	1.478%	1.555%	1.630%	1.743%	1.861%	1.961%	2.101%	2.246%
Optimized Algorithm	1.066%	1.239%	1.417%	1.517%	1.612%	1.723%	1.841%	1.946%	2.088%	2.256%
Complete Schedule	1.077%	1.258%	1.443%	1.542%	1.634%	1.752%	1.862%	1.958%	2.095%	2.254%
Last-Day Algorithm	1.077%	1.291%	1.468%	1.550%	1.663%	1.768%	1.866%	1.992%	2.126%	2.245%

Except for the ninth day in advance, the algorithm always offers better accuracy. The Optimized Algorithm has an average improvement of 0.024% compared to the current schedule.

5.4. Computational Burden

The Spanish electricity system operator requires future load of 19 electrical regions. Nowadays, the entire forecasting horizon spans up to 240 h, thus the total of future loads that can be predicted extends to 4560, which require 10.16 min. However, if the quarter-hour system is employed, the number of future intervals to forecast will multiply by four. This new system will entail 18,240 numbers to be calculated in 40.62 min, which is unfeasible since REE requires results before 7 min have passed.

Table 5 shows the execution time for every scheduling in the worst-case scenario. That is forecasting 19 electric regions, during the hours of the day with the maximum number of future intervals to forecast. Execution times have been estimated employing Equation (2).

Table 5. Maximum execution times.

Scheduling	Run Hour with Maximum Intervals to Forecast	Number of Intervals to Forecast	Execution Time (Minutes)
Current planning	9:00 a.m. Look at Table 1.	3933 (207 × 19)	8.77
Optimized algorithm	Any hour. Every time it is executed it has a constant number of future intervals to forecast.	1349 (71 × 19)	3.01
Complete schedule	0:00 a.m. The system forecasts the entire current day and the following nines.	4560 (240 × 19)	10.16
Last-day selection	0:00 a.m. The system forecasts the entire current day and one of the following days.	912 (48 ×19)	2.04

Last-day selection and optimized algorithm manage to compute predictions under 7 min and the first one requires less time. However, the optimized algorithm offers better accuracy in most cases as indicated in Figure 9 and Table 4.

According to Equation (2) and quarter-hour intervals, the maximum number of forecasts to compute in 7 min is 3140. So, there is time to forecast 165 intervals in every electrical region. Therefore 165 is the maximum value that can be used on the algorithm as number N of forecasts.

6. Conclusions

European electricity operators need to develop systems with quarter-hour intervals and work in coordination with the rest of the operators in Europe. Figure 8 shows that accuracy is not proportional to the number of calculations, therefore a criterion is necessary to decide which predictions will be calculated. The increase in frequency and granularity can impose an extra constraint in forecasting models that can be detrimental to accuracy. In order to avoid any accuracy losses to the Spanish TSO, this research has developed an algorithm that organizes the calculation schedule of a STLF system throughout the day. The schedule obtained is adapted to the computational capacity of the computer while actually increasing the system accuracy from 1.089% and 1.276% to 1.066% and 1.239% for the current-day and next-day forecast respectively, with an average improvement of 0.023% for all previous days. The methodology described can be applied to any forecasting technique, even if computational burden is not an issue because it has been proven that limiting the number of forecasts can be beneficial for accuracy, as it has been demonstrated for the case of REE.

On the other hand, according to results, the main contribution of the work is to reduce the computational load of a predictive system without sacrificing accuracy. This will allow a transition to the quarter-hour system with an optimal execution schedule.

Furthermore, the error analysis provides a deeper understanding of how each temperature forecast update reduces the error on distant days but not so much on proximate ones, and how recent loads affect forecasting error drastically in the next 3 h but only marginally beyond hours 8 or 9.

This paper offers a first approach to improving forecasting systems through calculation planning, not only for electricity STLF but also for other time series forecasting systems, as well as other forecasting intervals such as quarter-hour intervals. Applying a similar study to other time series prediction systems could improve them in a similar way.

As future work, it is proposed to use the algorithm to plan the new quarter-hour system of the Spanish TSO. Each advance has a different impact on the operator's management, so forecasting errors have different impacts. To take this into account, each error can be multiplied by a weight factor according to the advance. In this way, with slight changes on the algorithm, it is possible to calculate schedules based on costs according to errors.

Institutional Review Board Statement

Not applicable.

Informed Consent Statement

Not applicable.

Data Availability Statement

The data that support the findings of this study are openly available at https://www.esios.ree.es/es/analisis/1293?compare_indicators=545,544&start_date=10-07-2021T00:00&geoids= (accessed on 15 May 2022) for historical demand records and https://opendata.aemet.es (accessed on 15 May 2022) for historical temperature records.

Conflicts of Interest

The authors declare no conflict of interest.

References

1. Zhang, Z.; Dou, C.; Yue, D.; Zhang, B. Predictive Voltage Hierarchical Controller Design for Islanded Microgrids Under Limited Communication. IEEE Trans. Circuits Syst. Regul. Pap. **2022**, 69, 933–945. [Google Scholar] [CrossRef]
2. Han, L.; Peng, Y.; Li, Y.; Yong, B.; Zhou, Q.; Shu, L. Enhanced Deep Networks for Short-Term and Medium-Term Load Forecasting. IEEE Access **2019**, 7, 4045–4055. [Google Scholar] [CrossRef]
3. Hong, T.; Wilson, J.; Xie, J. Long Term Probabilistic Load Forecasting and Normalization With Hourly Information. IEEE Trans. Smart Grid **2014**, 5, 456–462. [Google Scholar] [CrossRef]
4. Kong, W.; Dong, Z.Y.; Hill, D.J.; Luo, F.; Xu, Y. Short-Term Residential Load Forecasting Based on Resident Behaviour Learning. IEEE Trans. Power Syst. **2018**, 33, 1087–1088. [Google Scholar] [CrossRef]
5. Chen, Q.; Xia, M.; Lu, T.; Jiang, X.; Liu, W.; Sun, Q. Short-Term Load Forecasting Based on Deep Learning for End-User Transformer Subject to Volatile Electric Heating Loads. IEEE Access **2019**, 7, 162697–162707. [Google Scholar] [CrossRef]
6. Niu, D.-X.; Wanq, Q.; Li, J.-C. Short term load forecasting model using support vector machine based on artificial neural network. In Proceedings of the 2005 International Conference on Machine Learning and Cybernetics, Guangzhou, China, 18–21 August 2005; Volume 7, pp. 4260–4265. [Google Scholar]
7. Singh, S.; Hussain, S.; Bazaz, M.A. Short Term Load Forecasting Using Artificial Neural Network. In Proceedings of the 2017 Fourth International Conference on Image Information Processing (ICIIP), Shimla, India, 21–23 December 2017; p. 5. [Google Scholar]
8. Chen, K.; Chen, K.; Wang, Q.; He, Z.; Hu, J.; He, J. Short-Term Load Forecasting With Deep Residual Networks. IEEE Trans. Smart Grid **2019**, 10, 3943–3952. [Google Scholar] [CrossRef]
9. Wang, P.; Liu, B.; Hong, T. Electric load forecasting with recency effect: A big data approach. Int. J. Forecast. **2016**, 32, 585–597. [Google Scholar] [CrossRef]
10. Yang, L.; Yang, H. A Combined ARIMA-PPR Model for Short-Term Load Forecasting. In Proceedings of the 2019 IEEE Innovative Smart Grid Technologies—Asia (ISGT Asia), Chengdu, China, 21–24 May 2019; pp. 3363–3367. [Google Scholar]
11. López, M.; Valero, S.; Rodriguez, A.; Veiras, I.; Senabre, C. New online load forecasting system for the Spanish Transport System Operator. Electr. Power Syst. Res. **2018**, 154, 401–412. [Google Scholar] [CrossRef]
12. Bianchi, F.M.; De Santis, E.; Rizzi, A.; Sadeghian, A. Short-Term Electric Load Forecasting Using Echo State Networks and PCA Decomposition. IEEE Access **2015**, 3, 1931–1943. [Google Scholar] [CrossRef]
13. Ma, Y.; Zhang, Q.; Ding, J.; Wang, Q.; Ma, J. Short Term Load Forecasting Based on iForest-LSTM. In Proceedings of the 2019 14th IEEE Conference on Industrial Electronics and Applications (ICIEA), Xi'an, China, 19–21 June 2019; pp. 2278–2282. [Google Scholar]

14. Abedinia, O.; Amjady, N.; Zareipour, H. A New Feature Selection Technique for Load and Price Forecast of Electrical Power Systems. IEEE Trans. Power Syst. **2017**, 32, 62–74. [Google Scholar] [CrossRef]

15. Mamun, A.A.; Sohel, M.; Mohammad, N.; Haque Sunny, M.S.; Dipta, D.R.; Hossain, E. A Comprehensive Review of the Load Forecasting Techniques Using Single and Hybrid Predictive Models. IEEE Access **2020**, 8, 134911–134939. [Google Scholar] [CrossRef]

16. Hippert, H.S.; Pedreira, C.E.; Souza, R.C. Neural networks for short-term load forecasting: A review and evaluation. IEEE Trans. Power Syst. **2001**, 16, 44–55. [Google Scholar] [CrossRef]

17. Hong, T.; Fan, S. Probabilistic electric load forecasting: A tutorial review. Int. J. Forecast. **2016**, 32, 914–938. [Google Scholar] [CrossRef]

18. López, M.; Sans, C.; Valero, S.; Senabre, C. Empirical Comparison of Neural Network and Auto-Regressive Models in Short-Term Load Forecasting. Energies **2018**, 11, 2080. [Google Scholar] [CrossRef]

19. Sethi, R.; Kleissl, J. Comparison of Short-Term Load Forecasting Techniques. In Proceedings of the 2020 IEEE Conference on Technologies for Sustainability (SusTech), Santa Ana, CA, USA, 23–25 April 2020; pp. 1–6. [Google Scholar]

20. Jie-sheng, W.; Qing-wen, Z. Short-term electricity load forecast performance comparison based on four neural network models. In Proceedings of the The 27th Chinese Control and Decision Conference (2015 CCDC), Qingdao, China, 23–25 May 2015; pp. 2928–2932. [Google Scholar]

21. Mehmood, S.T.; El-Hawary, M. Performance Evaluation of New and Advanced Neural Networks for Short Term Load Forecasting. In Proceedings of the 2014 IEEE Electrical Power and Energy Conference, Calgary, AB, Canada, 12–14 November 2014; pp. 202–207. [Google Scholar]

22. Sun, X.; Luh, P.B.; Cheung, K.W.; Guan, W.; Michel, L.D.; Venkata, S.S.; Miller, M.T. An Efficient Approach to Short-Term Load Forecasting at the Distribution Level. IEEE Trans. Power Syst. **2016**, 31, 2526–2537. [Google Scholar] [CrossRef]

23. Rafi, S.H.; Nahid-Al-Masood, N.-A.-M. Highly Efficient Short Term Load Forecasting Scheme Using Long Short Term Memory Network. In Proceedings of the 2020 8th International Electrical Engineering Congress (iEECON), Chiang Mai, Thailand, 4–6 March 2020; pp. 1–4. [Google Scholar]

24. Kong, W.; Dong, Z.Y.; Jia, Y.; Hill, D.J.; Xu, Y.; Zhang, Y. Short-Term Residential Load Forecasting Based on LSTM Recurrent Neural Network. IEEE Trans. Smart Grid **2019**, 10, 841–851. [Google Scholar] [CrossRef]

25. Rafi, S.H.; Nahid-Al-Masood; Deeba, S.R.; Hossain, E. A Short-Term Load Forecasting Method Using Integrated CNN and LSTM Network. IEEE Access **2021**, 9, 32436–32448. [Google Scholar] [CrossRef]

26. Mohammed, J.; Bahadoorsingh, S.; Ramsamooj, N.; Sharma, C. Performance of exponential smoothing, a neural network and a hybrid algorithm to the short term load forecasting of batch and continuous loads. In Proceedings of the 2017 IEEE Manchester Power Tech, Manchester, UK, 18–22 June 2017; pp. 1–6. [Google Scholar]

27. Veljanovski, G.; Atanasovski, M.; Kostov, M.; Popovski, P. Application of Neural Networks for Short Term Load Forecasting in Power System of North Macedonia. In Proceedings of the 2020 55th International Scientific Conference on Information, Communication and Energy Systems and Technologies (ICEST), Niš, Serbia, 10–12 September 2020; pp. 99–101. [Google Scholar]

28. Weyermüller, E.; Vermeulen, H.J.; Groch, M. Short-Term Load Forecasting using Minimalistic Adaptive Neuro Fuzzy Inference Systems. In Proceedings of the 2020 International SAUPEC/RobMech/PRASA Conference, Cape Town, South Africa, 29–31 January 2020; pp. 1–6. [Google Scholar]

29. Liu, S.; Gu, S.; Bao, T. An Automatic Forecasting Method for Time Series. Chin. J. Electron. **2017**, 26, 445–452. [Google Scholar] [CrossRef]

30. Panapongpakorn, T.; Banjerdpongchai, D. Short-Term Load Forecast for Energy Management Systems Using Time Series Analysis and Neural Network Method with Average True Range. In Proceedings of the 2019 First International Symposium on Instrumentation, Control, Artificial Intelligence, and Robotics (ICA-SYMP), Bangkok, Thailand, 16–18 January 2019; pp. 86–89. [Google Scholar]

31. Di, S. Power System Short Term Load Forecasting Based on Weather Factors. In Proceedings of the 2020 3rd World Conference on Mechanical Engineering and Intelligent Manufacturing (WCMEIM), Shanghai, China, 4–6 December 2020; pp. 694–698. [Google Scholar]

32. Jiang, H.; Zhang, Y.; Muljadi, E.; Zhang, J.J.; Gao, D.W. A Short-Term and High-Resolution Distribution System Load Forecasting Approach Using Support Vector Regression With Hybrid Parameters Optimization. IEEE Trans. Smart Grid **2018**, 9, 3341–3350. [Google Scholar] [CrossRef]

33. McIlvenna, A.; Herron, A.; Hambrick, J.; Ollis, B.; Ostrowski, J. Reducing the computational burden of a microgrid energy management system. Comput. Ind. Eng. **2020**, 143, 106384. [Google Scholar] [CrossRef]

34. Weimar, M.; Somani, A.; Etingov, P.; Miller, L.; Makarov, Y.; Loutan, C.; Katzenstein, W. Benefit Cost Analysis of Improved Forecasting for Day-Ahead Hourly Regulation Requirements. In Proceedings of the 2018 IEEE Power Energy Society General Meeting (PESGM), Portland, OR, USA, 5–10 August 2018; pp. 1–5. [Google Scholar]

35. López, M.; Sans, C.; Valero, S.; Senabre, C. Classification of Special Days in Short-Term Load Forecasting: The Spanish Case Study. Energies **2019**, 12, 1253. [Google Scholar] [CrossRef]

Anexo B. Automatic Selection of Temperature Variables for Short-Term Load Forecasting.

Automatic Selection of Temperature Variables for Short-Term Load Forecasting

Alfredo Candela Esclapez*, Miguel López García, Sergio Valero Verdú and Carolina Senabre Blanes.

Electrical Engineering Area, Miguel Hernández University, Av. de la Universidad, s/n, 03202 Elche, Spain

*Author to whom correspondence should be addressed.
Academic Editor: Gaetano Zizzo

(This article belongs to the Topic Short-Term Load Forecasting)

Abstract

Due to the infeasibility of large-scale electrical energy storage, electricity is generated and consumed simultaneously. Therefore, electricity entities need consumption forecasting systems to plan operations and manage supplies. In addition, accurate predictions allow renewable energies on electrical grids to be managed, thereby reducing greenhouse gas emissions. Temperature affects electricity consumption through air conditioning and heating equipment, although it is the consumer's behavior that determines specifically to what extent. This work proposes an automatic method of processing and selecting variables, with a two-fold objective: improving both the accuracy and the interpretability of the overall forecasting system. The procedure has been tested by the predictive system of the Spanish electricity operator (Red Eléctrica de España) with regard to peninsular demand. During the test period, the forecasting error was consistently reduced for the forecasting horizon, with an improvement of 0.16% in MAPE and 59.71 MWh in RMSE. The new way of working with temperatures is interpretable, since they separate the effect of temperature according to location and time. It has been observed that heat has a greater influence than the cold. In addition, on hot days, the temperature of the second previous day has a greater influence than the previous one, while the opposite occurs on cold days.

Keywords: accuracy; interpretability; short-term load forecasting; temperature analysis; temperature processing.

1. Introduction

On a national scale, it is not feasible to store energy on electrical grids before transmitting it to consumers. Therefore, electrical operators maintain a real-time balance between produced and consumed energy. To maintain this balance, it is necessary to forecast the future electric load. Forecasting is necessary in the very short-term for the

control of generators, and in the short and medium term for resource supply and operations planning. In addition, long-term forecasting is required for the construction and maintenance of facilities. This paper focuses on short-term load forecasting (STLF), ranging from hours to several days in advance, being necessary for energy and the economic management in electrical companies, such as marketers, demand aggregators, generators, etc.

Predicting demand accurately is crucial to reliably operating power generation, transmission and distribution. Making decisions based on inaccurate predictions can lead to additional costs, breakdowns and even blackouts. Furthermore, accurate forecasts allow better management of renewable energies, so load forecasting can help reduce greenhouse gas emissions indirectly.

The electrical load depends on many variables, such as time of the day, temperature, day of the week or industrial activity, and it even has a random component, so there is always some error. In addition, these variables show interaction among them. For example, temperature has a greater effect during the afternoon than during early morning, since air conditioning units are generally less used while people sleep. This paper deals specifically with temperature variables and how they can be automatically selected and processed to properly capture their effect on load and, therefore, forecast electrical load more accurately.

1.1. Literature Review

Over the last decades, many works have been published developing predictive models, and so a wide variety of models have been built. Some of them are based on statistical models, such as ARIMA and the Hidden Markov Model [1], the autoregressive [2,3], exponential smoothing grey model [4], the exponential smoothing model [5], or a single ARIMA [6]. Other models are based on machine learning, such as the radial basis function neural network [7], fuzzy interaction regression [8] or convolutional neural network with long short-term memory [9]. There are also hybrid forecasting systems that combine artificial intelligence with statistical techniques like ARIMA and support vector machine [10], state-space models combined with a neural network [11] or multivariable regression with a long short-term memory network [12].

In recent years, machine learning techniques have received more attention than statisticals. For example, ref. [13] designs a deep-learning model to forecast wind speed and, consequently, electric energy generation; a long short-term memory neural network and a convolutional neural network are combined as a core of the forecasting system. A long short-term memory model is used with a hyperparameter adjustment in [14]. Another work [15] employs a neural network to forecast the load of individual families. Convolutional neural networks can extract non-linear features to feed support vector machines as forecasting systems [16]. An artificial neural network is integrated with an evolutionary algorithm to avoid local optima and obtain convergence [17].

The number of forecasting hybrid techniques has also increased recently. As an example, a fuzzy c-means clustering is employed in [18] using a random forest model and a deep neural network. In [19], an exponential smoothing state-space model and an artificial neural network are combined. The system from [20] combines a SARIMAX with a long-short term memory network to obtain a better forecasting performance.

During the last years, smart grids received more attention due to increased access to data through smart meters. For example, ref. [21] employed a multivariable linear regression to forecast trend and a long short-term memory neural network to model nonlinear behavior of an electric load. In [22], k-means clustering is employed to divide data into sets, they are divided into training and test sets, and a convolutional neural

network is finally trained and employed to forecast the load. Another example is [23], which evaluates different machine-learning models for smart grids. In [24], a list of methods for low voltage forecasting are also compared, which mainly consist of kernel density estimation, simple seasonal linear regression, and autoregressive and exponential smoothing.

When it comes to predicting demand, selecting and processing exogenous variables may be more important than the mathematical model used. Other previous works have focused on processing temperature data to accurately forecast load. An example to this is the regressive algorithm of [25], which uses the climate data from five previous days in a model. It is updated with similar previous days employing the shortest Euclidean distance. Fuzzification has also been applied to the temperature before using it in a multi-layered LSTM [26]. This allows the model to adapt to temperature changes and improve its performance. The heat island effect has been taken into account by means of satellite images to correct the temperature before using it in an Elman Neural Network [27], also using the temperature of previous days; however, real predictive systems do not usually have satellite data. A predictive system was developed in Nepal [28] with a feed-forward neural network that uses temperature, working days, holidays, time of the day, month, and previous data. Previously, they analyzed the demand/temperature sensitivity and obtained different values for the cold and hot degree days, then the difference between room heating and cooling systems is obtained.

Mentioned works [25,26,27,28] offer a treatment of climatic variables in order to improve accuracy, but leave interpretability on the background or do not mention it. In contrast, other research has focused on the analysis of the relationship between temperature and demand, such as the use of a linear regression model to extract the correlation in Vietnam [29], where it was observed how the relationship varies throughout the year. In Beijing [30], the relationship was analyzed with linear regression using two demand/temperature lines. One of them is used above a temperature threshold value while the other one is used below. This provides two demand-temperature equations depending on whether it is cold or hot. For this, a threshold temperature is established to separate both behaviors; however, the possibility of an intermediate range of temperatures is not contemplated. In the United Kingdom, the effect that cold temperatures have on demand due to the use of heat pumps was studied [31]. This allowed the calculations of demand forecasts for heat pumps according to temperature.

In Spain, a predictive system that uses differentiated temperature and the effects of daylight at each hour of the day was developed in [32]. The model, called "smooth transition regression model with double threshold", allows for the distinguishing of the demand/temperature sensitivity for periods of economic activity and rest. Therefore, the predictive model also allows analytical conclusions to be drawn, this being its focus. In this paper we work with an interpretable approach to use temperature by linearizing it with three demand-temperature lines. On the contrary, in [32], temperature was preprocessed by means of a third degree polynomial function against logarithmic demand. In addition, our system works with a model for each hour of execution and forecast, which also considers the cycles of economic activity; this data together with the month implicitly considers daylight; there are also 54 variables that define type of day, reinforcing the information about economic activity as well as allowing the types of day to be distinguished.

In the literature there are also works about the automation of STLF. In 1997, a predictive regressive system was programmed for the Irish Electricity Supply Board [33]. The forecasting calculation and the periodic updating of the model are automated, and the STLF system uses backward elimination to discard temperature variables that are not

useful and an algorithm to rule out outliers. More presently, an automatic predictive system that updates and uses a specific model, such as the Stochastic Hour Ahead Proportion Analysis Trained by Multivariable Regression, is presented in [34], which includes a graphical user interface.

Currently, automation can go a step further through open-source libraries that automate the process of generating predictive models, which allows building prediction systems without a need for experts. For example, Auto-Sklearn and Python's TPOT generate machine learning models. They were used to build models that predicted the consumption levels of appliances in a household and of an industrial office building [35].

There is also the possibility of working at an intermediate point of automation using a library of already defined models. This was the case of the creation of an automatic model selection system using a semi-Markov process and a modified hidden Markov chain [36].

1.2. Paper Contributions

According to [37], there is already a large number of STLF models, each one being the best according to the circumstances. Therefore, a new model is not offered in this paper. Instead, a model-independent temperature data preprocessing technique is developed. In the same way, the model used is also not dependent on the temperature preprocessing. All this allows the proposed technique to by applied to any other forecasting engine using temperature information

By applying this processing technique, this paper seeks to improve the STLF system implemented in the Spanish Transmission System Operator, Red Eléctrica de España (REE) (Municipality of Alcobendas, Spain) and developed by the Miguel Hernández University [38]. The system has been operating for more than five years, and during this time REE and the university have been working on improvements [39,40]. The forecasting system is considered as an adequate benchmark for load forecasting in Spain due to its continuous use and enhancement by the Spanish Transmission System Operator (TSO).

To predict the demand of the Spanish peninsula, the previous REE system had temperature data available from 28 meteorological stations, of which five were used. Stations were chosen by expert advice, following subjective criteria of demography and climatological regions of Spain. This implies that the previous system was not built in an automatic and repeatable way, nor did it have an interpretable way of processing temperatures. As a consequence, many coefficients of the autoregressive models had opposite signs to what was expected, compensating for other effects. In addition, there were 30 variables to represent the temperatures of the forecast day and the two previous ones, which, as shown in this paper, is an unnecessary amount.

Three improvements are offered regarding temperature management:
- Final prediction accuracy.
- Variable selection automation.
- Interpretability of variables.

The new approach consists of working with the following new temperature variables:
- Average temperature from chosen stations.
- Temperature averages from previous days.
- Individual temperatures from chosen stations.
- Individual temperatures from previous days.

The new predictive system starts from the same database, however it is capable of automatically determining how many stations to use, which ones to use, and how many previous days should be considered.

This new way of constructing the temperature variables has replaced the one previously used by the predictive system. To test it, it has been trained with the years from 2012 to 2018, after which 2019 was predicted. An execution of the predictive system has been simulated with the same data availability as under normal conditions. In the simulation, the current day and the following nine days were predicted, executing the system in each of the 24 h of the day. Different ways of processing temperatures have been tested, and the best one obtained higher and more consistent accuracy than the old system.

The new way of working with temperatures is more interpretable since it separates the effects of temperature, according to location and time. Based on the zones, lags and training coefficients, the regions that affect demand can be deduced along with their temperature, how many previous days of temperature affect demand, and by how much.

The new predictive system is also intended to be the test subject for future studies of the temperature-demand relationship.

This paper is organized as follows: Section 2 explains the prediction system used to test the processing of temperature data, Section 3 exposes an updated version of the tested system, Section 4 explains the rest of preprocessing methods tested, Section 5 presents the execution of the simulations to test the preprocessing methods, Section 6 shows the simulation results, and Section 7 presents the conclusions. Section Nomenclature shows variable meanings.

2. Previous Forecasting System

This section explains important aspects to bear in mind from the previous REE system. Design details are shown in the previous work [38].

2.1. Data Employed

Temperature data is taken from the State Meteorological Agency, which consists of measurements and forecasts up to nine days in advance of daily temperatures.

The previous predictive system and the proposed modifications use the same variables except for temperature: holiday information and historical electrical load of the Spanish national network. Holiday information was acquired from the official state gazette (BOE), whilst historical load was provided by REE.

Data are classified into three sets according to purpose: training, validation and testing. Training data are used to calculate internal coefficients of predictive models. Some input data are not applied directly to models, but they are pre-processed using coefficients called hyperparameters. Validation data is used to test and correct these hyperparameters after training models. Test data are used to test trained models. The test data set must be independent and not have any matches with other datasets to ensure generalizability.

2.2. Forecasting Models

The REE forecasting system [38] uses two different model types: an exogenous autoregressive model and a group of exogenous autoregressive networks. Both models employ identical inputs to forecast the peninsular load. They use the following inputs in the same way:
- Temperature predictions for current and the next nine days.
- Peninsular load from the previous hour to calculate the forecast.
- Average load of 52 previous weeks.

- Calendar information, which distinguishes different national and regional holidays including Christmas, weekdays, previous and following days after the time change, month of the year and August week.

The output is the forecasted load for an hour of one of the following nine days or the current one. To obtain multiple forecasted hours, multiple models are then trained with their available inputs and expected output.

Both types of models are employed to calculate forecasts. Their individual results are then combined into a weighted average to obtain final predictions for the operator, so two coefficients from zero to one are applied to each forecast. Both coefficients are calculated to minimize the Mean Absolute Percentage Error (MAPE) of the last 30 days. The forecast horizon spans from the current day up to the next ninth day.

Each neural model is made up of ten feed-forward neural networks with feedback. Every neural network generates its own forecast. The highest and lowest values are then discarded and, finally, the average is calculated to obtain the final neural prediction.

Equation (1) represents the autoregressive model.

$$\ln(y_t) = \sum_{i=1}^{d} c_{t-i}\, \beta_i + \sum_{k=1}^{n} X_{k\,t}\, \Psi_k + \varepsilon_t \tag{1}$$

where y is the time series of forecast load for an hour of the day, t is the day whose demand is forecast, c is the time series of errors made by the model itself (difference between real value and prediction), β is the series of coefficients associated with the errors, d is the number of previous days that are taken into account, X is the exogenous input vector to predict a day t composed of a number k of variables, Ψ are their respective coefficients and ε is a Gaussian random variation with zero mean.

To operate with the natural logarithm instead of the directly forecast load, it is expressed according to (2).

$$y_t = e^{\varepsilon t} e^{\sum_{i=1}^{d} c_{t-i}\, \beta_i} \prod_{k=1}^{n} e^{X_{k\,t}\, \Psi_k} \tag{2}$$

In (2) the entire expression is made up of a series of multiplications of e raised to two multiplied elements, so the effect of an exogenous variable can be isolated according to (3). Therefore, each input variable can be interpreted as a load variation proportional to the Euler number (e) raised to the variable by its coefficient.

$$y_t = y_t'\, e^{A\,\Psi_a} \tag{3}$$

Being A any exogenous variable desired to analyze, Ψ_a its respective coefficient and y_t' the demand without taking said variable into account. That is, variable y_t' is calculated as shown in (1) or (2) discarding the variable A and its respective coefficient Ψ_a.

The autoregressive model predicts the natural logarithm of the demand in (1) for interpretability reasons. In this way, the demand can be expressed as a series of multiplications in (2) and isolate the influence of the variable to be analyzed in (3), that is, as a multiplication factor for the demand. For example, given a variable A and its respective coefficient Ψ_a, if the result of $e^{A\,\Psi_a}$ is 1.05, the variable A increases demand by 5%.

2.3. Use of Temperature

For measurements and forecasts, there exist daily maximum and minimum values. The daily temperature is then represented by the mean of both values.

The old predictive system does not use this average temperature directly, but preprocesses it with a linearization. To do this, two thresholds are first calculated, and

they separate temperature into three intervals: cold, hot and warm. Equations (4) and (5) are then applied, resulting in two new variables that indicate the degree of cold and heat.

$$CD_z = \begin{cases} 0, & T_z \geq Thc_z \\ Thc_z - T_z, & T_z < Thc_z \end{cases} \tag{4}$$

$$HD_z = \begin{cases} 0, & T_z \leq Thh_z \\ T_z - Thh_z, & T_z > Thh_z \end{cases} \tag{5}$$

Where *CD* is the cold degree, *T* is the temperature, Thc_z is the cold threshold for zone *z*, *HD* is the heat degree and Thh_z is the heat threshold for zone *z*. Then, there is only a pair of thresholds for each zone.

These two thresholds are the hyperparameters used to process temperature. All variables have subscript *z* because they are specific for each zone.

To calculate thresholds Thc_z and Thh_z for each weather station, the method from the same paper where the forecasting system is explained [33] has been used. The method consists of creating a demand-temperature curve divided into 3 straight lines (cold, warm and hot), so that the three lines are delimited by the thresholds. Then, thresholds and line coefficients are calculated by minimizing the Root Mean Square Error (RMSE) of the triple curve with respect to the real demand. After applying minimization, the thresholds obtained are the results.

The heat degree and cold degree of each region are used as inputs to the prediction system, the selected regions being Zaragoza, Madrid, Biscay, Seville, and Barcelona. In addition, these variables are also used for the temperature data of the previous day and the previous one. Then there is a total of 30 variables: 5 regions for 2 degree variables for 3 days.

3. Updated Forecasting System

As an alternative benchmark, a modified version of the old REE system has been tested, which is called the Updated Forecasting System. It still works with variables *CD* and *HD* from (4) and (5), but the difference lies in using a pair of thresholds Thc_z and Thh_z for each hour of each zone z. Then, this method forecasts load in a similar way to the original system, following the next steps:

Step 1, calculate Thc_z and Thh_z for each hour of each zone, with historical data.

Step 2, calculate *CD* and *HD* with temperatures from the training dataset.

Step 3, train models with *CD, HD* and the rest of inputs, which are not temperature data.

Step 4, calculate again *CD* and *HD* with temperatures from the test dataset.

Step 5, forecast with *CD, HD* and the rest of inputs, which are not temperature data.

Although temperatures are daily values, a pair of thresholds is used for each hour of the day. Pairs of thresholds are updated with data from 2011 to 2018, no special days or holidays are considered to minimize the effect of other factors on load. For each hour of the day, a couple of thresholds has been obtained using the demand for that same hour.

When discarding days of the data, they become discontinuous, but this is not an inconvenient, since the procedure to obtain thresholds does not use the autoregressive model, as explained in the previous section.

4. Alternative Processing Methods

This section explains the different alternative methods of temperature processing. All procedures use variables presented from (6) to (14).

$$TM_t = \frac{1}{nz} \sum_{z=1}^{nz} T_{z\,t} \qquad (6)$$

$$HN_t = \begin{cases} 0, & TM_t \le Thh_n \\ TM_t - Thh_n, & TM_t > Thh_n \end{cases} \qquad (7)$$

$$CN_t = \begin{cases} 0, & TM_t \ge Thh_n \\ Thh_n - TM_t, & TM_t < Thh_n \end{cases} \qquad (8)$$

Where *TM* is the time series for the mean national temperature, *t* is the forecasted day, and T_z is the time series for temperature from zone *z*. As an example, $T_{2\,3}$ represents the temperature during the third day in the second zone. The number of zones is *nz*, *CN* is the cold degree time series for the national mean, Thc_n is the cold national threshold, *HN* is the heat degree time series for the national mean, and Thh_n is the heat national threshold. As in the updated version, there are a few different thresholds depending on the time of the day.

$$PC_{nl\,t} = CN_{t-nl} - CN_t \qquad (9)$$

$$PH_{nl\,t} = HN_{t-nl} - HN_t \qquad (10)$$

Where PC_l is the previous cold degree time series for *nl* previous days and PH_l is the previous heat degree time series.

$$IC_{z\,t} = CD_{z\,t} - CN_t \qquad (11)$$

$$IH_{z\,t} = HD_{z\,t} - HN_t \qquad (12)$$

Where IC_z is the individual cold degree difference of zone *z* and IH_z is the individual heat degree difference of zone *z*. For example, $IC_{2\,3}$ represents the cold degree difference during the third day in the second zone.

$$PIC_{z\,zl\,t} = CD_{z\,t-zl} - CN_{t-zl} \qquad (13)$$

$$PIH_{z\,zl\,t} = HD_{z\,t-zl} - HN_{t-zl} \qquad (14)$$

4.1. Combinatorial Brute Force

This method looks for the best zone and lag combination so that all possible combinations are tested.

4.1.1. Steps

Step 1, individual thresholds. Individual thresholds (Thc_z and Thh_z) are obtained for all available zones.

Step 2, number and zone selection. All possible choices that include five zones are tried. For each combination of zones, the R squared for a linear model is calculated between temperature matrix and peninsular demand, this matrix is made up of time series CDz and HDz. Next, the combination of zones with the highest R squared is chosen. The whole process is repeated for one, two, three and four zones, so that five zone lists are obtained. This step is summarized in Figure 1.

Figure 1. Second step of Combinatorial Brute Force.

Step 3, peninsular thresholds. For each zone list, Thc_n and Thh_n are calculated.

Step 4, peninsular and individual lags. For each list, all possible combinations of individual lags zl for each zone and national nl are tested, which can be 0, 1 or 2. During each iteration, an autoregressive model is trained with all the exogenous variables simulating real training (for the fourth day before, executing at 10:00 a.m. and predicting

at 6:00 p.m.). The combination with the lowest MAPE in the validation period is chosen as the result. This step is summarized in Figure 2.
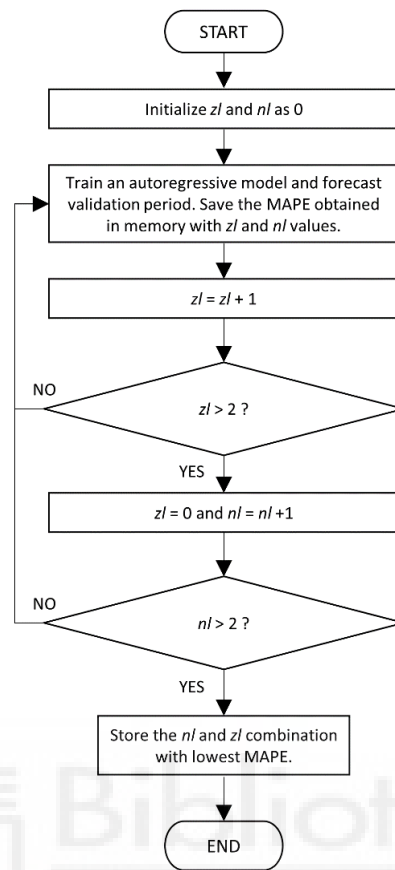

Figure 2. Fourth step of Combinatorial Brute Force.

4.1.2. Datasets

For steps 1, 2 and 3, only days that are not holidays or special weekdays are considered, in order to minimize the effect of other factors on demand. Data from 2011 to 2018 have been used.

For step 4, every day from 2011 to 2017 has been used as a training period and data from 2018 have been taken as the validation to calculate error and compare combinations.

4.2. Sequential Brute Force

This algorithm follows the same steps as the combinational one, but it searches for the best thermal zones one by one instead of all possible combinations. To do this, step 2 is changed to the following:

For each zone, the matrix composed with time series CD_z and HD_z is created, obtaining a matrix composed by two time-series. Then, R squared is calculated with respect to load, employing a linear model and the matrix itself; this process is repeated for all the rest of the zones. The first registered zone is the one with the highest squared. After that, the second zone is searched. Then, the R squared is calculated by concatenating the matrix of the first registered zone with each matrix of the other zones. The second registered zone will be the one that offers the best correlation between the load and the concatenated matrices. This loop is repeated up to five times, adding the registered zones one by one

to the previous matrices, thus obtaining a list of the five best zones. Since zones were added in correlation order, the list can be shortened to use less zones by removing the last elements. This step is summarized in Figure 3.
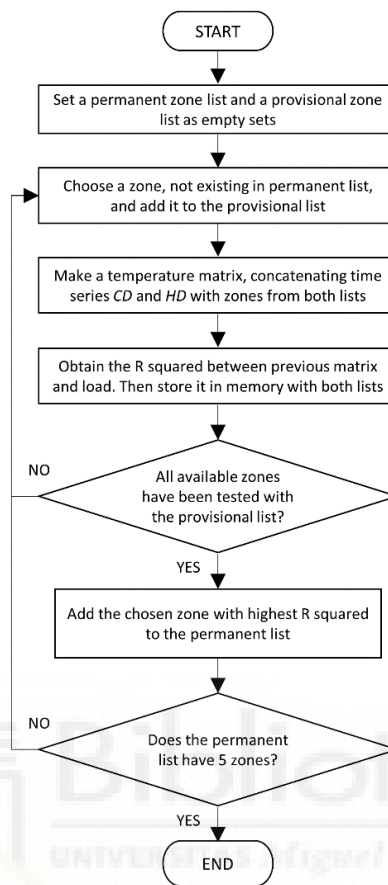

Figure 3. Second step of Sequential Brute Force.

4.3. Combinatorial Completeness

This technique follows the same steps and datasets as the Combinatorial Brute Force, but it uses all possible variables to take advantage of all the information. To do this, step 2 only obtains the list of five zones, and step 4 automatically chooses two previous individual days, *zl* and *nl*, since it is the maximum possible value.

4.4. Sequential Completeness

This method is also analog to the Sequential Brute Force, with the difference that this method takes advantage of all the information. Therefore, it results as follows:

Step 1, individual thresholds. Individual thresholds (Thc_z and Thh_z) are obtained for all available zones.

Step 2, number and zone selection. For each zone, the matrix composed of time series CD_z and HD_z is created. Then, R squared is calculated with respect to load with a linear model. This process is then repeated for the rest of the zones and, finally, the one that achieves the highest R squared is selected and the first zone is registered. Subsequently, the second zone is searched. The R squared is calculated by concatenating the matrix of the first zone with each one of the others. The second registered zone will be the one that offers the best combination. This process is repeated up to five times, adding the

registered zones one by one, thus obtaining a list of the best five zones. This step is also summarized in Figure 3, since it is identical to Sequential Brute Force, but it is explained again to show a general view.

Step 3, peninsular thresholds. Thc_n and Thh_n are calculated for the list of zones obtained.

Step 4, peninsular and individual lags. Two previous individual days, zl and peninsular $nl,$ are chosen since it is the maximum value.

5. Forecasting Simulation

The REE models have been trained and used to forecast 2019 in a simulation with each preprocessing option. The only difference between models is the input temperature variables set, which has been explained in previous sections.

5.1. Training

All models have been trained with data from 2012 to 2018. Seven years of training have been used to ensure that all possible special days are included, offering better accuracy in the process. [39].

When training the models, there are two options regarding temperature data. One option is to use only real measurements. The second option uses forecasted values along with measurements, respecting the data availability of real time.

An example of the second option is the case of a model that forecasts the current day and uses the real temperature from the previous day. It would use the temperature forecast as data for the current day and real measurements from the previous day.

If the first training option is used, some weight will be assigned to the temperature variables to deal with precise temperature data. If the second option is used, the temperature data will be based on forecasts, so there will be some error. Consequently, they will have less correlation with the real demand and lower weights will be assigned to them. If a predictive model is trained with measurements only, although it will actually work with predictions, the error induced in the temperature forecasts will affect the accuracy of the load forecast. Therefore, training is executed with the second option for this work. In addition, coefficients of autoregressive models will reflect the temperature-demand correlation.

5.2. Forecasting

The tests of this work have been carried out with Matlab R2020a with Windows 10 Home as operating system on a computer with an Intel Core i7-8700 as CPU and 16 GB RAM.

The year 2019 has been used as the test dataset, so it has been predicted to calculate the errors of all systems. To calculate forecasts, a predictive system execution has been simulated throughout the year, so the current and the following nine days have been forecasted during every hour of the year. Therefore, the 24 hours of the day have been predicted for the whole year every hour since nine days before the forecasted day.

Data availability has been considered. Therefore, during the simulation, data that would be available at each moment has been used. For example, to forecast an hour of the following day, temperature measurements are not used. Instead, temperature forecasts

from one day in advance are used. The data employed on this work have been provided by REE and the Spanish State Meteorology Agency (AEMET).

Figure 4 is a summary of the process carried out in this paper to obtain forecasts and analyses.
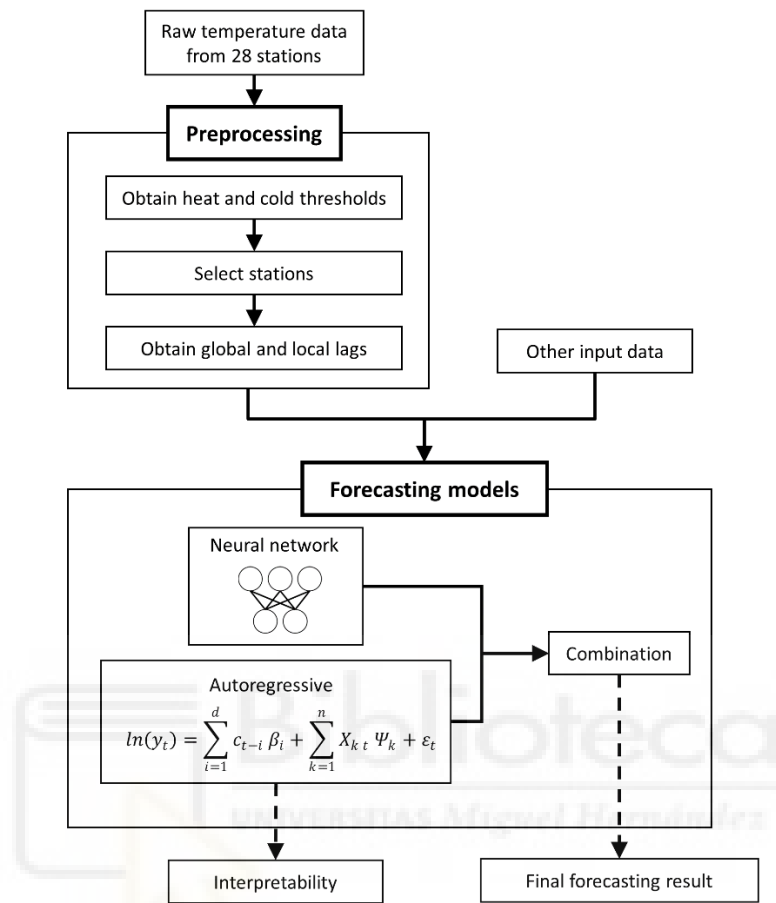

Figure 4. Process summary.

6. Results

Regardless of temperature processing, a predictive system is made up of autoregressive and neural models, so final forecasts are obtained from the combination of both results. The performance of results (combinatorial) is analyzed to evaluate the usefulness of the system from the point of view of an electrical operator. On the other hand, the performance of the autoregressive approach is analyzed to validate it as an analytical model to study the temperature-demand relationship in the future.

MAPE is used as an accuracy indicator since it represents the average of relative error and it is easy to interpret from an analytical perspective. RMSE is also used as a global accuracy indicator, because it employs the quadratic error and it reports higher error in case of higher variability; therefore, it represents more precisely the real costs suffered by the operator.

6.1. Autoregressive Model Accuracy

Figure 5 shows the MAPE for all of the hours of the year from every autoregressive system; in other words, from the autoregressive models with each preprocessing method,

including the original standard system, which is named as Previous. Each MAPE value is displayed according to how long in advance the load has been predicted, from one hour to nine days before. The abscissa axis represents the order of execution in chronological order, so that the first execution is the one carried out at 12:00 a.m. on the previous ninth day. Temperature data arrive at 9:00 a.m. each day, and these moments are reflected in the graph with vertical dotted lines.
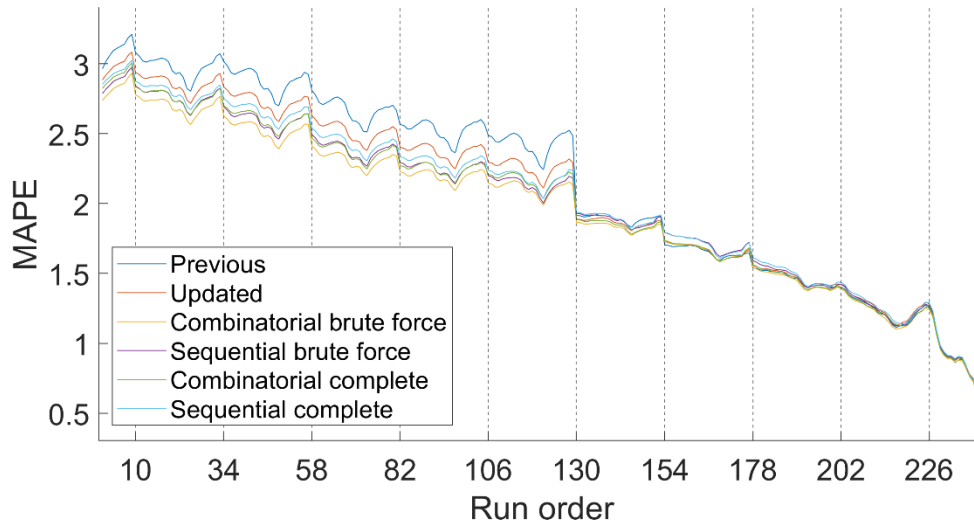

Figure 5. Error of autoregressive models in function of run order.

Table 1 shows the average error for each forecasting system from all forecast horizons, including RMSE.

Table 1. Error Average of Autoregressive Models.

Name	MAPE (%)	RMSE (MWh)
Previous	2.149	863.33
Updated Forecasting System	2.069	831.48
Combinatorial Brute Force	1.964	789.86
Sequential Brute Force	2.010	802.82
Combinatorial Completeness	2.002	804.94
Sequential Completeness	2.039	815.67

All processing methods outperform Previous with 4 or more days in advance. During that interval, the Combinatorial Brute Force is consistently the best, considering MAPE and RMSE. The accuracy for the remaining days is very similar for all methods.

6.2. Autoregressive Error Difference vs. Time Ahead of the Forecast.

On the sixth day of execution, at 9:00 a.m. (execution 130) there is a very pronounced error jump on the previous version. At the time of the jump there are only two factors that vary: temperatures and last recorded load. To check which of these factors causes the jump, two versions of the old REE system have been trained: one acts as if temperature

at the jump time was known in earlier forecasts; on the other hand, the second acts as if it was the load at jump time that was known. The respective simulation is shown in Figure 6.
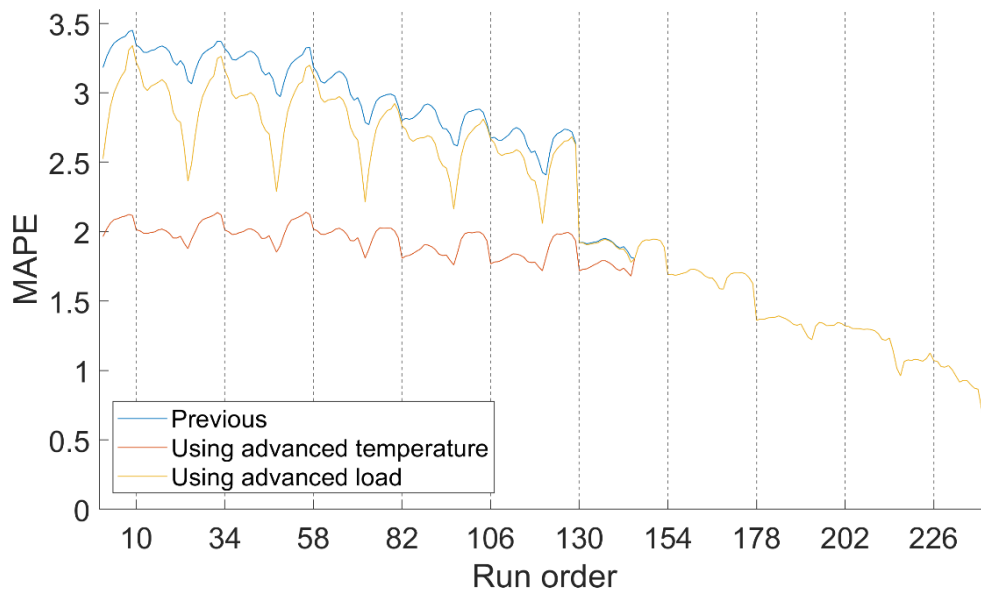

Figure 6. Error of previous system and versions with advanced variables.

Figure 6 allows us to conclude that it is temperature that lowers the accuracy during the first execution days, because the model using temperature from later days shows a very similar pattern until the seventh day.

Once the temperature is located as a factor that causes this difference in precision, the correlation between temperature and demand was analyzed. For this, the time series of training temperature has been isolated; that is, variables *CD*, *HD* and their lagged versions. Subsequently, R squared values of these time series have been calculated. Finally, the R squared average for each anticipation has been drawn in Figure 7. The process is performed for the previous and updated system. Vertical lines indicate the moments when temperature data arrives. It has only been used on weekdays and working days to avoid the influence of other variables.
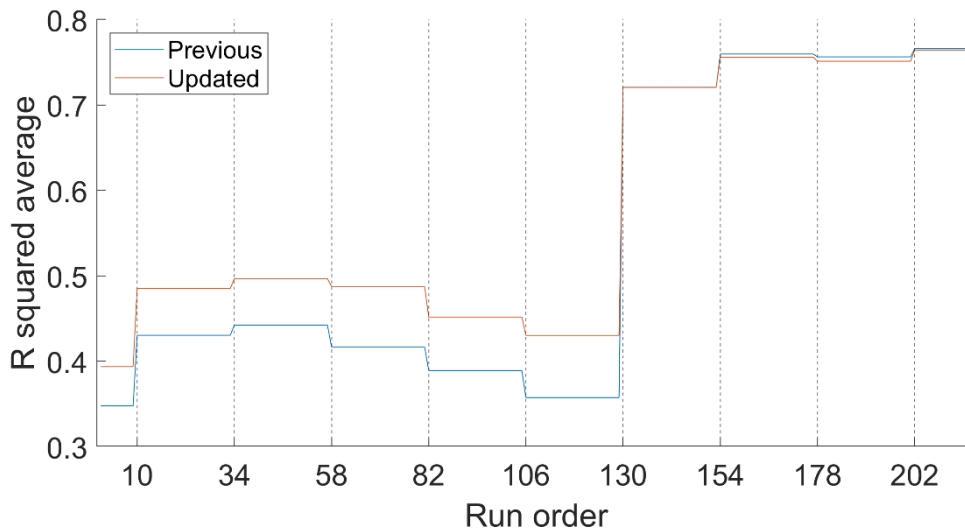
Figure 7. R squared average of temperature time series.

Correlation is constant between data collection moments, since during these intervals temperature time series do not change. Correlations behave similarly to precision. At 9:00 a.m. on the sixth day there is a jump. Previous to this jump, the updated system offers a better performance, while later there is no appreciable difference between systems. Therefore, a simple change to using hourly thresholds considerably improves the relationship between temperature and demand.

In conclusion, between available temperature variables and load, there is a correlation jump on the sixth day. This correlation variation causes the abrupt accuracy improvement, since accuracy depends on the accuracy of available temperature data.

6.3. Hybrid Systems Accuracy

Figure 8 shows the MAPE of hybrid systems, since these produce the final forecasts for the operator, while Figure 9 shows the RMSE. To summarize data from Figures 8 and 9, Table 2 shows the error average of hybrid systems from all advances, also known as run orders.
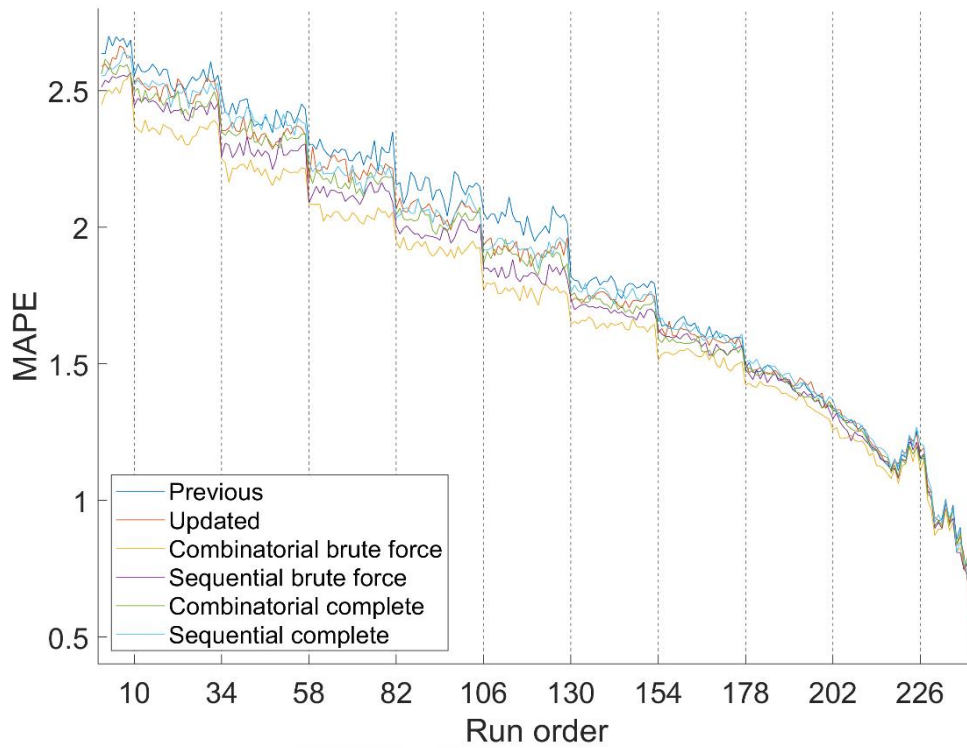
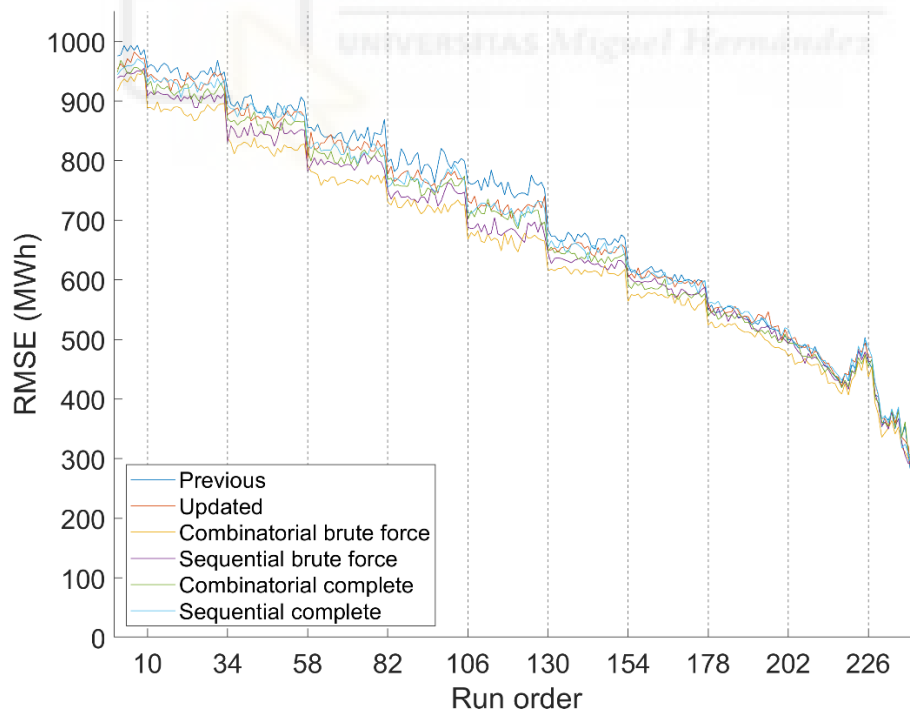**Figure 8.** Error of hybrid models in function of run order.

Figure 9. RMSE of hybrid models in function of run order.

Table 2. Error Average of Hybrid Systems.

Name	MAPE (%)	RMSE (MWh)
Previous	1.953	767.98
Updated Forecasting System	1.906	767.92
Combinatorial Brute Force	1.793	708.27
Sequential Brute Force	1.850	727.11
Combinatorial Completeness	1.878	737.28
Sequential Completeness	1.914	750.41

Regarding both metrics, the Combinatorial Brute Force version is more accurate than the rest overall. It also offers better accuracy with almost all forecast horizons, so it consistently performs better. Combinatorial Brute Force is thus considered as the best preprocessing method for the REE forecasting system.

6.4. Autoregressive Interpretability

Once an autoregressive model has been obtained, it can be used to read its coefficients and draw conclusions from the training period.

The winner procedure for the autoregressive model (Combinatorial Brute Force) has obtained three zones:Córdoba, Tarragona and Getafe. It has also obtained two previous days of temperature used at a peninsular level (nl), while at the local level it has obtained zero previous days in each of the zones (zl).

To quantify the change that one variable undergoes when another varies, sensitivity is calculated. Applying it to the autoregressive model of (3) through (15).

$$S_A = \frac{\partial y_t}{\partial A} = y_t' \, e^{A \, \Psi_a} \, \Psi_a = y_t \, \Psi_a \qquad (15)$$

Where S_A is the sensitivity of any exogenous variable A. Since sensitivity depends on forecasted load, for each demand value there is a different sensitivity, instead of a fixed value, as would result from a linear model that predicts the demand directly, as shown in (16) and (17), which is not the case.

$$y_t = \sum_{i=1}^{d} c_{t-i} \, \beta_i + \sum_{k=1}^{n} X_{k \, t} \, \Psi_k + \varepsilon_t \qquad (16)$$

$$S_A = \frac{\partial y_t}{\partial A} = \Psi_a \qquad (17)$$

Once the autoregressive models have been trained with Sequential Brute Force, all hours of 2019 have been predicted, simulating the calculations that were made 9 days before at 5:00 p.m. The resulting demands have been multiplied by coefficients of their respective models, and then the sensitivities of 2019 have been obtained. Finally, sensitivity averages have been calculated, and they have been drawn on Figures 10–12.
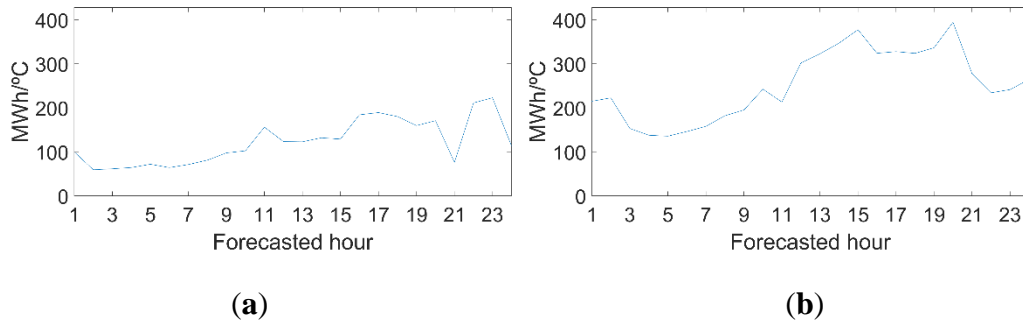
(a)   **(b)**

Figure 10. Sensitivity of peninsular variables for every forecasted hour. (**a**) Peninsular cold degree sensitivity (CN). (**b**) Peninsular heat degree sensitivity (HN).
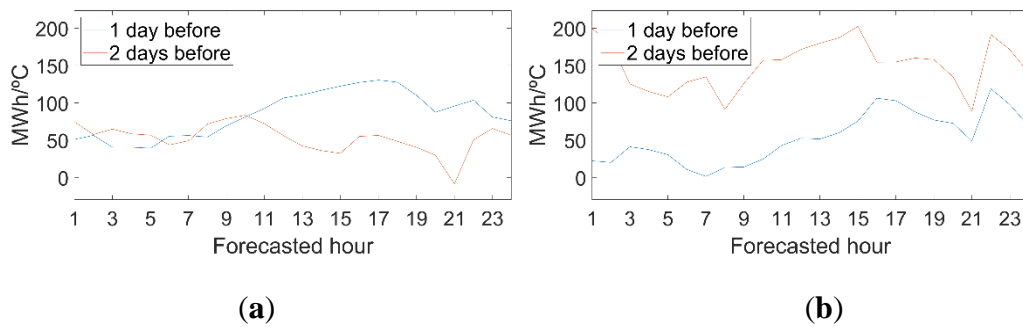

(a)   **(b)**

Figure 11. Sensitivity of previous peninsular variables for every forecasted hour. (**a**) Previous cold degree sensitivity (PC). (**b**) Previous heat degree sensitivity (PH).
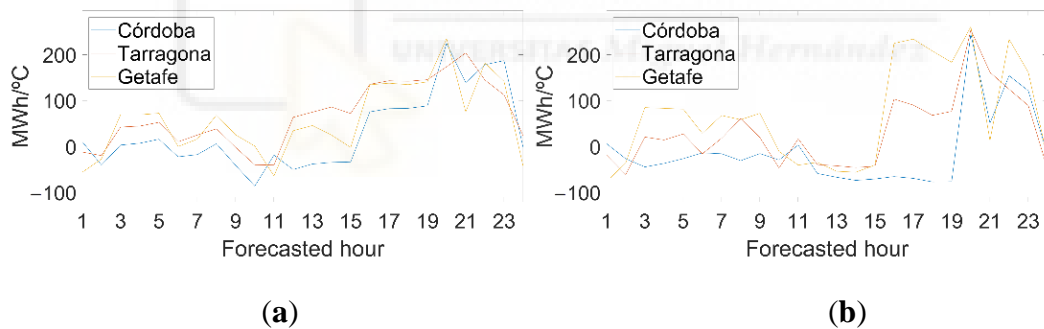

(a)   **(b)**

Figure 12. Sensitivity of local variables for every forecasted hour. (**a**) Individual cold degree difference (IC). (**b**) Individual heat degree difference (IH).

Since there are no previous individual days, sensitivities of their respective variables $PIC_{z\,l}$ and $PIH_{z\,l}$ do not exist. According to the algorithm used, individual previous days are not obtained because they do not improve forecasting accuracy. Therefore, they do not provide relevant information.

The sensitivities of peninsular heat are greater than cold (Figure 10); therefore, the heat effect is more influential than cold. In addition, both peninsular variables have lower values during the early morning hours, so temperature has less influence on rest periods.

On Figure 11 there are positive values. Therefore, on a peninsular scale, if it has been colder or hotter on previous days, the load will increase. In addition, in hot seasons the temperature of the second previous day has a greater influence than the previous one, while the opposite occurs for cold seasons.

Figure 12 represents the effect of one area being colder or hotter than the rest.

7. Conclusions

In this paper, a method has been developed to preprocess temperature data which improves the accuracy of forecasting electricity demand on a national scale. To do that, the peninsular demand of Spain for 2019 has been predicted. Preprocessing has been tested with the STLF system of the Spanish electrical operator REE. Forecasts have been made simulating the execution of the system with the same data availability that would be available under normal operating conditions. Simulations have been carried out for all horizons with the REE predictive system; therefore, its performance can be evaluated as the forecasted moment approaches.

Different data processing methods for temperature have been tested. The most accurate method selects five combinations of zones with the highest R squared with respect to the peninsular demand. Then, for each zone combination, all the combinations of the number of previous days of individual temperatures and their average are tested. Finally, we get the one that offers the best precision to predict the prior year to the one we wish to forecast.

The method of processing temperatures is automatic, so it selects the zones and variables with the greatest estimated influence on demand. Consequently, the implementation on a national scale does not require additional studies and the interpretability of the chosen zones is straightforward.

Incorporating temperature data preprocessing globally improves MAPE by 0.16% and RMSE by 59.71 MWh, as can be seen in Table 2. In addition, said improvement is consistent with respect to how early the forecasts are made, as shown in Figures 8 and 9.

The new variables that are incorporated into the system are interpretable. The significance is expressed in Tables 1–3, which allows for analysis with statistical models such as the REE autoregressive ones. These models also show an improvement in accuracy. The impact of the variables on the demand is obtained as the sensitivity expressed in (15). In addition, the sensitivity is expressed with an interpretable unit (MWh/°C). In the Spanish peninsula, the variable sensitivities show that hot temperatures influence load more than cold ones, but both have a lower influence on rest periods. According to the results, load is affected by the temperature of previous days, so heat from the second previous day has a notorious influence in the same way that cold from the previous day does.

It has been observed that the availability of temperature forecasts notably affects the accuracy of electricity demand, since there is a close relationship between how early a thermal forecast is made and the load forecasts. In conclusion, the most recent thermal forecasts for the forecasted moment should be used.

This paper is focused on predictive and non-analytic applications. In terms of future work, we propose to incorporate this new approach for processing temperatures into statistical models, and to use them as a tool to analyze relationships between temperature and electrical demand on both a national and regional scale, including smart grids. Another proposed future work is the implementation of the proposed methodology in other large-scale predictive system, in order to improve their accuracy and compare the employed preprocessing methods with different systems.

The sustainability of the energy systems is linked to the management of renewable resources, which, in turn, have a stochastic component that make them unreliable. The

ability to forecast not only electric demand but also electric generation is key to ensuring an effective way to harness renewable energies. The preprocessing techniques described can also be applied to these fields where multiple climatological temperatures are used as input; for example, wind forecasting and, consequently, energy generation forecasting for wind generators and, therefore, can get us closer to a sustainable energy system.

Author Contributions

Conceptualization, A.C.E. and M.L.G.; methodology, A.C.E. and M.L.G.; software, A.C.E., M.L.G. and C.S.B.; validation, M.L.G. and S.V.V.; formal analysis, A.C.E.; investigation, A.C.E. and M.L.G.; resources, S.V.V.; data curation, C.S.B. and M.L.G.; writing—original draft preparation, A.C.E.; writing—review and editing, M.L.G.; visualization, A.C.E.; supervision, S.V.V.; project administration, S.V.V.; funding acquisition, S.V.V. All authors have read and agreed to the published version of the manuscript

Institutional Review Board Statement

Not applicable.

Informed Consent Statement

Not applicable.

Data Availability Statement

The data that support the findings of this study are openly available at https://www.esios.ree.es/es/analisis/1293?compare_indicators=545,544&start_date=10-07-2021T00:00&geoids= (accessed on 15 August 2022) for historical demand records and https://opendata.aemet.es (accessed on 15 August 2022) for historical temperature records.

Conflicts of Interest

The authors declare no conflict of interest.

Nomenclature

Input variables

Symbol	Name	Explanation
CN	Cold degree for national mean.	Cold effect for the entire peninsula
HN	Heat degree for national mean.	Heat effect for the entire peninsula
PC_l	Previous cold degree.	Effect of previous day l being colder than today.
PH_l	Previous heat degree.	Effect of previous day l being hotter than today.
IC_z	Individual cold degree difference.	Effect of region z being colder than the nation.
IH_z	Individual heat degree difference.	Effect of region z being hotter than the nation.
$PIC_{z\,l}$	Previous individual cold degree.	Effect of region z being colder than the nation, for one previous day.
$PIH_{z\,l}$	Previous individual heat degree.	Effect of region z being hotter than the nation, for one previous day.

Hyperparameters

Symbol	Name	Explanation
Thh_z	Heat threshold for zone z.	Above this temperature, it is hot and people tend to use refrigeration equipment. For the zone z.
Thc_z	Cold threshold for zone z.	Below this temperature, it is cold and people tend to use heating equipment. For the zone z.
Thh_n	Peninsular heat threshold.	Above this temperature, it is hot and people tend to use refrigeration equipment. For the entire peninsula.
Thc_n	Peninsular cold threshold.	Below this temperature, it is cold and people tend to use heating equipment. For the entire peninsula.
nz	Number of zones employed.	Number of zones whose temperature influences peninsular load.
z	Zones employed.	Which zones have temperature that influences peninsular load.
nl	Number of previous days for peninsular temperature.	Number of previous days whose average peninsular temperature influence load.
zl	Number of previous days for local temperature.	Number of previous days whose temperature at zone z influences load.

Other variables

Symbol	Name
y	Time series of forecasted load.
c	Time series of errors.
B	Series of coefficients associated with the forecasting errors.
X	Exogenous input vector.
Ψ	Exogenous coefficients.
ε_t	Gaussian random variation with mean zero.
A	Exogenous variable desired to analyze.
y'	Time series of load without a variable considered.
T_z	Time series of temperature from zone z.
TM	Time series of mean national temperature.
CD_Z	Cold degree for zone z.
HD_Z	Heat degree for zone z.

References

1. Hermias, J.P.; Teknomo, K.; Monje, J.C.N. Short-Term Stochastic Load Forecasting Using Autoregressive Integrated Moving Average Models and Hidden Markov Model. In Proceedings of the 2017 International Conference on Information and Communication Technologies (ICICT), Karachi, Pakistan, 30–31 December 2017; pp. 131–137. [Google Scholar]
2. Baharudin, Z.; Kamel, N. Autoregressive Method in Short Term Load Forecast. In Proceedings of the 2008 IEEE 2nd International Power and Energy Conference, Ohor Bahru, Malaysia, 1–3 December 2008; pp. 1603–1608. [Google Scholar]
3. Lisi, F.; Shah, I. Forecasting Next-Day Electricity Demand and Prices Based on Functional Models. Energy Syst. **2020**, 11, 947–979. [Google Scholar] [CrossRef]
4. Mi, J.; Fan, L.; Duan, X.; Qiu, Y. Short-Term Power Load Forecasting Method Based on Improved Exponential Smoothing Grey Model. Math. Probl. Eng. **2018**, 2018, 3894723. [Google Scholar] [CrossRef]
5. Ji, P.; Xiong, D.; Wang, P.; Chen, J. A Study on Exponential Smoothing Model for Load Forecasting. In Proceedings of the 2012 Asia-Pacific Power and Energy Engineering Conference, Shanghai, China, 27–29 March 2012; pp. 1–4. [Google Scholar]
6. Wei, L.; Zhen-gang, Z. Based on Time Sequence of ARIMA Model in the Application of Short-Term Electricity Load Forecasting. In Proceedings of the 2009 International Conference on Research Challenges in Computer Science, Shanghai, China, 28–29 December 2009; pp. 11–14. [Google Scholar]
7. Zhang, Z.; Yu, D. RBF-NN Based Short-term Load Forecasting Model Considering Comprehensive Factors Affecting Demand Response. Zhongguo Dianji Gongcheng Xuebao/Proc. Chin. Soc. Electr. Eng. **2018**, 38, 1631–1638. [Google Scholar] [CrossRef]
8. Hong, T.; Wang, P. Fuzzy Interaction Regression for Short Term Load Forecasting; Springer: Berlin/Heidelberg, Germany, 2013. [Google Scholar]
9. Alhussein, M.; Aurangzeb, K.; Haider, S.I. Hybrid CNN-LSTM Model for Short-Term Individual Household Load Forecasting. IEEE Access **2020**, 8, 180544–180557. [Google Scholar] [CrossRef]
10. Karthika, S.; Margaret, V.; Balaraman, K. Hybrid Short Term Load Forecasting Using ARIMA-SVM. In Proceedings of the 2017 Innovations in Power and Advanced Computing Technologies (i-PACT), Vellore, India, 21–22 April 2017; pp. 1–7. [Google Scholar]
11. Villalba, S.A.; Bel, C.A. Hybrid Demand Model for Load Estimation and Short Term Load Forecasting in Distribution Electric Systems. IEEE Trans. Power Deliv. **2000**, 15, 764–769. [Google Scholar] [CrossRef]
12. Rafi, S.H.; Masood, N.-A.; Deeba, S.R. An Effective Short-Term Load Forecasting Methodology Using Convolutional Long Short Term Memory Network. In Proceedings of the 2020 11th International Conference on Electrical and Computer Engineering (ICECE), Dhaka, Bangladesh, 17–19 December 2020; pp. 278–281. [Google Scholar]
13. Chen, Y.; Zhang, S.; Zhang, W.; Peng, J.; Cai, Y. Multifactor Spatio-Temporal Correlation Model Based on a Combination of Convolutional Neural Network and Long Short-Term Memory Neural Network for Wind Speed Forecasting. Energy Convers. Manag. **2019**, 185, 783–799. [Google Scholar] [CrossRef]

14. Bouktif, S.; Fiaz, A.; Ouni, A.; Serhani, M.A. Multi-Sequence LSTM-RNN Deep Learning and Metaheuristics for Electric Load Forecasting. Energies **2020**, 13, 391. [Google Scholar] [CrossRef]

15. Kong, W.; Dong, Z.Y.; Jia, Y.; Hill, D.J.; Xu, Y.; Zhang, Y. Short-Term Residential Load Forecasting Based on LSTM Recurrent Neural Network. IEEE Trans. Smart Grid **2019**, 10, 841–851. [Google Scholar] [CrossRef]

16. Imani, M. Electrical Load-Temperature CNN for Residential Load Forecasting. Energy **2021**, 227, 120480. [Google Scholar] [CrossRef]

17. Singh, P.; Dwivedi, P.; Kant, V. A Hybrid Method Based on Neural Network and Improved Environmental Adaptation Method Using Controlled Gaussian Mutation with Real Parameter for Short-Term Load Forecasting. Energy **2019**, 174, 460–477. [Google Scholar] [CrossRef]

18. Liu, F.; Dong, T.; Hou, T.; Liu, Y. A Hybrid Short-Term Load Forecasting Model Based on Improved Fuzzy C-Means Clustering, Random Forest and Deep Neural Networks. IEEE Access **2021**, 9, 59754–59765. [Google Scholar] [CrossRef]

19. Sulandari, W.; Subanar, S.; Suhartono, S.; Utami, H. Forecasting Electricity Load Demand Using Hybrid Exponential Smoothing-Artificial Neural Network Model. Int. J. Adv. Intell. Inform. **2016**, 2, 131–139. [Google Scholar] [CrossRef]

20. Pooniwala, N.; Sutar, R. Forecasting Short-Term Electric Load with a Hybrid of ARIMA Model and LSTM Network. In Proceedings of the 2021 International Conference on Computer Communication and Informatics (ICCCI), Coimbatore, India, 27–29 January 2021; pp. 1–6. [Google Scholar]

21. Li, J.; Deng, D.; Zhao, J.; Cai, D.; Hu, W.; Zhang, M.; Huang, Q. A Novel Hybrid Short-Term Load Forecasting Method of Smart Grid Using MLR and LSTM Neural Network. IEEE Trans. Ind. Inform. **2021**, 17, 2443–2452. [Google Scholar] [CrossRef]

22. Dong, X.; Qian, L.; Huang, L. Short-Term Load Forecasting in Smart Grid: A Combined CNN and K-Means Clustering Approach. In Proceedings of the 2017 IEEE International Conference on Big Data and Smart Computing (BigComp), Jeju-si, Korea, 13–16 February 2017; pp. 119–125. [Google Scholar]

23. Alquthami, T.; Zulfiqar, M.; Kamran, M.; Milyani, A.H.; Rasheed, M.B. A Performance Comparison of Machine Learning Algorithms for Load Forecasting in Smart Grid. IEEE Access **2022**, 10, 48419–48433. [Google Scholar] [CrossRef]

24. Haben, S.; Giasemidis, G.; Ziel, F.; Arora, S. Short Term Load Forecasting and the Effect of Temperature at the Low Voltage Level. Int. J. Forecast. **2019**, 35, 1469–1484. [Google Scholar] [CrossRef]

25. Ruzic, S.; Vuckovic, A.; Nikolic, N. Weather Sensitive Method for Short Term Load Forecasting in Electric Power Utility of Serbia. IEEE Trans. Power Syst. **2003**, 18, 1581–1586. [Google Scholar] [CrossRef]

26. Zhichao, R.; Chao, C.; Yingying, D.; Wentao, Z.; Jun, W.; Ruixiao, Z. Short-Term Load Forecasting of Multi-Layer LSTM Neural Network Considering Temperature Fuzzification. In Proceedings of the 2020 IEEE Sustainable Power and Energy Conference (iSPEC), Chengdu, China, 23–25 November 2020; pp. 2398–2404. [Google Scholar]

27. Wang, M.; Yu, Z.; Chen, Y.; Yang, X.; Zhou, J. Short-Term Load Forecasting Considering Improved Cumulative Effect of Hourly Temperature. Electr. Power Syst. Res. **2022**, 205, 107746. [Google Scholar] [CrossRef]

28. Rajbhandari, Y.; Marahatta, A.; Ghimire, B.; Shrestha, A.; Gachhadar, A.; Thapa, A.; Chapagain, K.; Korba, P. Impact Study of Temperature on the Time Series

Electricity Demand of Urban Nepal for Short-Term Load Forecasting. Appl. Syst. Innov. **2021**, 4, 43. [Google Scholar] [CrossRef]

29. Tung, N.X.; Dat, N.Q.; Thang, T.N.; Solanki, V.K.; Anh, N.T.N. Analysis of Temperature-Sensitive on Short-Term Electricity Load Forecasting. In Proceedings of the 2020 IEEE-HYDCON, Hyderabad, India, 11–12 September 2020; pp. 1–7. [Google Scholar]

30. Shi, H.H.; Weng, W.G.; Zhai, Z.G.; Zhang, X.L. The Relationship Analysis of Temperature and Electric Load. AMM **2012**, 256–259, 2644–2647. [Google Scholar] [CrossRef]

31. Anderson, A.; Stephen, B.; Telford, R.; McArthur, S. A Probabilistic Model for Characterising Heat Pump Electrical Demand versus Temperature. In Proceedings of the 2020 IEEE PES Innovative Smart Grid Technologies Europe (ISGT-Europe), Hague, The Netherlands, 26–28 October 2020; pp. 1030–1034. [Google Scholar]

32. Moral-Carcedo, J.; Pérez-García, J. Time of Day Effects of Temperature and Daylight on Short Term Electricity Load. Energy **2019**, 174, 169–183. [Google Scholar] [CrossRef]

33. Hyde, O.; Hodnett, P.F. An Adaptable Automated Procedure for Short-Term Electricity Load Forecasting. IEEE Trans. Power Syst. **1997**, 12, 84–94. [Google Scholar] [CrossRef]

34. Antoja, A.J.D.; Lafamia, P.A.O.; Yang, C.A.B.; Magwili, G.V.; Santiago, R.V.M. Automated Short-Term Load Forecasting Using Modified Stochastic Hour Ahead Proportion (SHAP) Analysis. In Proceedings of the 2019 IEEE 11th International Conference on Humanoid, Nanotechnology, Information Technology, Communication and Control, Environment, and Management (HNICEM), Laoag, Philippines, 29 November–1 December 2019; pp. 1–6. [Google Scholar]

35. Wang, C.; Bäck, T.; Hoos, H.H.; Baratchi, M.; Limmer, S.; Olhofer, M. Automated Machine Learning for Short-term Electric Load Forecasting. In Proceedings of the 2019 IEEE Symposium Series on Computational Intelligence (SSCI), Xiamen, China, 6–9 December 2019; pp. 314–321. [Google Scholar]

36. Duan, Q.; Liu, J.; Zhao, D. Short Term Electric Load Forecasting Using an Automated System of Model Choice. Int. J. Electr. Power Energy Syst. **2017**, 91, 92–100. [Google Scholar] [CrossRef]

37. Hong, T.; Fan, S. Probabilistic Electric Load Forecasting: A Tutorial Review. Int. J. Forecast. **2016**, 32, 914–938. [Google Scholar] [CrossRef]

38. López, M.; Valero, S.; Rodriguez, A.; Veiras, I.; Senabre, C. New Online Load Forecasting System for the Spanish Transport System Operator. Electr. Power Syst. Res. **2018**, 154, 401–412. [Google Scholar] [CrossRef]

39. López, M.; Sans, C.; Valero, S.; Senabre, C. Empirical Comparison of Neural Network and Auto-Regressive Models in Short-Term Load Forecasting. Energies **2018**, 11, 2080. [Google Scholar] [CrossRef]

40. López, M.; Sans, C.; Valero, S.; Senabre, C. Classification of Special Days in Short-Term Load Forecasting: The Spanish Case Study. Energies **2019**, 12, 1253. [Google Scholar] [CrossRef]

Agradecimientos

A mi director y mi codirector de tesis por guiarme y aconsejarme en todo momento.

A mis padres y mi pareja por apoyarme y ayudarme en todo momento.